M. Tech (Power Electronics and Systems)

Performance Analysis of Bidirectional SEPIC/ZETA Converter for Battery Energy Storage System

DISSERTATION/THESIS

SUBMITTED IN PARTIAL FULFILLMENT OF THE REQUIREMENTS
FOR THE AWARD OF THE DEGREE
OF

MASTER OF TECHNOLOGY
IN
POWER ELECTRONICS & SYSTEMS

Submitted by:

PRASHANT SINGH

2K22/PES/11

Under the supervision of

DR. ALKA SINGH
(Professor, EED, DTU)

DR. ANKITA ARORA
(Assistant Professor, EED, DTU)

DEPARTMENT OF ELECTRICAL ENGINEERING
DELHI TECHNOLOGICAL UNIVERSITY
(Formerly Delhi College of Engineering)Bawana Road, Delhi-110042

MAY 2024

Prashant Singh

2024

DEPARTMENT OF ELECTRICAL ENGINEERING

DELHI TECHNOLOGICAL UNIVERSITY

(Formerly Delhi College of Engineering)

Bawana Road, Delhi-110042

CANDIDATE'S DECLARATION

I, **PRASHANT SINGH**, Roll No. 2K22/PES/11 student of M. Tech (Power Electronics & Systems), hereby declare that the project Dissertation titled **"Performance Analysis of Bidirectional SEPIC/ZETA Converter for Battery Energy Storage System"** which is submitted by me to the Department of Electrical Engineering Department, Delhi Technological University, Delhi in partial fulfillment of the requirement for the award of the degree of Master of Technology, is originaland not copied from any source without proper citation. This work has not previously submitted for the award of any Degree, Diploma.

Place: Delhi **(Prashant Singh)**

Date: 31/05/2024

DEPARTMENT OF ELECTRICAL ENGINEERING

DELHI TECHNOLOGICAL UNIVERSITY

(Formerly Delhi College of Engineering)

Bawana Road, Delhi-110042

CERTIFICATE

I hereby certify that the project Dissertation titled **"Performance Analysis of Bidirectional SEPIC/ZETA Converter for Battery Energy Storage System"** which is submitted by Prashant Singh, Roll No. 2K22/PES/11, Department of Electrical Engineering, Delhi Technological University, Delhiin partial fulfilment of the requirement for the award of the degree of Master of Technology,is a record of the project work carried out by the student under my supervision. To the best of my knowledge this work has not been submitted in part or full for any Degree or Diplomato this University or elsewhere.

Place: Delhi

Date: 31.05.2024

DR. ALKA SINGH

(SUPERVISOR)

DR. ANKITA ARORA

(CO-SUPERVISOR)

DEPARTMENT OF ELECTRICAL ENGINEERING
DELHI TECHNOLOGICAL UNIVERSITY
(Formerly Delhi College of Engineering)
Bawana Road, Delhi-110042

ACKNOWLEDGEMENT

I would like to express my gratitude towards all the people who have contributed their precious time and effort to help me without whom it would not have been possible for me to understand and complete the project.

I would like to thank **Dr. Alka Singh** (Professor, Department of Electrical Engineering, DTU, Delhi) and **Dr. Ankita Arora** (Assistant Professor, Department of Electrical Engineering, DTU, Delhi) my Project guide and co-guide respectively, for supporting, motivating, and encouraging me throughout the period of this work was carried out. His readiness for consultation always, his educative comments, his concern and assistance even with practical things have been invaluable. I would also like to thank the Centre of Excellence for Electric Vehicles and Related Technologies, Delhi Technological University for providing necessary facilities for performing my research work.

Finally, I must express my very profound gratitude to my parents, seniors and to my friends for providing me with unfailing support and continuous encouragement throughout the research work.

Date: 31/05/2024

Prashant Singh
M. Tech (Power Electronics & Systems)
Roll No. 2K22/PES/11

ABSTRACT

This research is centred on the detailed analysis, control design, and performance enhancement of Zeta converters, which play a crucial role in various applications such as Battery Energy Storage Systems (BESS), motor drives, power factor correction equipment, and solar power systems.

A significant portion of the study is dedicated to discussing two prevalent control strategies: Voltage Mode Control (VMC) and Current Mode Control (CMC). These strategies are vital in regulating the output of the Zeta converter. By employing state-space averaging and linearization techniques, the research derives transfer functions that establish the relationship between the converter's input and output parameters. These transfer functions are instrumental in analysing the small-signal behaviour of the converter, which is crucial for designing robust control systems.

The control schemes' effectiveness is assessed based on key performance indicators such as steady-state error, transient response, and robustness to parameter changes. In addition to the ideal scenarios, the research delves into the complexities introduced by parasitic elements inherent in non-ideal Zeta converters. These parasitic elements, including the resistance in the inductor winding, the equivalent series resistance (ESR) in capacitors, and losses in switches and diodes, significantly impact the converter's operational characteristics, stability, and efficiency. A comprehensive mathematical model is developed to elucidate the interrelationships of these parasitic elements within the context of closed-loop voltage mode control. This model addresses the intricacies added by parasitic components and demonstrates its efficacy through simulations, providing insights into achieving stable and efficient converter performance despite these non-idealities. The research extends to the practical implementation of a bidirectional SEPIC/ZETA DC-DC converter, particularly relevant for BESS applications. This converter facilitates bidirectional power flow, enabling battery charging and discharging operations between the battery and the grid or other power sources. The proposed converter design employs a state-space circuit-averaged modelling technique to derive the transfer function necessary for managing the switching pulses via a PID controller in both SEPIC and ZETA modes. The tuning process for the PID controller utilizes the classic Ziegler-Nichols method, known for its efficacy in achieving optimal control settings.

TABLE OF CONTENT

LIST OF FIGURES

LIST OF TABLES

LIST OF ABBREVIATIONS

PID	Proportional Integral Derivative
BESS	Battery Energy Storage System
HEV	Hybrid Electric Vehicle
UPS	Uninterrupted Power Supply
SEPIC	Single Ended Primary Inductor Converter
HVDC	High Voltage Direct Current
RES	Renewable Energy Sources
VMC	Voltage Mode Control
CMC	Current Mode Control
ESR	Equivalent Series Resistance
MPPT	Maximum Power Point Tracking
BMS	Battery Management System
CCM	Continuous Conduction Mode
PWM	Pulse Width Modulation
LED	Light Emitting Diode
CV	Constant Voltage
CC	Constant Current
PV	Photovoltaic
BDC	Bidirectional Converter
PI	Proportional Integral
ZN	Ziegler Nichols
SOC	State Of Charge
EV	Electric Vehicle
PSO	Particle Swarm Optimization
GA	Genetic Algorithm

LIST OF SYMBOLS

V_{IN}	Input Voltage
I_{IN}	Input Voltage
V_0	Output Voltage
D	Duty Cycle
f_{SW}	Switching Frequency
P_0	Output Power
L_1	Inductor 1
L_2	Inductor 2
I_{L_1}	Inductor 1 current
I_{L_2}	Inductor 2 current
$\Delta i_{L_1}, \Delta i_{L_2}$	Ripple in inductors
C_1	Capacitor 1
C_2	Capacitor 2
$\Delta v_{C_1}, \Delta v_{C_2}$	Ripple in capacitors
R	Resistance
T_S	Switching Time
I_{ref}	Reference Current
V_{ref}	Reference Voltage
V_C	Controlled Voltage
V_{err}	Error Voltage
R_{DS}	MOSFET ON Resistance
r_{L_1}	Inductor 1 ESR

r_{C_1}	Capacitor 1 ESR
R_D	Diode Resistance
r_{L_2}	Inductor 2 ESR
r_{C_2}	Capacitor 2 ESR
V_{BUS}	Bus Voltage
$V_{Battery}$	Battery Voltage
$I_{Battery}$	Battery Current
C_C	Coupling Capacitor

CHAPTER 1
INTRODUCTION

1.1 Overview

The growing demand for versatile and efficient power electronic systems has sparked a new wave of research focused on DC-DC converters. ZETA converters have attracted considerable attention in this domain due to their ability to perform both boost and buck voltage steps while generating a non-inverted output [1-2]. This study aims to elucidate the operation of converters, particularly emphasizing their voltage and current mode control mechanisms. The design of Controllers incorporating Proportional-Integral-Derivative (PID) will be highlighted, especially concerning load and line regulation.

Zeta converters, a variant of the buck-boost family, present efficient solutions for applications requiring both step-up and step-down capabilities [3]. Their unique architectural design offers several benefits, including reduced electromagnetic interference, decreased output ripple, expanded input voltage range, and improved efficiency ranging from 90 to 95 percent. Moreover, their cost-effectiveness makes them suitable for various power electronic applications such as bidirectional power flow, renewable energy systems, power factor correction, electric vehicles, portable electronics, etc. [4]-[8]. However, a thorough understanding of converter behavior under different conditions is essential to ensure operational stability. Exploring this topic effectively can be achieved through small signal analysis.

Small signal analysis is highly advantageous in power converter research, enabling the modeling of dynamic characteristics near an established operating point. This approach is critical for understanding the stability and transient response of Zeta converters in the presence of disturbances and variations. This research delves into the principles and methodologies of small signal analysis to illuminate the operational dynamics and system performance implications of Zeta converters. Additionally, evaluating steady-state conditions is crucial for determining the operational performance of the Zeta converter [9]-[10].

Despite the perceived advantages of the ZETA converter, its practical application is often hindered by the presence of parasitic elements, which can disrupt its operation and efficiency. These elements introduce voltage drops, current losses, and additional dynamics, negatively impacting the converter's efficiency, stability, and overall performance. Therefore, there is a critical need to investigate and improve our understanding of non-ideal ZETA converters and their closed-loop voltage mode control to effectively analyze, optimize, and enhance system performance [11]-[13].

This research aims to thoroughly examine non-ideal ZETA converters and emphasize the importance of employing closed-loop voltage mode control for optimal performance. The evaluation of imperfections in the ZETA converter begins with a comprehensive analysis of parasitic elements, including resistances, inductances, and capacitances within components and interconnections, which introduce additional losses and affect dynamic performance. After assessing the complexities inherent in non-ideal ZETA converters, the study delves into the design and effectiveness of closed-loop voltage mode control. The primary goal of this control mechanism is to manage output voltage effectively while minimizing the impact of parasitic elements. A detailed theoretical framework, comprising mathematical models and analytical methodologies, is examined to support the assessment and enhancement of closed-loop voltage mode control [14]-[17].

The importance of clean energy sources has surged due to the detrimental effects of fossil fuel usage on the environment. In recent times, there has been rapid development in PV system, fuel-cell, and wind-power generating systems. However, these systems often face challenges in providing stable power output. To address this issue, hybrid power systems combining renewable energy sources with batteries have emerged. In such systems, when renewable sources fail to meet the power demand, batteries step in to supply the shortfall. Additionally, these batteries can be used to store excess energy generated. Battery Energy Storage System (BEES) is generally performed as a storage system for energy. Bidirectional DC-DC converters play a crucial role in facilitating power transfer between different DC sources, making them essential components in renewable energy hybrid

power systems, hybrid electric vehicles (HEV), and uninterruptible power supplies (UPS).[18]-[21]

The Bidirectional SEPIC/ZETA converter is used in various applications like EV battery management system, UPS, HVDC transmission, smart grid, etc [22]**.** This paper explores the transfer function by performing converter's mathematical analysis relating the converter's output voltage to the duty cycle of its switches. The focus is on battery charging and discharging operations, with a deep dive into the different modes of the SEPIC/ZETA converter so that battery is charging and discharging with constant current**.** To optimize the performance of the PID controllers, the Ziegler-Nichols method is employed to determine the appropriate values for the proportional (K_p), integral (K_i), and derivative (K_d) gains**.** The proportional component of controllers enhances transient response speed, while the integral component improves steady-state response and diminishes steady-state error. Meanwhile, the derivative component aids transient response and mitigates ripples and overshoots.[23]

1.2 Grid-Integrated Renewable Energy Systems

These systems generate electricity from renewable sources. When linked to the grid, they can either supply surplus energy or draw energy to meet demand. The battery storage system serves as a buffer, storing excess energy during low demand periods and providing it back to the grid during high demand.

Key Components of the System

The system comprises several essential parts:

- Renewable Energy Sources (RES): Includes solar panels and wind turbines, which produce DC or AC power.
- Battery Storage System: Stores excess energy and provides power when needed.
- Bidirectional DC-DC Converter: Manages the flow of electricity between the battery and the grid.
- Inverter: Converts DC from renewable sources and the battery to AC for the grid.
- Grid: The primary electrical network distributing power to consumers.

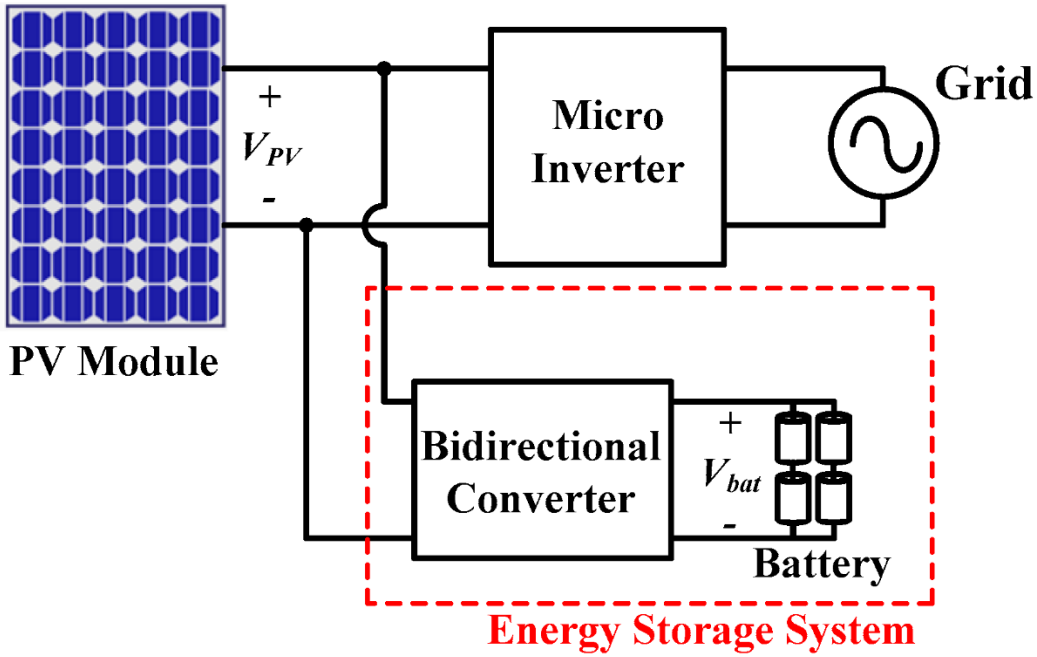

Fig.1. 1Bidirectional Converter in Grid System

1.3 Operational Flow

Energy Generation and Supply

During the daytime, when renewable generation is high and demand is low, the system may produce more electricity than needed. This excess energy is directed towards charging the battery through the bidirectional DC-DC converter. If the battery is fully charged, the surplus energy can be fed into the grid.

Battery Charging

In charging mode, the bidirectional DC-DC converter reduces the voltage from renewable sources to match the battery's charging needs. This ensures efficient and safe charging, preventing overcharging by regulating current and voltage. The converter shifts from grid-connected mode to battery charging when demand is low, optimizing energy flow and storage.

Energy Discharge and Supply

During the evening or night, when renewable generation is low and demand is high, the stored energy in the battery is utilized. The battery discharges to provide additional power to the load. In discharging mode, the bidirectional DC-DC converter increases the battery voltage to match the load or grid voltage requirements, ensuring efficient conversion and supply of stored energy. The converter manages the energy flow from the battery, preventing deep discharging and extending the battery's lifespan.

1.4 Role of the Bidirectional DC-DC Converter

Voltage Regulation

The bidirectional DC-DC converter is crucial in managing voltage levels between the battery and the grid or load. It adjusts the voltage to ensure efficient energy transfer, stepping down the voltage when charging the battery and stepping it up during discharging to match grid or load requirements.

Current Control

This converter plays a key role in controlling the current flow to the battery. It prevents overcharging by regulating the current during the charging process, ensuring the battery is charged safely. Conversely, during discharge, it controls the current to avoid deep discharging, which helps in extending the battery's lifespan.

Power Flow Management

The converter dynamically manages the direction of power flow. During periods of excess energy generation, it directs surplus power to the battery for storage. When energy demand is high, it allows the stored energy to flow from the battery to the grid or load. This bidirectional flow ensures that energy is efficiently stored and utilized as needed.

Efficiency Enhancement

By optimizing the conversion process, the bidirectional DC-DC converter minimizes energy losses, enhancing the overall efficiency of the renewable energy system. It ensures that the maximum amount of generated renewable energy is effectively used or stored, contributing to a more reliable and sustainable energy supply.

1.5 Literature Review

Verma, Singh, and Rao (2013) [24] offers a comprehensive examination of control strategies for DC-DC converters. It categorizes various techniques, highlighting their principles, advantages, and limitations. The paper delves into traditional methods like PWM and modern approaches such as digital control, discussing their application contexts and performance impacts. This review is essential for understanding the evolving landscape of DC-DC converter control methodologies, providing a solid foundation for both theoretical and practical advancements in the field.

Slobodan Cuk and R.D. Middlebrook (2017) [25] detail a novel approach to DC-DC switching converters. This innovation, associated with the California Institute of Technology, introduces a unique topology for power conversion, emphasizing efficiency and performance improvements over existing methods. The document outlines the theoretical framework and practical implementation, highlighting key design principles that address common issues such as voltage regulation and energy loss. This work has significantly influenced the development of modern power electronics by providing a foundational technique widely adopted in various applications.

Middlebrook et al., (2013) [26] presents a comprehensive framework for modeling the power stages of switching converters. Their approach introduced lays the foundation for understanding and designing efficient power conversion systems. By unifying various methods, they offer a versatile tool for analyzing the behavior of different converter topologies. This methodology not only enhances the accuracy of performance predictions but also simplifies the design process, making it a cornerstone reference in the field of power electronics. Their contributions have significantly influenced subsequent research and development in power converter technology.

Cuk and Middlebrook (2014) [27] introduces a novel topology for DC-to-DC

converters, aimed at optimizing performance. The proposed topology addresses key limitations of existing designs, enhancing efficiency, and reducing ripple. The authors provide a comprehensive analysis of the converter's operation, detailing its theoretical foundations and practical implications. Experimental results are presented to validate the theoretical predictions, demonstrating significant improvements over traditional converter designs. This pioneering work has laid the groundwork for numerous advancements in power electronics, highlighting the importance of innovative topological approaches in the development of efficient and reliable DC-to-DC converters.

Niculescu et al. (2009) [28] present a streamlined steady-state analysis of the PWM Zeta converter. This study is documented in the proceedings of the WSEAS International Conference on Mathematics and Computers in Science and Engineering. The authors, Niculescu, Mioara-Purcaru, Niculescu, Purcaru, and Marian, focus on simplifying the analysis method to make it more accessible. Their work addresses the efficiency and practicality of the PWM Zeta converter in various applications, offering insights into its performance. The paper contributes to the field by providing a more straightforward approach to understanding and utilizing this type of power converter.

Niculescu, Purcaru, and Niculescu (2006) [29] presents a comprehensive steady-state analysis of the PWM SEPIC converter. The study is detailed in the proceedings of the 10th WSEAS International Conference on Circuits, offering insights into the converter's behavior under steady-state conditions. The authors employ theoretical and simulation-based approaches to examine the performance and operational efficiency of the SEPIC converter. Key aspects discussed include voltage and current waveforms, as well as the impact of various parameters on converter stability and efficiency. The findings are relevant for optimizing converter design in practical applications.

Adrian Ioinovici (2013) [30] offers an in-depth analysis of the essential principles and mechanisms underlying hard-switching converters. The book meticulously explains the

theoretical foundations, operational dynamics, and practical applications of these converters, highlighting their role in power electronics. Ioinovici delves into various circuit configurations, design considerations, and performance metrics, providing both theoretical insights and practical guidelines. His work is a valuable resource for understanding the complexities of hard-switching converters, serving as a comprehensive reference for students, researchers, and professionals in the field of power electronics.

Wu and Chen's (1998) [31] explores the innovative approach of modeling Pulse Width Modulation (PWM) DC/DC converters using fundamental converter units. The paper delves into the intricacies of PWM converters, emphasizing the significance of a comprehensive model for accurate analysis and design. By synthesizing basic converter units, the authors propose a novel methodology to construct PWM converter models, enhancing understanding and facilitating advancements in converter technology. Their findings underscore the importance of such models in optimizing converter performance and efficiency. Wu and Chen's contribution marks a pivotal advancement in the field of power electronics, offering valuable insights for future research and development endeavors.

Vuthchhay and Bunlaksananusorn (2008) [32] paper focuses on the dynamic modeling of a Zeta converter using the state-space averaging technique. The study provides valuable insights into the behavior of Zeta converters under varying operating conditions. By employing state-space averaging, the authors offer a comprehensive approach to understanding the converter's performance, which is crucial for optimizing its design and control strategies. The paper's contribution lies in its ability to bridge theoretical modeling with practical application, aiding engineers in developing efficient and reliable power electronics systems. This work serves as a significant reference for researchers and practitioners in the field of electrical engineering and power electronics.

J. Kochcha and Sarawut Sujitjorn (2010) [33] delves into the operational principles

and design intricacies of the Isolated Zeta Converter when operating in continuous conduction mode. This study presents a comprehensive analysis of the converter's functioning and provides guidelines for its efficient design. By investigating its operational characteristics and design considerations, the authors contribute valuable insights into the utilization and optimization of the Isolated Zeta Converter, offering a significant resource for researchers and practitioners in the field of power electronics.

Preeja, P., and Kayalvizhi, S.V. (2013) [34] focuses on enhancing the transient response of the Cuk converter by employing Sliding Mode Control (SMC) and Fuzzy Logic Control (FLC) techniques. The Cuk converter is widely used in various applications due to its non-isolated nature and ability to provide a negative output voltage. The authors investigate the effectiveness of SMC and FLC in improving the converter's dynamic response under varying load conditions. Through simulation and experimental validation, they demonstrate significant enhancements in transient response, highlighting the potential of these control strategies for practical implementation in power electronics systems.

Banaei, Reza, and Bonab (2019) [35] introduces a high-efficiency nonisolated buck-boost converter utilizing the ZETA converter architecture. It addresses the demand for energy-efficient power conversion systems. The proposed converter offers advantages such as reduced voltage stress on switches, decreased conduction losses, and improved efficiency. Through detailed analysis and experimental validation, the paper demonstrates the effectiveness of the converter in enhancing efficiency and performance compared to conventional methods. The findings signify a significant contribution to the field of power electronics, offering potential applications in various industrial and commercial sectors.

Kim (2007) [36] introduces a novel bidirectional PWM Sepic/Zeta DC-DC converter design. It addresses the need for efficient energy conversion in bidirectional power flow applications. The converter offers advantages in terms of voltage regulation, power factor correction, and bidirectional power flow control. Kim's design incorporates Pulse Width

Modulation (PWM) techniques, enhancing its performance and versatility. This research contributes to the advancement of power electronics, particularly in renewable energy systems and electric vehicles. By integrating Sepic and Zeta converter topologies, Kim's design demonstrates improved efficiency and reliability in bidirectional power conversion, making it a significant contribution to the field.

N. Gorji et al. (2019) [37] provides a comprehensive overview of topologies and control schemes for bidirectional DC-DC power converters. It discusses various converter designs and their applications, focusing on their ability to efficiently transfer power bidirectionally. The authors highlight the importance of these converters in renewable energy systems, electric vehicles, and energy storage systems. Through a systematic review, they analyze different control strategies employed to regulate voltage and current in both buck and boost modes. The paper serves as a valuable resource for researchers and engineers working in the field of power electronics, offering insights into the latest advancements and trends.

Jain, Daniele, and Jain (2000) [38] a novel bidirectional DC-DC converter topology is proposed for low-power applications. The converter's architecture is designed to efficiently manage power flow bidirectionally, crucial for applications like battery-powered systems and renewable energy sources. Through a comprehensive analysis, the paper demonstrates the converter's effectiveness in achieving high efficiency and low power losses. The topology's practicality and suitability for low-power scenarios make it a significant contribution to the field of power electronics. This work serves as a foundational reference for researchers and engineers working on similar power management systems.

Caricchi et al. (1999) [39] present a significant advancement in electrical vehicle technology. The authors introduce a novel 20kW water-cooled prototype of a buck-boost bidirectional DC-DC converter, aimed at enhancing the efficiency and performance of

electrical vehicle motor drives. Through detailed analysis and experimentation, they demonstrate the feasibility and effectiveness of their proposed topology. This paper contributes valuable insights into the development of high-power converters for electric vehicles, addressing crucial challenges in power electronics and sustainable transportation systems.

Peng et al. (2004) [40] introduce a novel Zero Voltage Switching (ZVS) bidirectional DC-DC converter designed for fuel cell and battery applications. The converter addresses the challenges of efficient energy transfer and reduced switching losses in bidirectional power flow systems. Through detailed analysis and experimental validation, the authors demonstrate the converter's effectiveness in achieving Zero Voltage Switching (ZVS) operation, enhancing efficiency, and minimizing electromagnetic interference. This pioneering work contributes significantly to the advancement of bidirectional power conversion technology, particularly in sustainable energy systems like fuel cells and batteries, offering valuable insights for future research and practical applications in the field of power electronics.

Ma and Lee (2001) [41] proposed a pioneering solution for uninterruptible power supply (UPS) systems with their paper "A Novel Uninterruptible dc-dc Converter for UPS Applications." This work presents a unique dc-dc converter design tailored specifically for UPS applications. By addressing the challenges of uninterrupted power delivery, the authors contribute significantly to the field of industrial applications. Their approach, detailed in IEEE Transactions on Industry Applications, offers insights into enhancing the reliability and efficiency of UPS systems. Through meticulous analysis and experimentation, Ma and Lee offer a promising avenue for improving power supply resilience in critical sectors.

Mittal et al. (2023) [42] introduces a novel approach to optimize the operation of a grid-connected bi-directional electric vehicle (EV) charger using the Nonlinear Autoregressive

with exogenous inputs and Local Model Network (NARLMMN) algorithm. The proposed system integrates solar photovoltaic (PV) arrays to harness renewable energy for EV charging, enhancing sustainability. By employing NARLMMN, the charger's control mechanism achieves efficient power management, ensuring optimal utilization of available energy resources while maintaining grid stability. This research contributes to the advancement of smart grid technology by addressing challenges related to EV integration and renewable energy utilization within the grid framework.

Mittal et al. (2022) [43] explores Electric Vehicle (EV) control in both Grid-to-Vehicle (G2V) and Vehicle-to-Grid (V2G) modes using a Second Order Generalized Integrator (SOGI) controller. With the increasing integration of EVs into the grid, effective control mechanisms are crucial for optimizing energy flow. The SOGI controller offers advantages in terms of robustness and efficiency in controlling power flow between the grid and EVs. The study likely provides insights into enhancing grid stability, energy management, and overall efficiency in EV-grid integration, which are critical for the sustainable development of smart grids.

Sable, Lee, and Cho (2011) [44] present a pivotal advancement in battery charging technology with their paper, "A Zero-Voltage-Switching Bidirectional Battery Charger/Discharger for the NASA EOS Satellite." Their innovative design mitigates switching losses and enhances efficiency by achieving zero-voltage switching. The study demonstrates a bidirectional charger/discharger, critical for satellite applications where energy management is paramount. By focusing on NASA's EOS satellite, the authors highlight the practical implications of their work in space exploration. This paper serves as a cornerstone for future research in efficient and reliable energy systems, particularly in the demanding conditions of space missions.

1.6 Research Objective

This research aims to comprehensively explore Zeta converters, encompassing theoretical

and practical dimensions. Its primary objectives include evaluating control strategies, specifically Voltage Mode Control (VMC) and Current Mode Control (CMC), to ascertain their comparative effectiveness in regulating Zeta converters. Furthermore, the study seeks to analyze the influence of parasitic elements on the performance of non-ideal Zeta converters, focusing on factors such as resistance in inductor windings, equivalent series resistance (ESR) in capacitors, and losses in switches and diodes. Additionally, the research endeavors to validate the practical viability of bidirectional SEPIC/ZETA DC-DC converters, particularly in the context of energy storage systems.

The overarching goal is to advance the understanding and refinement of control techniques for Zeta converters, thereby enhancing their robustness, efficiency, and stability across diverse applications. By addressing theoretical complexities, investigating practical challenges, and demonstrating real-world applications, this research contributes to the ongoing development of Zeta converters, facilitating their broader adoption and utility in various fields such as battery energy storage, motor drives, power factor correction, and solar power systems. Ultimately, the research outcomes are expected to inform the design and implementation of more reliable and efficient Zeta converter systems, thereby supporting the advancement of sustainable energy technologies and power system management practices.

1.7 Thesis Organization

The structure of the Thesis is arranged as follows:

Chapter 1: In this chapter, the reader is introduced to general overview of ZETA Converter and is provided with its application like Bidirectional Converter and discussed about the role of bidirectional converter in grid system. Additionally, the chapter address the literature survey and research objective.

Chapter 2: In this chapter, we explore small signal analysis, steady-state analysis, and control technique design for Ideal Zeta converters. By implementing voltage mode control, we achieve a constant output voltage (CV) despite variations in load and line conditions, while current mode control ensures a consistent output current (CC). These insights underscore the Ideal Zeta converter's effectiveness in maintaining stable performance under varying conditions, highlighting significant advancements in power electronics.

Chapter 3: In this chapter, we model the non-ideal ZETA converter and design a controller to maintain a constant output voltage amid load and line variations. We analyze the impact of parasitic components on the converter's performance and emphasize the importance of closed-loop voltage mode control. By comparing the non-ideal and ideal ZETA converters in both open and closed-loop configurations, we highlight the necessity of advanced control techniques for optimal performance and reliability.

Chapter 4: This chapter models the Bidirectional SEPIC/ZETA converter and designs a control system to ensure constant current for battery charging and discharging, crucial for applications like EV battery management and smart grids. By analyzing SEPIC and ZETA modes and optimizing PI controllers using the Ziegler-Nichols method, we achieve efficient and stable battery management with a constant current, enhancing transient response and reducing steady-state error.

Chapter 5: In this chapter, the contribution of this thesis is summarized and the potential for future research opportunities is highlighted.

CHAPTER 2
MODELLING AND ANALYSIS OF IDEAL ZETA CONVERTER

2.1 Introduction

Zeta converters have emerged as a focal point in power electronic research due to their unique ability to execute dual voltage steps, boost and buck, while generating a non-inverted output. It utilizes a combination of both series and parallel switching to regulate the output voltage.

Belonging to the buck-boost family, Zeta converters offer efficient solutions for applications requiring both step-up and step-down capabilities. Their distinctive architectural design provides advantages such as reduced electromagnetic interference, decreased output ripple, expanded input voltage range, and impressive efficiency ranging from 90 to 95 percent. Affordable and versatile, Zeta converters find applications in bidirectional power flow, renewable energy systems, power factor correction, electric vehicles, and portable electronics.

Similar to the SEPIC converter, the Zeta converter is not affected by the polarity reversal issue. Moreover, the Zeta topology's uniform output current permits the use of smaller capacitors, which enhances load performance, in addition to its low output voltage ripple, which makes output regulation easier. Because of these characteristics, the Zeta converter is a better option when output power and voltage quality are important. However, the Zeta converter has the same problem as the Buck-Boost converter: a discontinuous input current, which can negatively impact MPPT performance. The fact that the control terminal on this converter is not grounded is another crucial issue that needs to be taken into account. Consequently, a sophisticated high side switch driver circuit is needed.

Real-Life Applications of ZETA Converter

1. **Solar Power System**: ZETA converters are used in solar power systems to efficiently convert the varying output voltage of solar panels to a stable voltage suitable for charging batteries or connecting to the grid.
2. **Grid-Tied Inverters**: In grid-tied inverters, ZETA converters facilitate the conversion of DC power from renewable energy sources (such as solar or wind) into AC power that can be fed into the grid.
3. **Electric Vehicle Charging Infrastructure**: ZETA converters play a role in electric vehicle charging stations, converting AC power from the grid to DC power suitable for charging vehicle batteries, and vice versa.
4. **Battery Management Systems (BMS)**: They are employed in BMS to manage the charging and discharging of batteries efficiently, ensuring optimal performance and longevity.

To ensure operational stability, it is imperative to have a thorough insight into the behavior of Ideal Zeta converters under different conditions. Small signal analysis proves highly advantageous in modeling dynamic characteristics around an operating point, enabling a comprehensive understanding of stability and transient response in the presence of disturbances and variations.

This chapter's primary aim is a comprehensive investigation into small signal analysis, steady-state analysis, and control technique design specific to Ideal Zeta converters. Evaluating the small signal model and understanding steady state conditions are crucial for shedding light on the operational dynamics and system performance implications of Ideal Zeta converters, contributing valuable insights to the field of power electronics.

2.2 Circuit Description

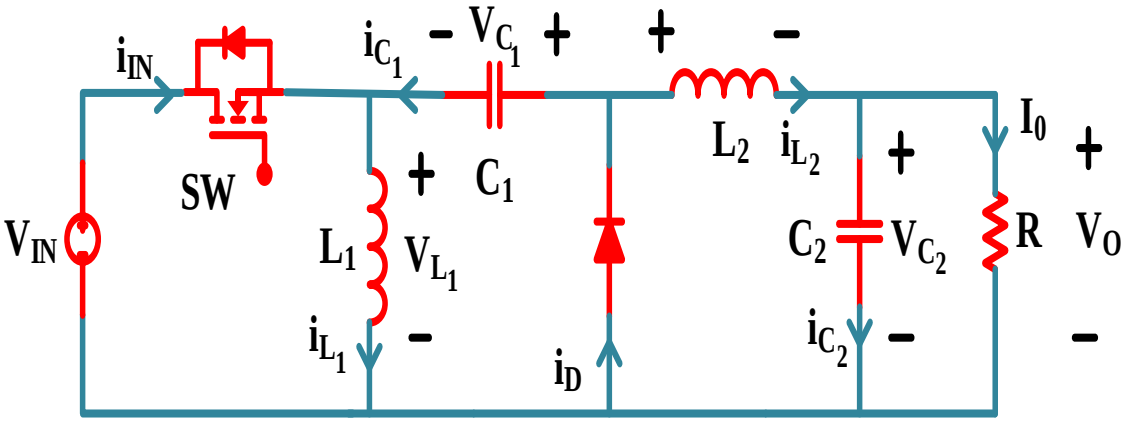

Fig.2. 1. Ideal ZETA converter circuit diagram

The Zeta converter, characterized by a non-linear fourth-order configuration because it has two capacitors and two inductors, belongs to the category of DC-DC converters designed to effectively modulate the output voltage in either an upward or downward direction. This converter is specifically categorized as a non-isolated type, signifying that there is a shared ground connection between the input and output voltages. Comprising two inductors ($\boldsymbol{L_1, L_2}$), two capacitors ($\boldsymbol{C_1, C_2}$), and a switch (**SW**), the Zeta converter's configuration is illustrated in Fig.2.1.

The Zeta converter is a non-isolated DC-DC converter that combines characteristics of both the buck and boost converters. It is called as Inverted SEPIC Converter because the inductor in the output stage replaced by a capacitor. This arrangement allows the Zeta converter to achieve a lower output ripple than the SEPIC converter.

2.3 Modes Of Operation

ZETA Converter has one switch and one diode which makes two switching states possible for operation.

Mode 1 [Switch SW is closed]:

In mode 1 Switch is closed as shown in Fig.2.2. When SW is On, the diode will be in

OFF state. The source voltage appears across the inductor $\boldsymbol{L_1}$ and causes its current to increase linearly, while the inductor $\boldsymbol{L_2}$ begins to store energy from the series capacitor via $\boldsymbol{C_1}$ the load which causes $\boldsymbol{i_{L_1}}$ and $\boldsymbol{i_{L_2}}$ to increase linearly.

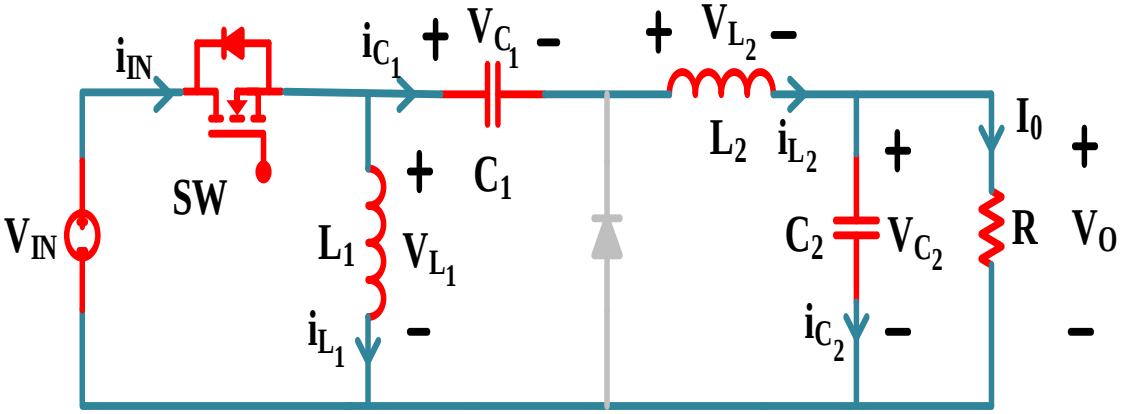

Fig.2. 2. Schematic diagram of Zeta converter in Mode 1 (SW is ON)

$$V_{IN} = V_{L_1} \tag{2.1}$$

$$i_{C_1} = -i_{L_2} \tag{2.2}$$

$$V_{L_2} = V_s + V_{C_1} - V_0 \tag{2.3}$$

$$i_{C_2} = i_{L_2} - i_0 \tag{2.4}$$

Mode 2 [Switch SW is Open]:

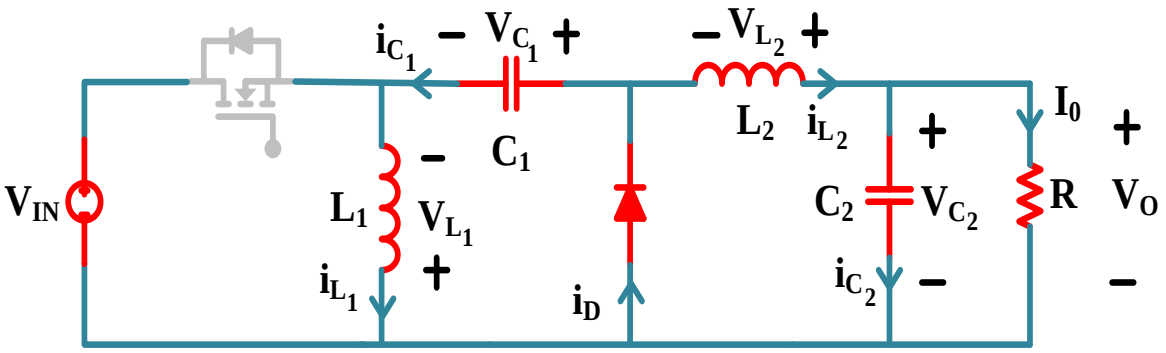

Fig.2. 3. Schematic diagram of Zeta converter in Mode 2 (SW is OFF)

In mode 2 Switch is open as shown in Fig.2.3. When SW is OFF, the diode will be in ON state. Inductor L_1 charges the capacitor C_1 in series, and Inductor L_2 provides the output power, or discharges through the load which causes i_{L_1} and i_{L_2} to decrease linearly. This is how the Zeta converter operates and its output current is continuous.

$$V_{L_1} = -V_{C_1} \tag{2.5}$$

$$i_{C_1} = i_{L_1} \tag{2.6}$$

$$V_{L_2} = -V_0 \tag{2.7}$$

$$i_{C_2} = i_{L_2} - i_0 \tag{2.8}$$

2.4 Circuit Parameters Expressions

Unlike buck boost and Cuk converters, ZETA converter has same polarity as source polarity, and this can be either higher or lower than the input voltage depending upon the duty cycle of the PWM given to the MOSFET switch. The expression relating the input (V_{IN}) and the output (V_O) voltages is evaluated using Volt-sec balance where D denotes the duty cycle.

Volt- Sec Balance:

The average voltage across the inductor over one period is always zero that is called

Volt-Sec Balance.

$$avg[v_L(t)] = V_L = \frac{1}{T}\int_{t_0}^{t_0+T} v_L(t)dt = 0 \tag{2.9}$$

Applying Volt-Sec Balance across Inductor L_1:

$$V_S * D * T_S - V_{C_1} * (1-D) * T_S = 0 \tag{2.10}$$

$$V_S * D * T_S = V_{C_1} * (1-D) * T_S \tag{2.11}$$

$$V_{C_1} = D * \frac{V_S}{1-D} \tag{2.12}$$

Applying Volt-Sec Balance across Inductor L_2:

$$\left(V_S + V_{C_1} - V_0\right) * D * T_S - V_0 * (1-D) * T_S = 0 \tag{2.13}$$

Put the value of V_{C_1} from eq.2.12 in eq.2.13 then we get

$$V_0 = D * \frac{V_S}{1-D} \tag{2.14}$$

Input Current(I_{IN}):

To compute the steady state value of input current I_{IN} power balance is required to pply.

Applying Power Balance:

$$P_{IN} = P_{OUT} \tag{2.15}$$

$$V_{IN} * I_{IN} = V_0 * I_0 \tag{2.16}$$

Put the value of V_0 from eq.2.14 in eq.2.16 then we get

$$V_{IN} * I_{IN} = V_{IN} * \frac{D}{1-D} * I_0 \tag{2.17}$$

$$I_{IN} = D * \frac{I_0}{1-D} \tag{2.18}$$

Inductor Current(I_{L_2}):

Inductor current is evaluated by utilizing Amp- Sec Balance.

Amp-Sec Balance: The average current through the capacitor over one period is always Zero that is called Amp- Sec Balance.

$$avg[i_C(t)] = I_C = \frac{1}{T}\int_{t_0}^{t_0+T} i_C(t)dt = 0 \tag{2.19}$$

Applying nodal at the output node we get

$$I_{L_2} - I_{C_2} - I_0 = 0 \tag{2.20}$$

By Amp -Sec Balance we can say $I_{C_2} = 0$ So above equation be like

$$I_{L_2} = I_0 \tag{2.21}$$

Inductor Current($\mathbf{I_{L_1}}$):

Amp-Sec Balance on Capacitor 1 (C_1):

$$-I_{L_1} * D * T_S + I_{L_1} * (1 - D) * T_S = 0 \tag{2.22}$$

$$I_{L_1} = I_{L_2} * \frac{D}{1 - D} \tag{2.23}$$

Put the value of I_{L_2} from eq. 2.22 in eq. 2.24 then we get

$$I_{L_1} = I_0 * \frac{D}{1 - D} \tag{2.24}$$

$$I_{L_1} = I_{IN} \tag{2.25}$$

Inductor Value($\mathbf{L_1}$):

For inductor value Volt Sec Balance is applied for any mode either on or off. Here for on mode is applied.

$$L_1 * \frac{di_{L_1}}{dt} = V_{L_1} \tag{2.26}$$

$$L_1 * \frac{\Delta I_{L_1}}{D * T_S} = V_{IN} \tag{2.27}$$

$$L_1 = D * \frac{V_{IN}}{\Delta I_{L_1} * f_{SW}} \tag{2.28}$$

$$L_1 = V_0 * \frac{(1 - D)}{\Delta I_{L_1} * f_{SW}} \tag{2.29}$$

$$L_1 = I_0 * R * \frac{1-D}{\Delta I_{L_1} * f_{SW}} \tag{2.30}$$

$$L_1 = R * \frac{(1-D)^2}{D * f_{SW} * \left(\frac{\Delta I_{L_1}}{I_{L_1}}\right)} \tag{2.31}$$

Inductor Value($\mathbf{L_2}$):

Similarly, as inductor (L_1) value Volt-Sec Balance is applied for either on or off mode. Here for on mode is applied.

$$L_2 * \frac{di_{L_2}}{dt} = V_{L_2} \tag{2.32}$$

$$L_2 * \frac{\Delta I_{L_2}}{(1-D) * T_S} = V_0 \tag{2.33}$$

$$L_2 = (1-D) * \frac{V_0}{\Delta I_{L_2} * f_{SW}} \tag{2.34}$$

$$L_2 = (1-D) * \frac{I_0 * R}{\Delta I_{L_2} * f_{SW}} \tag{2.35}$$

$$L_2 = (1-D) * \frac{I_{L_2} * R}{\Delta I_{L_2} * f_{SW}} \tag{2.36}$$

$$L_2 = (1-D) * \frac{R}{\left(\frac{\Delta I_{L_2}}{I_{L_2}}\right) * f_{SW}} \tag{2.37}$$

Capacitor Value($\mathbf{C_1}$):

For capacitor value Amp-Sec Balance is applied for any mode either on or off. Here for on mode is applied.

$$C_1 * \frac{\Delta V_{C_1}}{D * T_S} = I_{C_1} \tag{2.38}$$

$$C_1 * \frac{\Delta V_{C_1}}{D * T_S} = I_0 \tag{2.39}$$

$$C_1 = I_0 * \frac{D}{f_{SW} * \Delta V_{C_1}} \tag{2.40}$$

$$C_1 = \frac{V_0}{R} * \frac{D}{f_{SW} * \Delta V_{C_1}} \quad (2.41)$$

$$C_1 = \frac{V_{C_1}}{R} * \frac{D}{f_{SW} * \Delta V_{C_1}} \quad (2.42)$$

$$C_1 = \frac{D}{R * f_{SW} * \left(\frac{\Delta V_{C_1}}{V_{C_1}}\right)} \quad (2.43)$$

Capacitor Value(C_2):

Similarly, as capacitor (C_1) value Amp-Sec Balance is applied for either on or off mode. Here for on mode is applied.

$$C_2 * \frac{dV_0}{dt} = I_{C_2} \quad (2.44)$$

$$C_2 * dV_0 = I_{C_2} * dt \quad (2.45)$$

$$C_2 * dV_0 = \Delta Q \quad (2.46)$$

From graph of i_{C_2} we can say ΔQ will be

$$\Delta Q = \frac{1}{2} * \frac{T_S}{2} * \frac{\Delta I_{L_2}}{2} \quad (2.47)$$

Put the value of ΔQ from eq. 2.47 in eq. 2.48 then we get

$$C_2 * dV_0 = \frac{1}{2} * \frac{T_S}{2} * \frac{\Delta I_{L_2}}{2} \quad (2.48)$$

$$C_2 = \frac{T_S}{8} * \frac{\Delta I_{L_2}}{\Delta V_0} \quad (2.49)$$

Put the value of ΔI_{L_2} from eq.2.34 in eq.2.50 then we get

$$C_2 = \frac{(1-D)}{8 * f_{SW}^2 * \left(\frac{\Delta V_0}{V_0}\right) * L_2} \quad (2.50)$$

Waveforms Of Zeta Converter in CCM Mode:

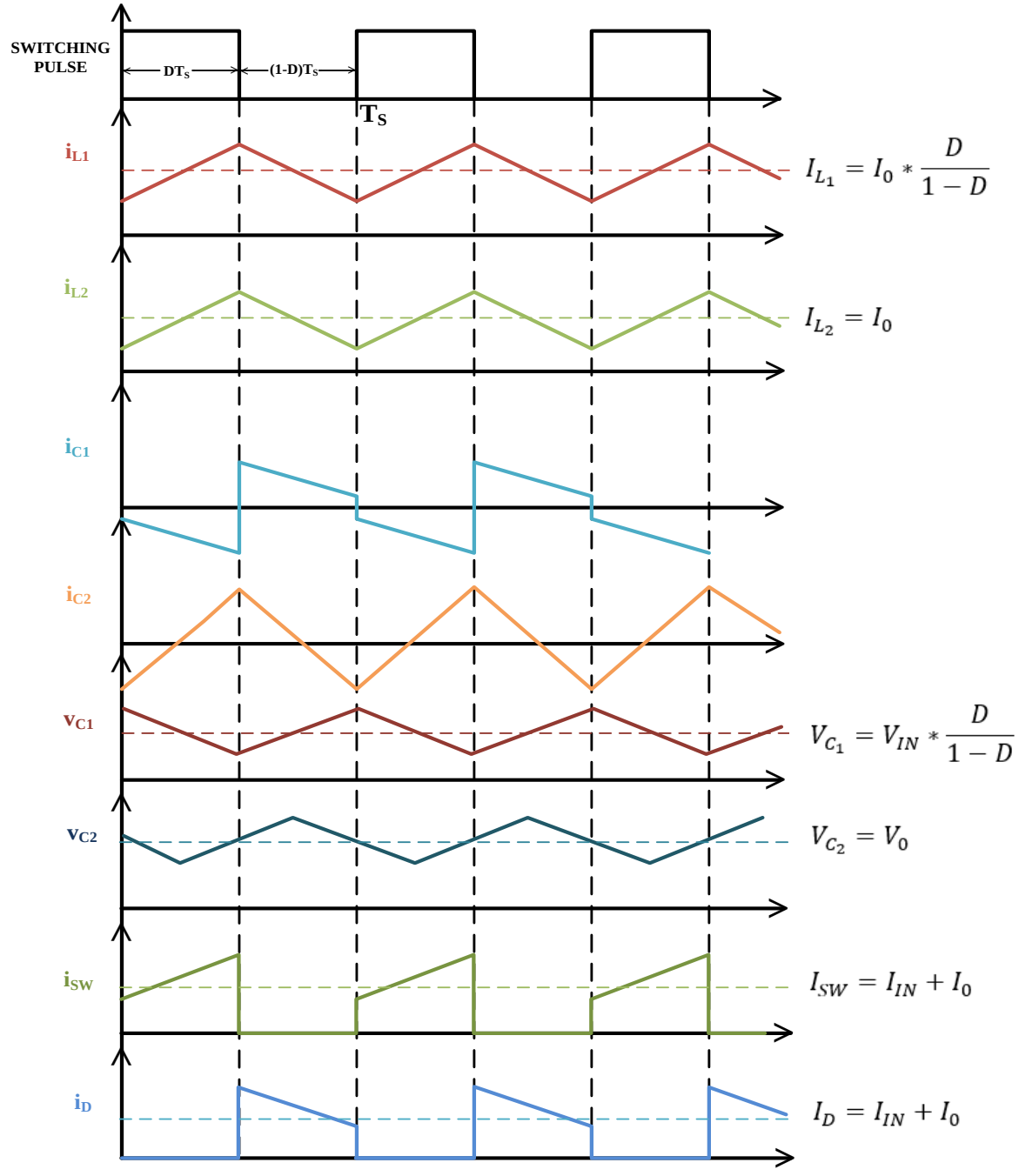

Fig.2. 4. Waveforms of ZETA Converter parameters

2.5 Circuit Parameter Calculation

Considering the input voltage $V_{IN} = 48V$, the output voltage $V_0 = 12V$, the switching frequency $f_{SW} = 50KHz$, output power $P_0 = 24W$, the ripple current in inductors($\Delta i_{L_1}, \Delta i_{L_2}$) and ripple in capacitor voltage ($\Delta V_{C_1}, \Delta V_{C_2}$) to be 5%.

Duty Cycle:

By using eq. 2.14

$$V_0 = D * \frac{V_S}{1 - D}$$

$$12 = D * \frac{48}{1 - D}$$

$$D = 0.2$$

Input Current($\mathbf{I_{IN}}$):

By using eq. 2.18

$$I_{IN} = D * \frac{I_0}{1 - D}$$

$$I_{IN} = 0.2 * \frac{(\frac{P_0}{V_0})}{1 - 0.2}$$

$$I_{IN} = 0.2 * \frac{(\frac{24}{12})}{0.8}$$

$$I_{IN} = 0.5A$$

Inductor Current ($\mathbf{I_{L_1}}$):

By using eq. 2.25

$$I_{L_1} = I_{IN}$$

$$I_{L_1} = 0.5A$$

Inductor Current $(\mathbf{I_{L_2}})$:

By using eq. 2.21

$$I_{L_2} = I_0$$

$$I_{L_2} = \frac{P_0}{V_0}$$

$$I_{L_2} = \frac{24}{12}$$

$$I_{L_2} = 2A$$

Inductor Value $(\mathbf{L_1})$:

By using eq. 2.31

$$L_1 = R * \frac{(1-D)^2}{D * f_{SW} * \left(\frac{\Delta I_{L_1}}{I_{L_1}}\right)}$$

$$L_1 = \frac{V_0}{I_0} * \frac{(1-D)^2}{D * f_{SW} * \left(\frac{\Delta I_{L_1}}{I_{L_1}}\right)}$$

$$L_1 = \frac{12}{2} * \frac{(1-0.2)^2}{0.2 * 50X10^3 * (0.05)}$$

$$L_1 = 7.68mH$$

Inductor Value$(\mathbf{L_2})$:

By using eq. 2.37

$$L_2 = (1-D) * \frac{R}{\left(\frac{\Delta I_{L_2}}{I_{L_2}}\right) * f_{SW}}$$

$$L_2 = (1-0.2) * \frac{(\frac{12}{2})}{(0.05) * 50X10^3}$$

$$L_2 = 1.92mH$$

Capacitor Value(C_1):

By using eq. 2.43

$$C_1 = \frac{D}{R * f_{SW} * \left(\frac{\Delta V_{C_1}}{V_{C_1}}\right)}$$

$$C_1 = \frac{0.2}{\frac{12}{2} * 50X10^3 * (0.05)}$$

$$C_1 = 13.33uF$$

Capacitor Value(C_2):

By using eq. 2.50

$$C_2 = \frac{(1-D)}{8 * f_{SW}^2 * \left(\frac{\Delta V_0}{V_0}\right) * L_2}$$

$$C_2 = \frac{(1-0.2)}{8 * (50X10^3)^2 * (0.05) * 1.92X10^{-3}}$$

$$C_2 = 0.4166uF$$

Table 2. 1 Parameters specification of Zeta converter

Parameter	Symbol	Values
Input Voltage	V_{IN}	48V
Output Voltage	V_0	12V
Duty Cycle	D	0.2
Switching Frequency	f_{SW}	50kHz
Output Power	P_0	24W
Inductor 1	L_1	7.68mH
Inductor 2	L_2	1.92mH
Inductor 1 current	I_{L_1}	0.5A
Inductor 2 current	I_{L_2}	2A
Ripple in inductors	$\Delta i_{L_1}, \Delta i_{L_2}$	$(5\%\ I_{L_1}, 5\% I_{L_2})$
Capacitor 1	C_1	13.33µF
Capacitor 2	C_2	0.4166µF
Ripple in capacitors	$\Delta V_{C_1}, \Delta V_{C_2}$	$(5\%\ V_{C_1}, 5\% V_{C_2})$

Waveforms of MATLAB Simulation Results with Specified Values:

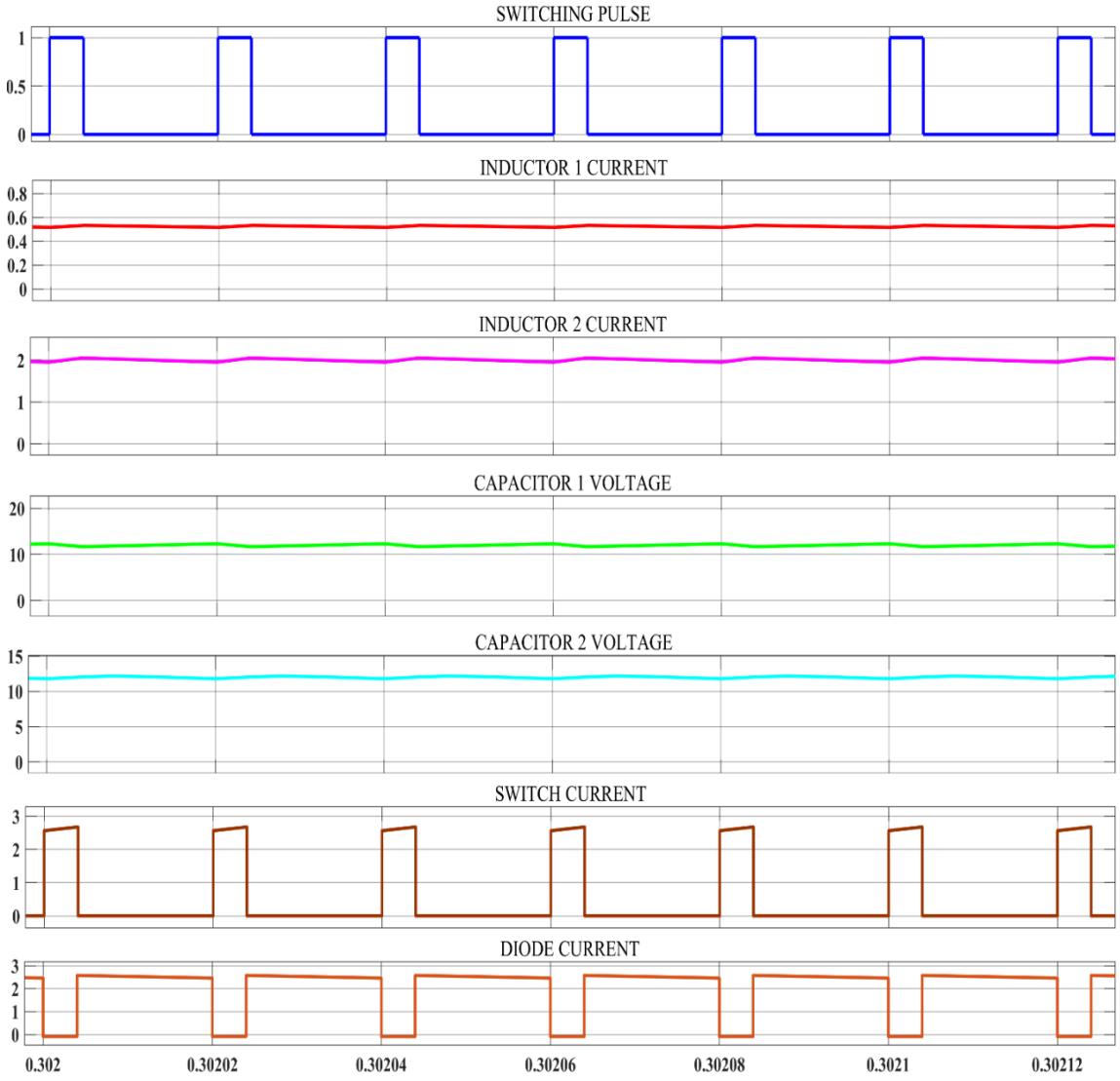

Fig.2. 5. Simulation Results with specified values

2.6 Small Signal and State Space Analysis

Small Signal Analysis is a key tool in the design and optimization of DC-DC converters, providing valuable insights into stability, transient response, and frequency characteristics. This analysis is crucial for ensuring the reliability and efficiency of the converters in various applications.

STEPS FOR SMALL SIGNAL ANALYSIS:

Identify The Operation Point

- Determine the steady-state operating point for the system. This is the nominal condition around which small signal analysis will be performed.

Averaging

- Classify system variables into fast and slow components based on their rates of change.
- Use averaging to eliminate fast variations and simplify the representation of the system.
- For periodic systems, apply time averaging to remove high-frequency components.
- Derive equations that describe the slow variations of the system.

Perturbation and linearization

- Identify variables representing small perturbations from the operating point.
- Linearize the system equations around the operating point, expressing them in terms of perturbation variables.
- Substitute perturbation variables into the linearized equations.
- Solve the resulting perturbation equations to obtain the relationship between perturbations in input and output.

Determine Transfer Function

- Identify transfer functions that relate small signal input variations to the corresponding small signal output variations.

In order to examine the small-signal characteristics of the converter, a small-signal model is developed using state space representation, which is obtained from the circuit equations.

The state variables of the Zeta converter are considered as inductor currents (i_{L_1}, i_{L_2}) and capacitor voltages (V_{C_1}, V_{C_2}), in this research paper. The controlled input variable is the input voltage, while the output variable is the output voltage. The Zeta converter is defined by the following equations:

$$x = \begin{bmatrix} i_{L_1} \\ i_{L_2} \\ V_{C_1} \\ V_{C_2} \end{bmatrix}, u = [V_{IN}], y = [V_0] \tag{2.51}$$

The state space representation of the system is described by the generalized set of equations:

$$\dot{x} = AX + BU \tag{2.52}$$

$$y = CX + EU \tag{2.53}$$

where the state matrix is denoted by A, the input matrix is denoted by B, the output matrix is denoted by C, and the input output coupling matrix is denoted by E.

State Space Equations:

The state space equations of the ZETA converter in mode 1 are as follows:

$$\frac{di_{L_1}}{dt} = \frac{V_{IN}}{L_1} \tag{2.54}$$

$$\frac{di_{L_2}}{dt} = \frac{V_{IN} + V_{C_1} - V_{C_2}}{L_2} \tag{2.55}$$

$$\frac{dV_{C_1}}{dt} = -\frac{i_{L_2}}{C_1} \tag{2.56}$$

$$\frac{dV_{C_2}}{dt} = \frac{i_{L_2}}{C_2} - \frac{V_{C_2}}{RC_2} \tag{2.57}$$

$$V_0 = V_{C_2} \tag{2.58}$$

$$\begin{bmatrix} \frac{di_{L_1}}{dt} \\ \frac{di_{L_2}}{dt} \\ \frac{dV_{C_1}}{dt} \\ \frac{dV_{C_2}}{dt} \end{bmatrix} = \begin{bmatrix} 0 & 0 & 0 & 0 \\ 0 & 0 & \frac{1}{L_2} & -\frac{1}{L_2} \\ 0 & -\frac{1}{C_1} & 0 & 0 \\ 0 & \frac{1}{C_2} & 0 & -\frac{1}{RC_2} \end{bmatrix} \begin{bmatrix} i_{L_1} \\ i_{L_2} \\ V_{C_1} \\ V_{C_2} \end{bmatrix} + \begin{bmatrix} \frac{1}{L_1} \\ \frac{1}{L_2} \\ 0 \\ 0 \end{bmatrix} [V_{IN}] \tag{2.59}$$

$$[V_0] = [0 \quad 0 \quad 0 \quad 1] \begin{bmatrix} i_{L_1} \\ i_{L_2} \\ V_{C_1} \\ V_{C_2} \end{bmatrix} + [0][V_{IN}] \tag{2.60}$$

$$\frac{di_{L_1}}{dt} = -\frac{V_{C_1}}{L_1} \tag{2.61}$$

$$\frac{di_{L_2}}{dt} = -\frac{V_{C_2}}{L_2} \tag{2.62}$$

$$\frac{dV_{C_1}}{dt} = \frac{i_{L_1}}{C_1} \tag{2.63}$$

$$\frac{dV_{C_2}}{dt} = \frac{i_{L_2}}{C_2} - \frac{V_{C_2}}{RC_2} \tag{2.64}$$

$$V_0 = V_{C_2} \tag{2.65}$$

$$\begin{bmatrix} \frac{di_{L_1}}{dt} \\ \frac{di_{L_2}}{dt} \\ \frac{dV_{C_1}}{dt} \\ \frac{dV_{C_2}}{dt} \end{bmatrix} = \begin{bmatrix} 0 & 0 & -\frac{1}{L_1} & 0 \\ 0 & 0 & 0 & -\frac{1}{L_2} \\ \frac{1}{C_1} & 0 & 0 & 0 \\ 0 & \frac{1}{C_2} & 0 & -\frac{1}{RC_2} \end{bmatrix} \begin{bmatrix} i_{L_1} \\ i_{L_2} \\ V_{C_1} \\ V_{C_2} \end{bmatrix} + \begin{bmatrix} 0 \\ 0 \\ 0 \\ 0 \end{bmatrix} [V_{IN}] \tag{2.66}$$

$$[V_0] = [0 \quad 0 \quad 0 \quad 1]\begin{bmatrix} i_{L_1} \\ i_{L_2} \\ V_{C_1} \\ V_{C_2} \end{bmatrix} + [0][V_{IN}] \tag{2.67}$$

The state space equations of the ZETA converter in mode 2 are as follows:

Averaging over one switching period is performed to remove the switching ripple component from the circuit calculations. Averaging these equations over one switching period yields the averaged switching model.

$$A = A_1 d + A_2(1-d) \tag{2.68}$$

$$B = B_1 d + B_2(1-d) \tag{2.69}$$

$$C = C_1 d + C_2(1-d) \tag{2.70}$$

$$E = E_1 d + E_2(1-d) \tag{2.71}$$

The nonlinear averaged state-space model must be linearized around an operational point before the small-signal model of Zeta converter can be derived. To do this, perturbations are made to the system's state variables, input variables, and parameters. Perturbations refer to small disturbances or changes introduced into these component values, which can lead to significant effects on the overall behaviour and performance of the system.

$$d = D + \hat{d} \tag{2.72}$$

$$x = X + \hat{x} \tag{2.73}$$

$$u = U + \hat{u} \tag{2.74}$$

$$y = Y + \hat{y} \tag{2.75}$$

Now, substituting the perturbed variables into the averaged state space model and assuming that steady state terms are zero and the effect of higher order terms is neglected. We get the linearized small signal model is obtained as follows:

$$s\hat{x}(s) = A\hat{x}(s) + B\hat{u}(s) + ((A_1 - A_2)X(s) + (B_1 - B_2)U(s))\hat{d}(s) \tag{2.76}$$

$$\hat{y}(s) = C\hat{x}(s) + E\hat{u}(s) + ((A_1 - A_2)X(s) + (E_1 - E_2)U(s))\hat{d}(s) \tag{2.77}$$

$$\frac{\hat{x}(s)}{\hat{d}(s)} = (sI - A)^{-1}((A_1 - A_2)X(s) + (B_1 - B_2)U(s)) \quad (2.78)$$

Using above Equation, the output-to-control transfer function can be obtained by substituting the values of the parameters from Table 2.1.

$$\frac{\widehat{v_0}(s)}{\hat{d}(s)} = \frac{7.501e10\, s^2 - 4.689e13\, s + 5.862e17}{s^4 + 4.001e05\, s^3 + 1.258e09\, s^2 + 3.126e12\, s + 7.816e15} \quad (2.79)$$

$$\frac{\widehat{i_0}(s)}{\hat{d}(s)} = \frac{3.125e04\, s^3 + 1.248e10\, s^2 - 7.572e12\, s + 9.77e16}{s^4 + 4.001e05\, s^3 + 1.258e09\, s^2 + 3.126e12\, s + 7.816e15} \quad (2.80)$$

2.7 Basics Of Control Systems

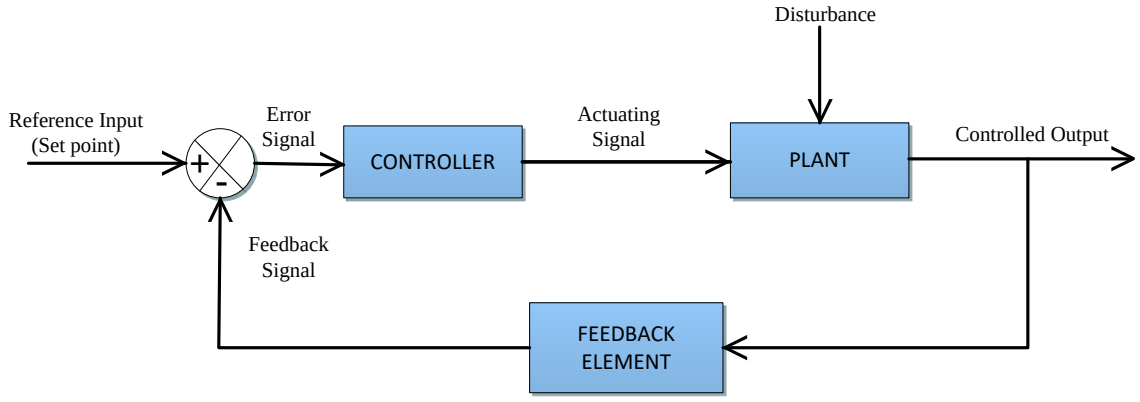

Fig.2. 6. Basic Block Diagram of Control System.

What Is Control System?

A control system is an arrangement of physical components designed to manage, command, direct, or regulate the behavior of other devices or systems. Its primary function is to ensure that the system behaves in a desired manner by manipulating its inputs based on feedback or predefined rules.

Components Of Control System

1. **Reference Input (Set point):** The desired value that the system aims to achieve. This is the target condition or the goal for the system, such as a specific temperature, speed, or position.

2. **Controller:** The device or algorithm that determines the necessary action to achieve the desired output. It compares the actual output with the input and computes an error signal, which is used to generate a control signal.
3. **Plant (Process):** The part of the system that performs the actual task and produces the output. This is the system being controlled, such as a heating system, motor, or any machinery.
4. **Output:** The actual value or behavior of the system after the control action has been applied. This is what is measured and fed back to the controller.
5. **Feedback:** The mechanism that measures the actual output and sends it back to the controller to compare with the desired setpoint. Feedback is essential for adjusting the control actions in real time

Types Of Control System

1. **Open Loop Control System:**

An open loop control system is one where the control action is not dependent on the output. There is no feedback to adjust the input based on the output, meaning the system cannot correct any errors or disturbances on its own.

Characteristics of Open Loop Systems:

- Simplicity and ease of design.
- Cost-effective and easy to implement.
- Lack of feedback means they are less accurate.
- Cannot correct errors automatically.

2. **Closed Loop Control System:**

A closed loop control system, also known as a feedback control system, uses feedback to compare the actual output with the desired output. The system adjusts the control actions based on the difference (error) between the actual output and the setpoint.

Characteristics of Closed Loop Systems:

- More accurate and reliable due to the feedback mechanism.

- Capable of correcting errors and compensating for disturbances.
- More complex and generally more expensive than open loop systems.
- Dynamic response can be tuned for optimal performance.

Difference Between Open Loop and Closed Loop Control System

Features	**Open Loop Control System**	**Closed Loop Control System**
Feedback	Not used	Used
Complexity	Simple	Complex
Accuracy	Generally, less accurate	Generally, more accurate
Response to disturbances	No automatic response	Automatic correction
Rise Time	Less	More
Settling Time	More	Less
Peak overshoot	High	Low
Cost	Generally lower	Generally higher
Examples	Toaster, Washing Machine	Thermostat-controlled HVAC, cruise control in cars.

2.8 Control Strategies

The Zeta converter is examined and evaluated in continuous conduction mode (CCM) and design of a closed-loop control mechanism for both voltage and current modes is discussed in this section. The transfer functions of the Zeta converter have been determined in Eq.2.80 and Eq.2.81, and a PID controller has been constructed for both the voltage and current loops. The efficacy of the closed-loop voltage and current mode control system is assessed by simulations conducted using MATLAB/Simulink.

2.8.1 Voltage Mode Control:

The Zeta converter, a non-linear system, is susceptible to variations in the input voltage, load current, and various external factors. Hence, the implementation of a closed-loop control system becomes imperative in order to effectively regulate the output voltage of the Zeta converter. In the absence of a closed-loop control system, it is observed that the output voltage exhibits fluctuations, thereby posing a potential risk of detrimental consequences to both the load and the converter.

The closed-loop voltage mode control technique is employed to effectively regulate the output voltage of the Zeta converter. This control method operates by dynamically adjusting the duty cycle of the converter in response to the error signal, which represents the discrepancy between the desired output voltage and the actual output voltage. By continuously monitoring and adapting the duty cycle, the closed-loop voltage mode control ensures that the Zeta converter maintains a stable and accurate output voltage as shown in fig.2.7. The closed-loop control system is widely recognised for its ability to deliver exceptional output voltage regulation and rapid transient response, rendering it highly suitable for a diverse range of applications necessitating bidirectional power flow.

The transfer function of PID controller is given as:

$$T_C(s) = K_{pro} + \frac{K_{in}}{s} + K_{der}s \tag{2.81}$$

where K_{pro}, K_{in}, K_{der} denote the proportional, integral, derivative gains which are selected as

$$K_{pro} = 0.001782, K_{in} = 3.688, K_{der} = 8.372 \times 10^{-8}$$

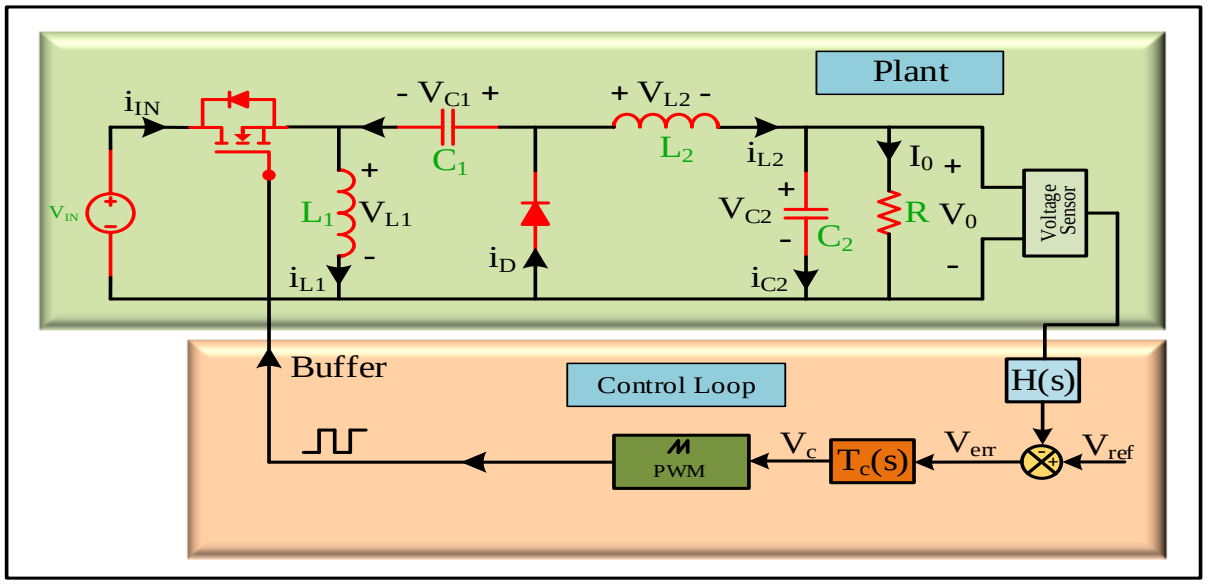

Fig.2. 7. Voltage Mode Control loop for Zeta Converter

2.8.2 Current Mode Control

The implementation of current mode control in Zeta converters is an essential approach employed to effectively manage the output current and maintain stable and efficient power conversion. The control methodology employed in this system is based on a closed-loop architecture, wherein the inductor current is constantly monitored and compared to a predetermined reference current. The control circuit utilizes contemporary current sensing methods, to provide an error signal that represents the disparity between the intended and real current magnitudes.

The error signal is subsequently subjected to processing by a controller, commonly referred to as a Proportional-Integral-Derivative (PID) controller, with the purpose of producing a control signal. The control signal is responsible for modulating the power switch, typically a MOSFET, by means of Pulse Width Modulation (PWM), so effectively altering the duty cycle as shown in fig.2.8 Consequently, the Zeta converter exhibits a rapid response to fluctuations in load or input voltage, so ensuring a consistent output current. This characteristic enhances stability and maximizes overall efficiency in a wide range of applications, including power supplies, LED drivers, and renewable energy systems.

The transfer function of PID controller is given as:

$$T_C(s) = K_{pro} + \frac{K_{in}}{s} + K_{der}s$$

where K_{pro}, K_{in}, K_{der} denote the proportional, integral, derivative gains which are selected as

$$K_{pro} = 0.01063, K_{in} = 29.05, K_{der} = 0.483 \times 10^{-8}$$

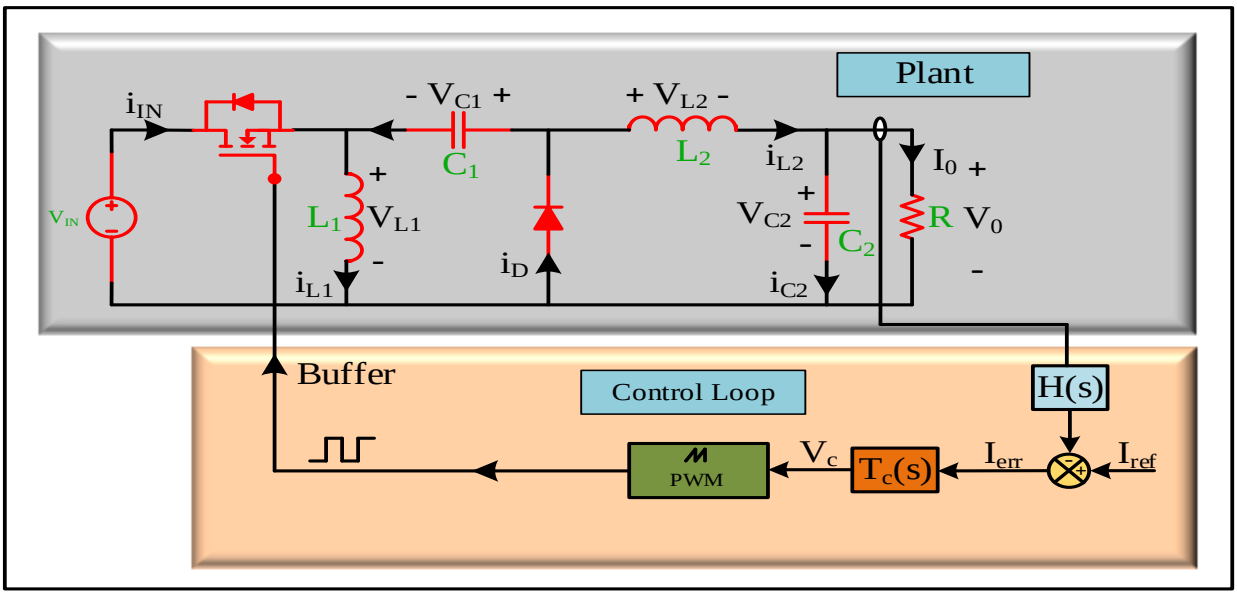

Fig.2. 8. Current Mode Control loop for ZETA Converter

2.9 Simulation Results

2.9.1 Closed Loop Voltage Control

Step Response Analysis:

The step response of the open loop and closed-loop voltage mode control, which is implemented using PID controller and applied to the Zeta converter, is illustrated in Fig. 2.9. The results obtained demonstrate that the closed-loop system displays a significant decrease in the percentage overshoot, measuring at 0.049%. The decrease indicates a noteworthy enhancement in the performance and stability of the system. The closed loop system exhibits a rise time of 8.35 ms and a settling time of 16 ms and The open loop system exhibits a rise time of 0.883 ms and a settling time of 19.998 ms.

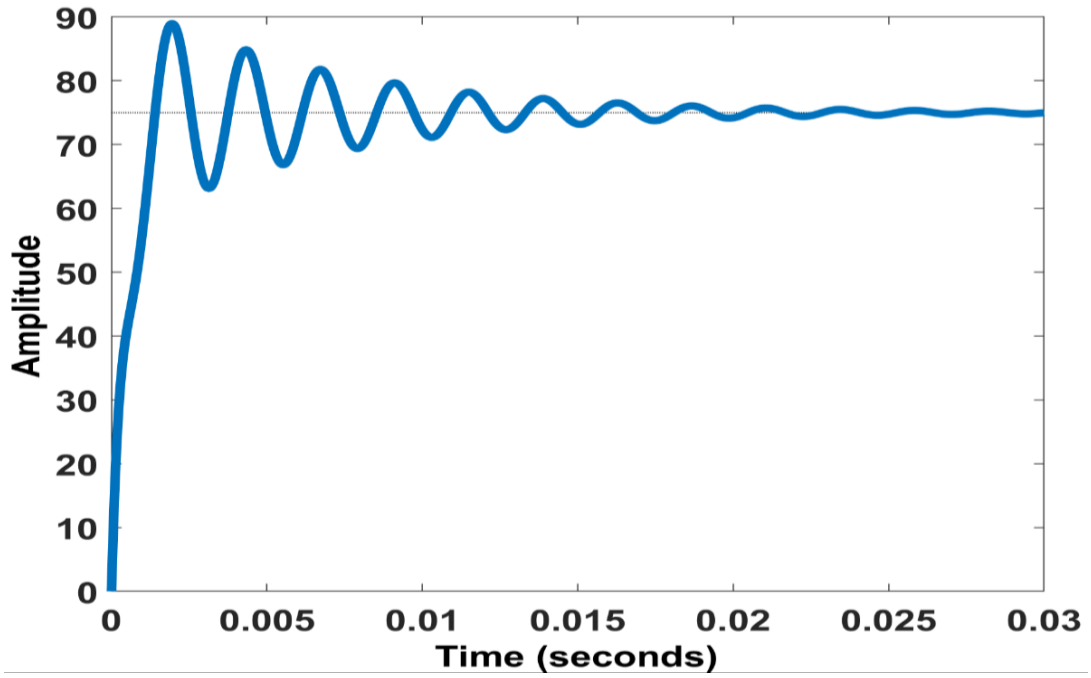

(a)

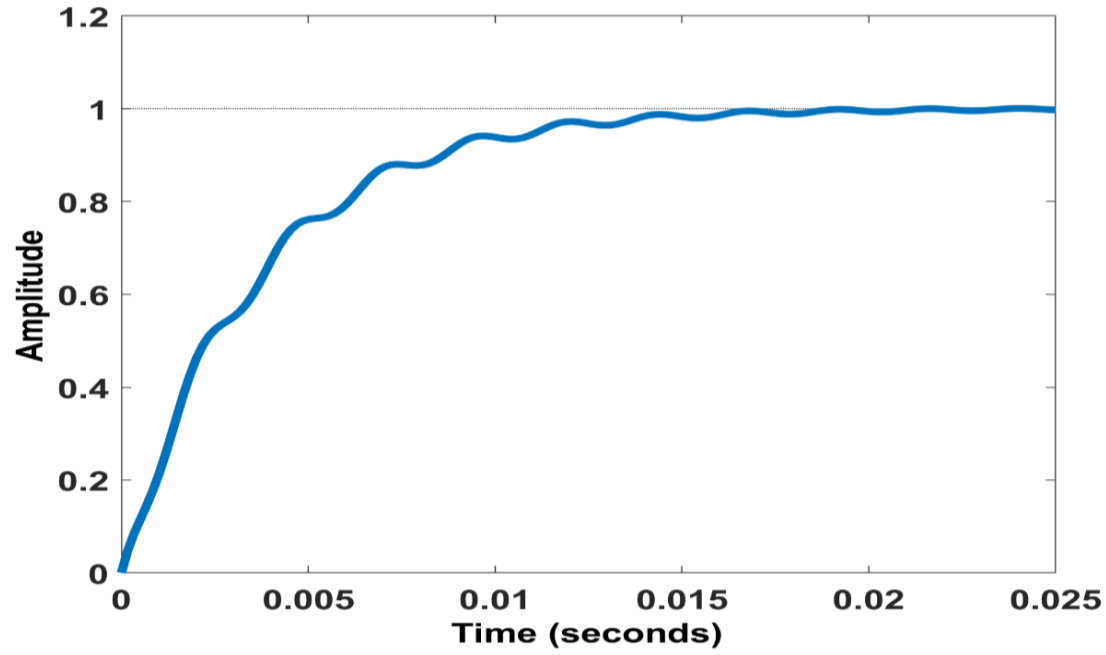

(b)

Fig.2. 9. Step Response (a) Open Loop (b) Close Loop

The comparison between open loop and closed loop voltage stability:

The performance of the Zeta converter under both open and closed-loop scenarios. Under constant load impedance of 6Ω, the converter displays a steady operational state. It is observed that the open-loop system's peak overshoot is 13.492%, the closed-loop application of the ZETA converter remarkably lowers the maximum peak overshoot to a mere 0.926%, signifying an enhanced system performance.

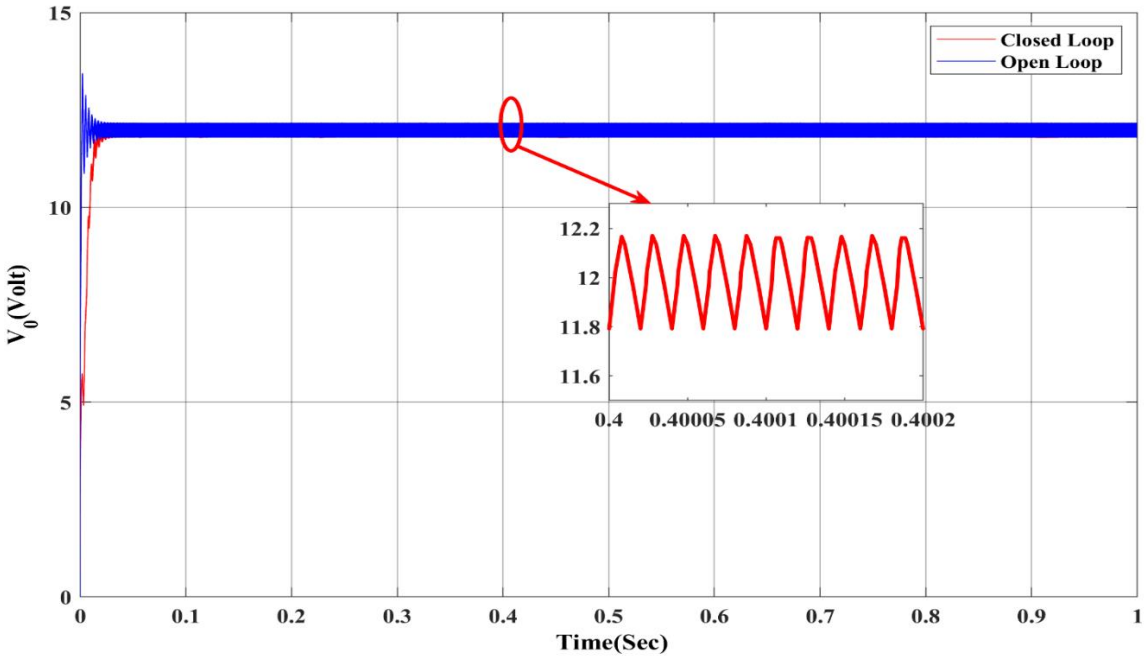

Fig.2. 10. Open loop vs closed loop Zeta converter output voltage

The regulation of output voltage under load variation:

Investigated the control has been designed and developed to ensure a consistent output voltage within predetermined parameters, and it diligently monitors the load and adjusts the duty cycle as required. As depicted in Fig.2.11, modifying the load resistance from 6Ω to 14Ω results in fluctuations in both the output voltage and load current of the Zeta converter. The data presented in the study provides evidence supporting the converter's capacity to maintain a consistent output voltage of 12V, even when subjected to varying load conditions in wide range.

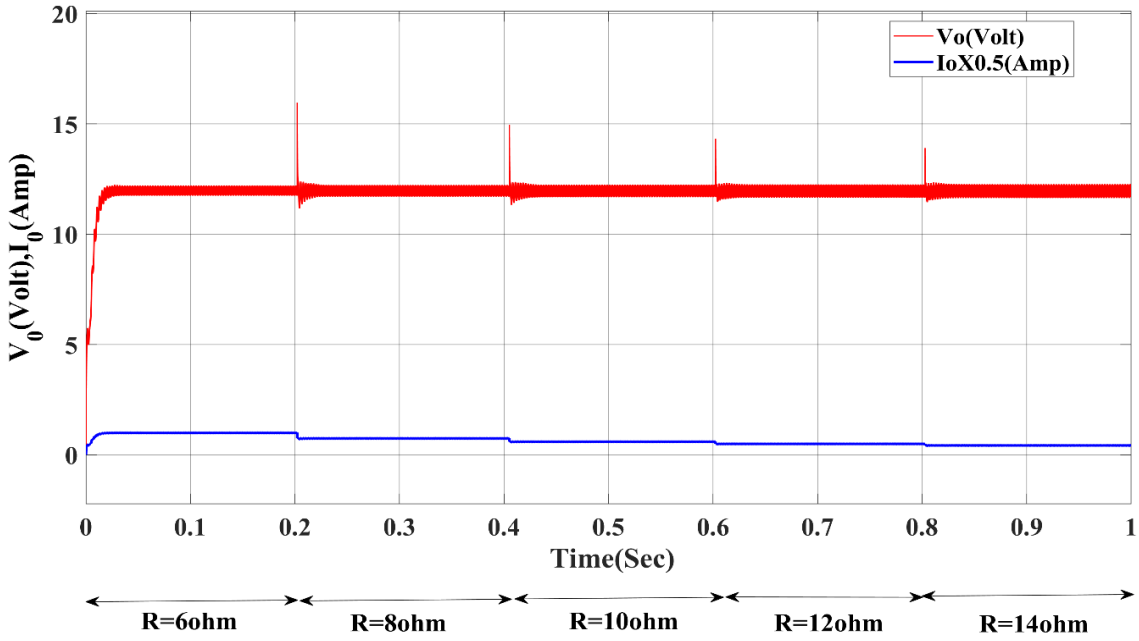

Fig.2. 11. Output Voltage and Current w. r. t. Load Variation

The regulation of load voltage with line variation:

The efficiency of power converters can be affected by line variations, which are also known as fluctuations or disruptions in the input voltage. The closed-loop voltage mode control mitigates these effects by adaptively modifying the duty cycle of the converter. The converter commences its operation once the line voltage has achieved stability and has reached a state of equilibrium. In order to replicate power outages, the voltage of the power line is modified in distinct increments ranging from 24V to 48V. Fig. 2.12 illustrates the ability of the control loop to maintain a consistent output voltage despite large fluctuations in the line voltage. This observation further confirms the effectiveness of well-designed control loop.

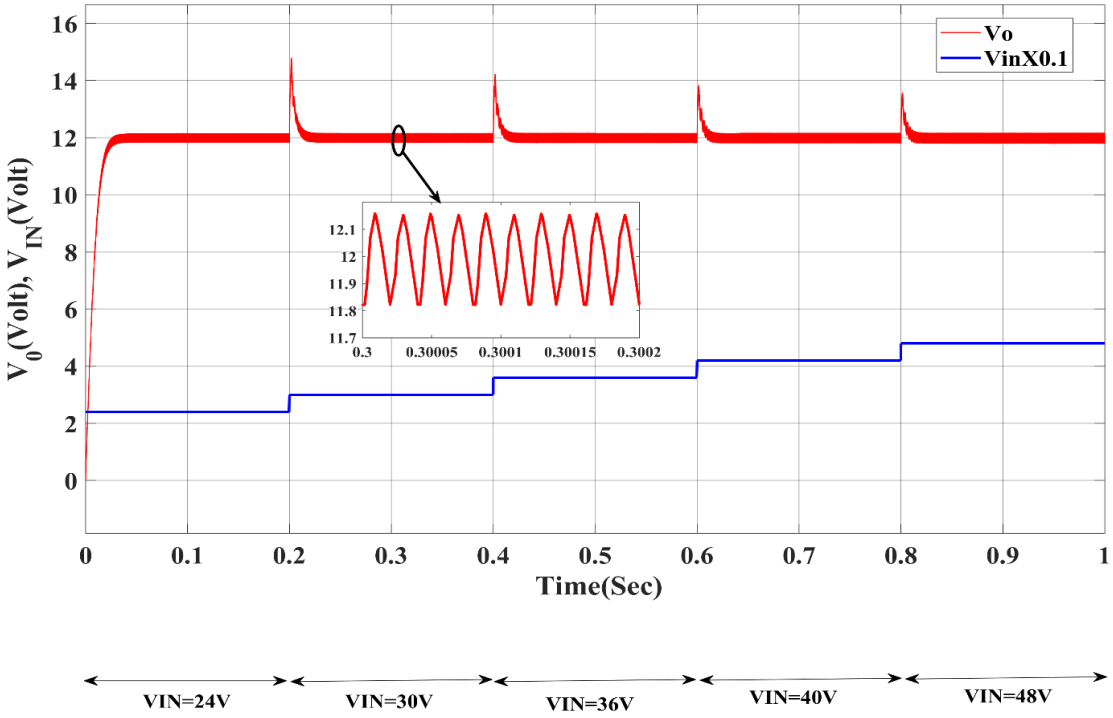

Fig.2. 12. Impact of Line variation on the Output Voltage

2.9.2 Closed Loop Current Control

Step Response Analysis:

The step response of Zeta converters with open loop control exhibits an unbounded reaction to variations in input conditions. Contrarily, in closed loop current mode control, a feedback loop is implemented to constantly monitor the inductor current and correct the system in real-time. As a result, the Zeta converter under closed loop control exhibits a rise time is 6.09ms, settling time of 13.3ms, and maximum peak overshoot is 0.587% and under open loop control exhibits a rise time is 1.34ms, settling time of 17.8ms, and maximum peak overshoot is 18.4% as shown in Fig.2.13.

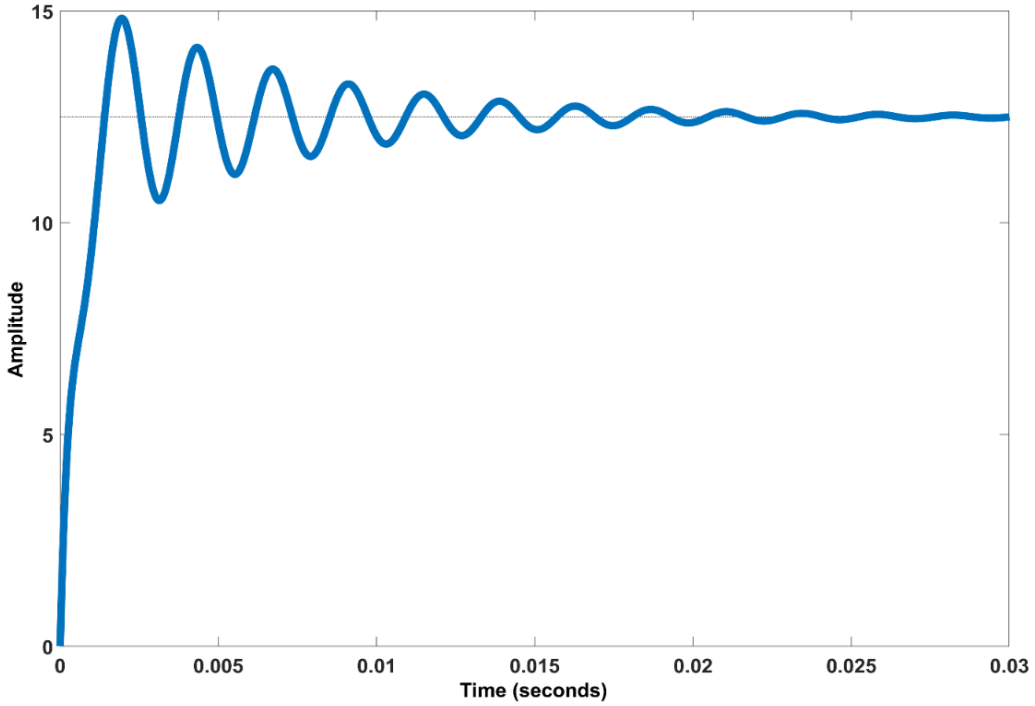

(a)

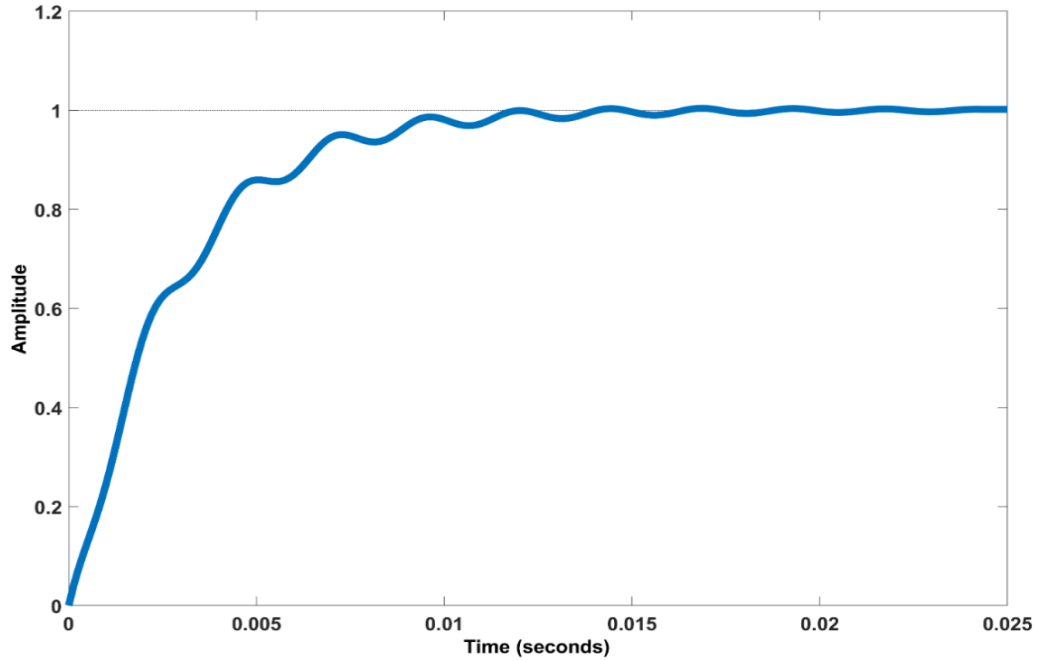

(b)

Fig.2. 13. Step Response (a) Open Loop Plant (b) Closed Loop Plant

The comparison between open loop and closed loop current stability:

The output current waveform for both open loop and closed loop current control modes, as they operate under a constant load. The simulation, employs a fixed load of 6Ω, reveals that the open-loop system manifests limited regulation abilities, exhibiting a maximum peak overshoot of 11.585%. Conversely, the closed-loop system displays a marked improvement in regulation which is further by evident by a significantly reduced peak overshoot of 2.778%.

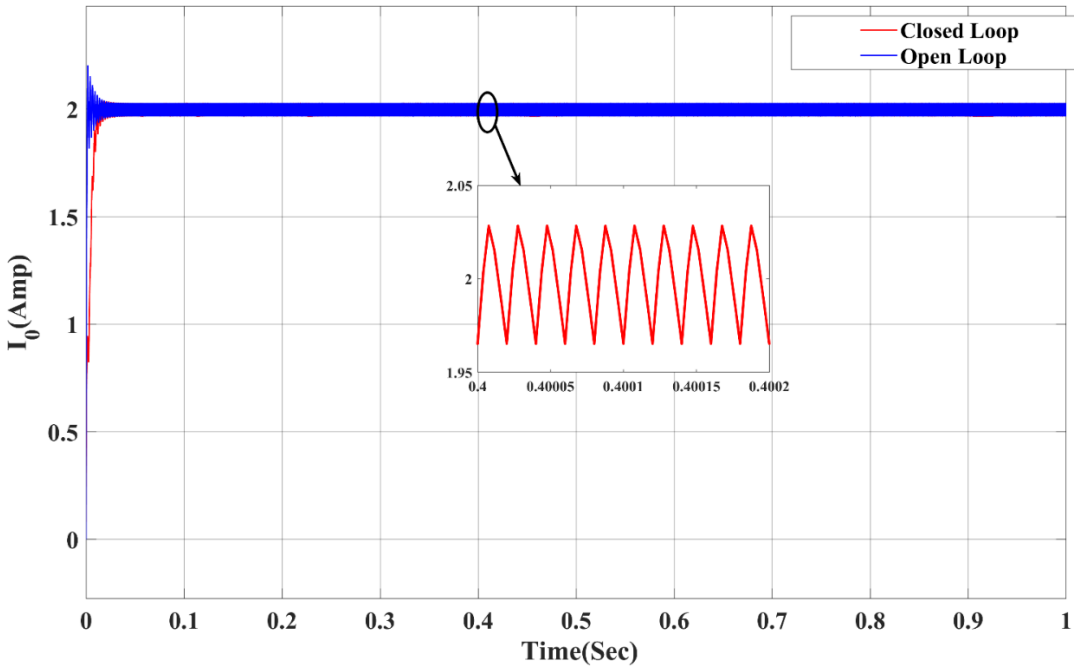

Fig.2. 14. Open loop vs Closed loop Zeta converter Output current

The regulation of output current under load variation:

The comprehensive analysis of the Zeta converter using closed loop current control under varying load conditions has produced significant results. Fig.2.15 shows the output voltage of the Zeta converter under varying load conditions, ranging from 3Ω to 12Ω. Despite the extensive range in the load values, the Zeta converter with closed loop current

control demonstrates an impressive ability to regulate the output current stability throughout at 2A.

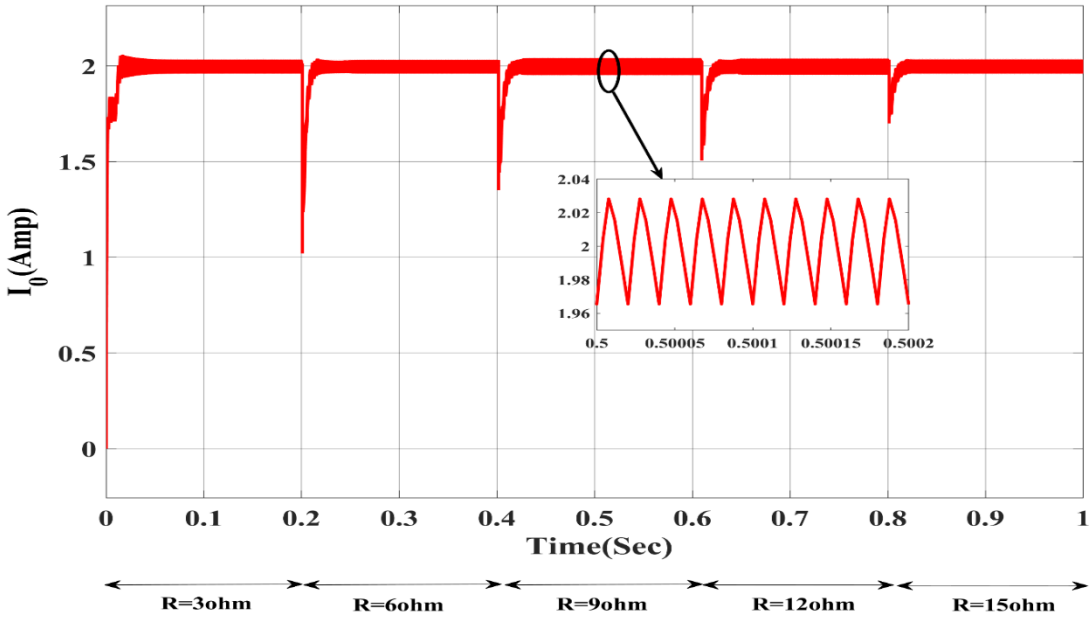

Fig.2. 15. Load regulation of Zeta converter under Current Mode control

The regulation of load voltage with line variation:

The evaluation of Zeta converter utilizing closed loop current control under varying input is discussed in Fig.2.16. The Zeta converter was subject to different input voltage levels between 24V to 48V, but control scheme works well to regulate the output current at steady value.

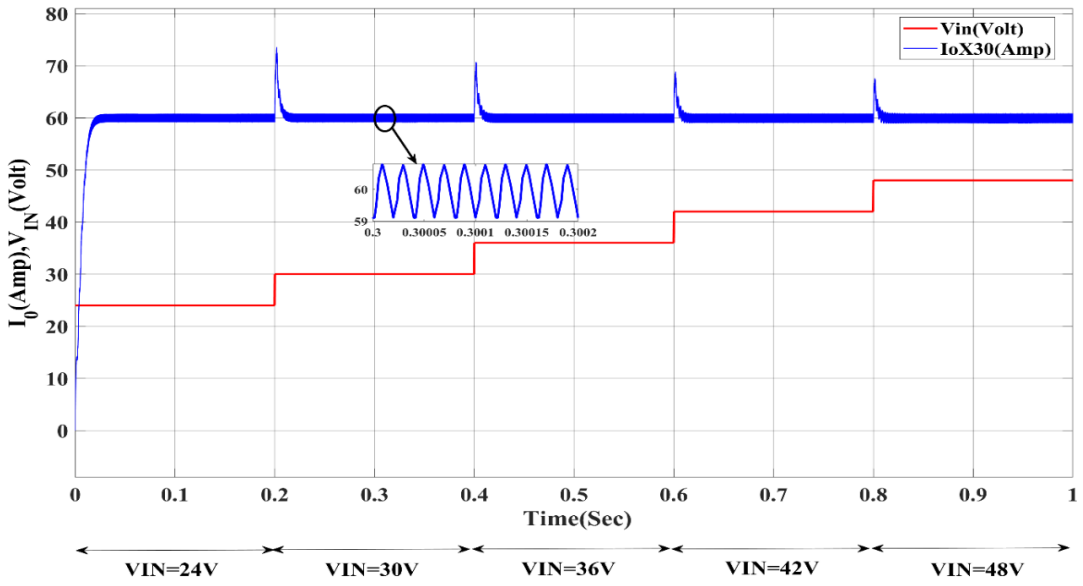

Fig.2. 16. Impact of Line variation on Output current

2.10 Conclusion

In this chapter, we delved deeply into small signal analysis, steady-state analysis, and control technique design for Ideal Zeta converters. By designing a robust control system, we achieved a constant output voltage (CV) despite variations in load and line conditions through voltage mode control. Similarly, we maintained a consistent output current (CC) in the face of load and line variations via current mode control. These findings underscore the effectiveness of Ideal Zeta converters in maintaining stable performance under varying operational conditions, thereby providing valuable insights, and contributing significantly to advancements in power electronics.

CHAPTER 3
COMPARISON BETWEEN IDEAL AND NON-IDEAL ZETA CONVERTER

3.1 Introduction

Switch-mode power supplies have become the preferred choice for power electronics designers due to the increasing need for efficient power conversion and energy management. ZETA converters have gained significant interest because of their numerous advantages. These advantages include the ability to have similar polarity of output voltage as input voltage, reduced current and voltage ripples, higher efficiency compared to buck-boost converters, and a compact design. However, despite the ZETA converter's appealing characteristics, practical applications often encounter issues due to parasitic components, which can hinder its operation and efficiency. These non-idealities result in voltage drops, current losses, and additional dynamics, which negatively impact the efficiency, stability, and overall performance of the converter. Therefore, it is crucial to investigate and improve our understanding of non-ideal ZETA converters and their closed-loop voltage mode control to effectively analyze, optimize, and enhance the performance of these systems.

This chapter aims to thoroughly examine the non-ideal ZETA converter and emphasize the importance of incorporating closed-loop voltage mode control to achieve optimal performance. The analysis begins with an in-depth investigation of the parasitic components affecting the ZETA converter. Parasitic resistances, inductances, and capacitances in the components and interconnections cause additional losses and influence the converter's dynamic response. Following a detailed exploration of these complexities in non-ideal ZETA converters, the discussion shifts to the design and efficiency of closed-loop voltage mode control. The primary goal of this control mechanism is to effectively regulate the output

voltage while minimizing the effects of parasitic components.

3.2 Modelling Of Non-Ideal Zeta Converter

The non-ideal ZETA converter, which includes parasitic components like winding resistance, Capacitor Equivalent Series Resistance (ESR), and losses from switches and diodes, as depicted in Figure 1, provides an in-depth look at the actual performance of these converters. Analyzing the steady state of a non-ideal ZETA converter involves considering the effects of parasitic elements on the system's functionality. The primary emphasis is on how the converter operates when subjected to a constant input voltage and maintains continuous regulation of the output voltage.

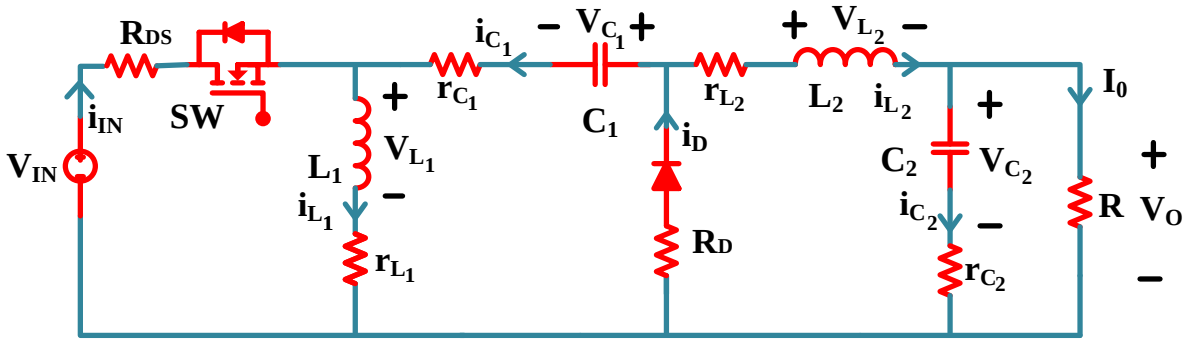

Fig.3. 1. Schematic Diagram of Non-Ideal ZETA Converter

As depicted in Fig.3.2, the ZETA converter's steady-state operation can be divided into two separate modes. The inductor L_1's current gradually increases during the first mode as a result of switch S being closed. Inductor L_1 is charged as a result of this procedure. In this mode, the inductor L_2 builds up energy while the coupling capacitor C_1 discharges, providing power to the load. In mode 2, the capacitor C_1 is being charged while the energy stored in the inductor L_1 is being discharged due to the switch S being in the open position. After being charged, the inductor L_2 is discharged, and power is applied to the load.

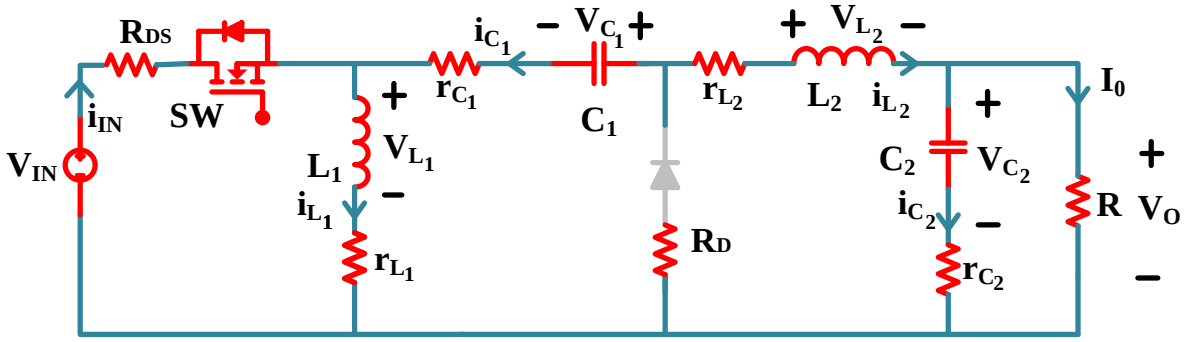

(a)

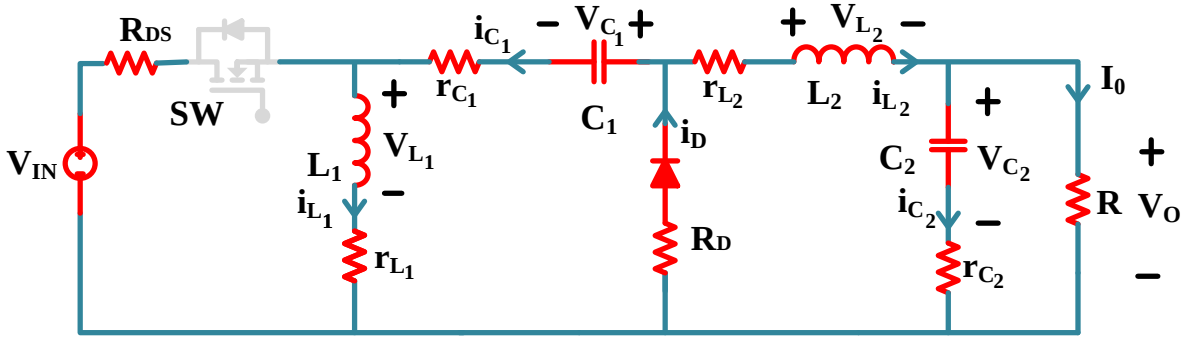

(b)

Fig.3. 2. Modes of Non-Ideal ZETA Converter(a) Mode 1 (b) Mode 2

Voltage ripple is caused by the output capacitor ESR, which can be reduced by using a low-ESR capacitor or raising the output capacitance. The output voltage is lowered due to the inductor winding resistance, but this can be mitigated by accounting for it in the control algorithm. A synchronous rectifier or a low on-resistance switch can be used to lessen the additional voltage drop caused by the switch on-resistance, which lowers the converter's efficiency.

The Non-Ideal Zeta converter is defined by the following equations:

$$x = \begin{bmatrix} i_{L_1} \\ i_{L_2} \\ V_{C_1} \\ V_{C_2} \end{bmatrix}, u = [V_{IN}], y = [V_0]$$

The state space representation of the system is described by the generalized set of equations:

$$\dot{x} = AX + BU$$

$$y = CX + EU$$

where the state matrix is denoted by A, the input matrix is denoted by B, the output matrix is denoted by C, and the input output coupling matrix is denoted by E.

The state space equations of Non-Ideal ZETA Converter in mode 1 is given by:

$$\frac{di_{L_1}}{dt} = \frac{V_{IN}}{L_1} - \frac{(r_{L_1} + R_{Ds})i_{L_1}}{L_1} - \frac{R_{Ds}i_{L_2}}{L_1} \tag{3.1}$$

$$\frac{di_{L_2}}{dt} = \frac{V_{IN}}{L_2} - \frac{R_{Ds}i_{L_1}}{L_2} - \frac{\left(R_{Ds} + r_{C_1} + r_{L_2} + \frac{\mathrm{R}r_{C_2}}{\mathrm{R} + r_{C_2}}\right)i_{L_2}}{L_2} + \frac{V_{C_1}}{L_2} - \frac{\left(\frac{\mathrm{R}}{\mathrm{R} + r_{C_2}}\right)V_{C_2}}{L_2} \tag{3.2}$$

$$\frac{dV_{C_1}}{dt} = -\frac{i_{L_2}}{C_1} \tag{3.3}$$

$$\frac{dV_{C_2}}{dt} = \frac{\frac{R}{\mathrm{R} + r_{C_2}}i_{L_2}}{C_2} - \frac{\frac{V_{C_2}}{\mathrm{R} + r_{C_2}}}{C_2} \tag{3.4}$$

$$V_o = \frac{\mathrm{R}r_{C_2}}{R + r_{C_2}}i_{L_2} + \frac{\mathrm{R}}{\mathrm{R} + r_{C_2}} \tag{3.5}$$

$$\begin{bmatrix} \frac{di_{L_1}}{dt} \\ \frac{di_{L_2}}{dt} \\ \frac{dV_{C_1}}{dt} \\ \frac{dV_{C_2}}{dt} \end{bmatrix} = \begin{bmatrix} -\frac{r_{L_1}+R_{Ds}}{L_1} & -\frac{R_{Ds}}{L_1} & 0 & 0 \\ -\frac{R_{Ds}}{L_2} & -\frac{R_{Ds}+r_{C_1}+r_{L_2}+\frac{\mathrm{R}r_{C_2}}{\mathrm{R}+r_{C_2}}}{L_2} & \frac{1}{L_2} & -\frac{\frac{R_o}{R_o+r_{C_2}}}{L_2} \\ 0 & -\frac{1}{C_1} & 0 & 0 \\ 0 & \frac{\frac{\mathrm{R}}{\mathrm{R}+r_{C_2}}}{C_2} & 0 & -\frac{\frac{1}{\mathrm{R}+r_{C_2}}}{C_2} \end{bmatrix} \begin{bmatrix} i_{L_1} \\ i_{L_2} \\ V_{C_1} \\ V_{C_2} \end{bmatrix} + \begin{bmatrix} \frac{1}{L_1} \\ \frac{1}{L_2} \\ 0 \\ 0 \end{bmatrix} [V_s] \tag{3.6}$$

$$[V_o] = \begin{bmatrix} 0 & \frac{Rr_{C_2}}{\mathrm{R}+r_{C_2}} & 0 & \frac{\mathrm{R}}{\mathrm{R}+r_{C_2}} \end{bmatrix} \begin{bmatrix} i_{L_1} \\ i_{L_2} \\ V_{C_1} \\ V_{C_2} \end{bmatrix} + \begin{bmatrix} 0 \\ 0 \\ 0 \\ 0 \end{bmatrix} [V_s] \tag{3.7}$$

The state space equations of Non-Ideal ZETA Converter in mode 2 is given by:

$$\frac{di_{L_1}}{dt} = -\frac{(r_{L_1}+r_{C_1}+R_D)i_{L_1}}{L_1} - \frac{R_D i_{L_2}}{L_1} - \frac{V_{C_1}}{L_1} \tag{3.8}$$

$$\frac{di_{L_2}}{dt} = -\frac{R_D i_{L_1}}{L_2} - \frac{\left(R_D + r_{L_2} + \frac{\mathrm{R}r_{C_2}}{\mathrm{R}+r_{C_2}}\right) i_{L_2}}{L_2} - \frac{\left(\frac{R_o}{R_o+r_{C_2}}\right) V_{C_2}}{L_2} \tag{3.9}$$

$$\frac{dV_{C_1}}{dt} = \frac{i_{L_1}}{C_1} \tag{3.10}$$

$$\frac{dV_{C_2}}{dt} = \frac{\frac{R}{R+r_{C_2}} i_{L_2}}{C_2} - \frac{\frac{V_{C_2}}{R+r_{C_2}}}{C_2} \tag{3.11}$$

$$[V_o] = \begin{bmatrix} 0 & \frac{Rr_{C_2}}{R+r_{C_2}} & 0 & \frac{R}{R+r_{C_2}} \end{bmatrix} \begin{bmatrix} i_{L_1} \\ i_{L_2} \\ V_{C_1} \\ V_{C_2} \end{bmatrix} + \begin{bmatrix} 0 \\ 0 \\ 0 \\ 0 \end{bmatrix} [V_s] \tag{3.12}$$

$$\begin{bmatrix} \frac{di_{L_1}}{dt} \\ \frac{di_{L_2}}{dt} \\ \frac{dV_{C_1}}{dt} \\ \frac{dV_{C_2}}{dt} \end{bmatrix} = \begin{bmatrix} -\frac{r_{L_1}+r_{C_1}+R_D}{L_1} & -\frac{R_D}{L_1} & -1/L_1 & 0 \\ -\frac{R_D}{L_2} & -\frac{R_D+r_{L_2}+\frac{Rr_{C_2}}{R+r_{C_2}}}{L_2} & 0 & -\frac{\frac{R}{R+r_{C_2}}}{L_2} \\ \frac{1}{C_1} & 0 & 0 & 0 \\ 0 & \frac{\frac{R}{R+r_{C_2}}}{C_2} & 0 & -\frac{\frac{1}{R+r_{C_2}}}{C_2} \end{bmatrix} \begin{bmatrix} i_{L_1} \\ i_{L_2} \\ V_{C_1} \\ V_{C_2} \end{bmatrix} + \begin{bmatrix} 0 \\ 0 \\ 0 \\ 0 \end{bmatrix} [V_s] \quad (3.13)$$

$$[V_o] = \begin{bmatrix} 0 & \frac{Rr_{C_2}}{R+r_{C_2}} & 0 & \frac{R}{R+r_{C_2}} \end{bmatrix} \begin{bmatrix} i_{L_1} \\ i_{L_2} \\ V_{C_1} \\ V_{C_2} \end{bmatrix} + \begin{bmatrix} 0 \\ 0 \\ 0 \\ 0 \end{bmatrix} [V_s] \quad (3.14)$$

Averaging over one switching period is performed to remove the switching ripple component from the circuit calculations. Averaging these equations over one switching period yields the averaged switching model using eq. (2.68) -(2.71)

$$A = A_1 d + A_2(1-d)$$
$$B = B_1 d + B_2(1-d)$$
$$C = C_1 d + C_2(1-d)$$
$$E = E_1 d + E_2(1-d)$$

The nonlinear averaged state-space model must be linearized around an operational point before the small-signal model of Zeta converter can be derived. To do this, perturbations are made to the system's state variables, input variables, and parameters. Perturbations refer to small disturbances or changes introduced into these component values, which can lead to significant effects on the overall behaviour and performance of the system using eq. (2.72) -(2.75)

$$d = D + \hat{d}$$

$$x = X + \hat{x}$$

$$u = U + \hat{u}$$

$$y = Y + \hat{y}$$

Now, substituting the perturbed variables into the averaged state space model and assuming that steady state terms are zero and the effect of higher order terms is neglected. We get the linearized small signal model is obtained as follows using eq. (2.76) – (2.78)

$$s\hat{x}(s) = A\hat{x}(s) + B\hat{u}(s) + ((A_1 - A_2)X(s) + (B_1 - B_2)U(s))\hat{d}(s)$$

$$\hat{y}(s) = C\hat{x}(s) + E\hat{u}(s) + ((A_1 - A_2)X(s) + (E_1 - E_2)U(s))\hat{d}(s)$$

$$\frac{\hat{x}(s)}{\hat{d}(s)} = (sI - A)^{-1}((A_1 - A_2)X(s) + (B_1 - B_2)U(s))$$

Using above Equation, the output-to-control transfer function can be obtained by substituting the values of the parameters from Table 3.1.

$$\frac{\widehat{v_0}(s)}{\hat{d}(s)} = \frac{7.454e10\ s\text{^}2\ -\ 4.495e13\ s\ +\ 5.712e17}{s\text{^}4\ +\ 4.004e05\ s\text{^}3\ +\ 1.396e09\ s\text{^}2\ +\ 3.22e12\ s\ +\ 8.764e15} \tag{3.15}$$

Table 3. 1 Design specification of Non-Ideal ZETA Converter

Parameters	Symbols	Values
Input Voltage	V_{IN}	48V
Output Voltage	V_o	12V
Duty Cycle	D	0.2
Switching Frequency	f_{sw}	50kHz
Output Power	P_0	24W
Inductor L_1	L_1	7.68mH
Inductor L_2	L_2	1.92mH
Current Ripple in Inductor L_1	Δi_{L_1}	5% I_{L_1}
Current Ripple in Inductor L_2	Δi_{L_2}	5% I_{L_2}
Inductors Resistance	r_{L_1}, r_{L_2}	0.2Ω
Capacitor C_1	C_1	13.33μF
Capacitor C_2	C_2	0.4166μF
Voltage Ripple in Capacitor C_1	ΔV_{C_1}	5% V_{C_1}
Voltage Ripple in Capacitor C_2	ΔV_{C_2}	5% V_{C_2}
Capacitor ESRs	r_{C_1}, r_{C_2}	1μΩ
MOSFET on Resistance	R_{DS}	0.45Ω
Diode on Resistance	R_D	0.3Ω

3.3 Control Strategy for Non-Ideal Zeta Converter

In this section, the Non-Ideal Zeta converter is analysed and assessed in continuous conduction mode (CCM), and the creation of a closed-loop voltage mode control mechanism is covered. A PID controller has been built for the voltage loops and the transfer functions of the Zeta converter have been found in Eq. 2.80. MATLAB/Simulink

simulations are used to evaluate the closed-loop voltage mode control system's effectiveness.

3.3.1 Voltage Mode Control

Several parasitic factors, such as winding resistances, equivalent series resistances (ESR), switch losses, and diode losses, affect how the non-ideal ZETA converter operates. Consequently, challenges arise in achieving the intended degree of output voltage regulation, minimising transient reactions, and guaranteeing the stability of system functioning. Owing to the inherent challenges presented by non-idealities, a closed-loop proportional-integral-derivative (PID) control system is imperative for optimising the ZETA converter's performance and guaranteeing its stability.

The basis of the voltage mode control methodology is the regulation of the output voltage by means of a comparison process with a reference voltage, followed by the generation of an error signal. As shown in Fig. 3.3, the error signal is then used to adjust the converter's duty cycle, which controls the output voltage. The design factors that must be considered when implementing voltage mode control in Non-ideal ZETA converters are covered in this section.

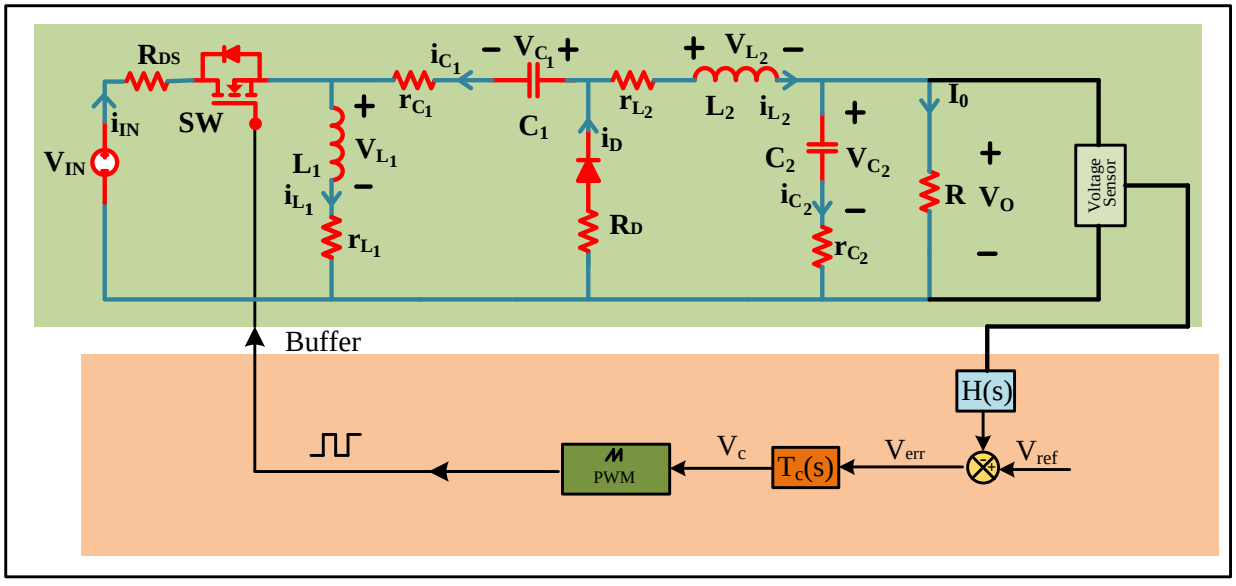

Fig.3. 3. Voltage Mode Control loop for Non-ideal Zeta Converter

The closed-loop control system is widely recognised for its ability to deliver exceptional output voltage regulation and rapid transient response, rendering it highly suitable for a diverse range of applications necessitating bidirectional power flow.

The transfer function of PID controller is given as:

$$T_C(s) = K_{pro} + \frac{K_{in}}{s} + K_{der}s$$

where K_{pro}, K_{in}, K_{der} denote the proportional, integral, derivative gains which are selected as

$$K_{pro} = 0.0010, K_{in} = 7.832, K_{der} = 2.09 \times 10^{-8}$$

3.4 Simulation Results

3.4.1 Closed Loop Voltage Control

Step Response Analysis:

The step response of the open loop and closed-loop voltage mode control, which is implemented using PID controller and applied to the Non-Ideal Zeta converter, is illustrated in Fig.3.4. The results obtained demonstrate that the closed-loop system displays a significant decrease in the percentage overshoot, measuring at 0.92%. The decrease indicates a noteworthy enhancement in the performance and stability of the system. The closed loop system exhibits a rise time of 3.63 ms and a settling time of 6.71 ms and the open loop system exhibits a rise time of 1.37 ms and a settling time of 11.7 ms.

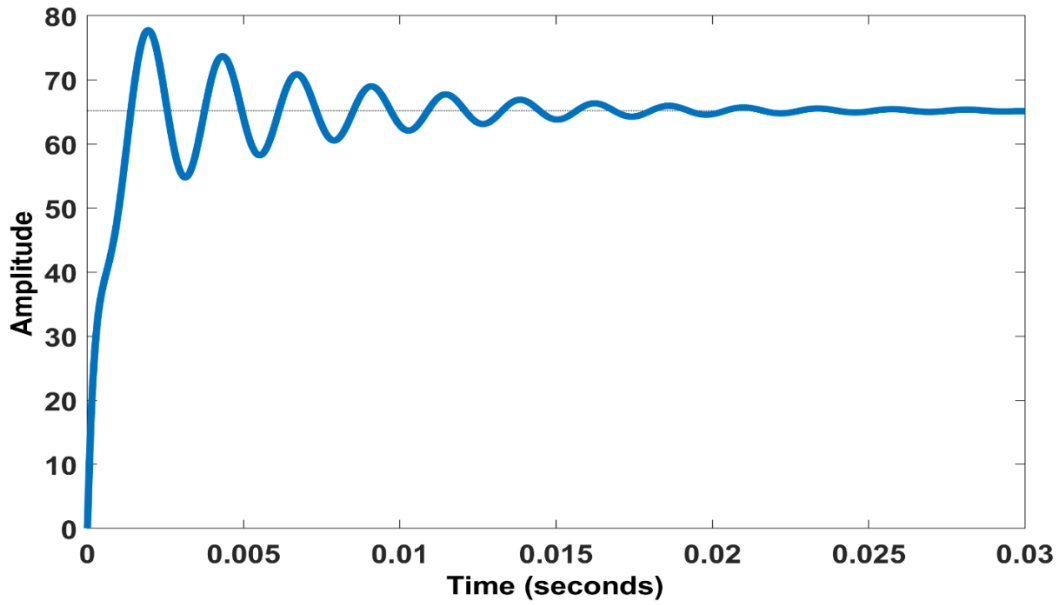

(a)

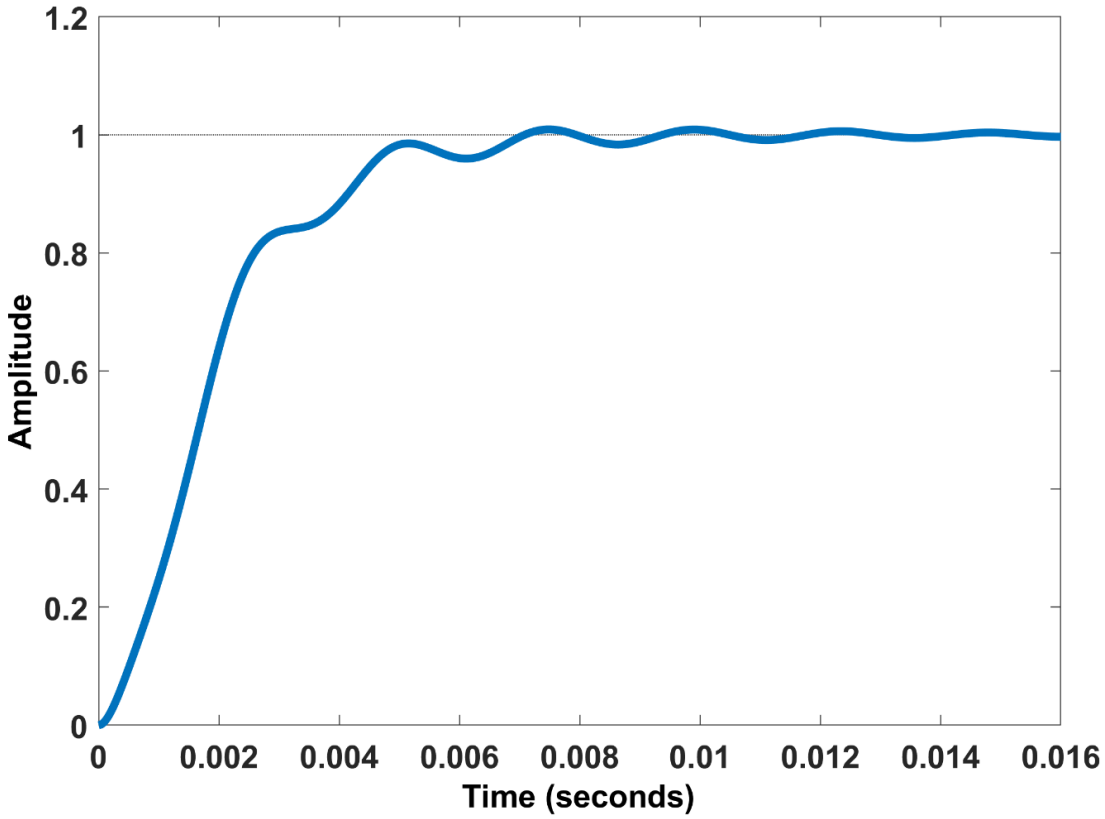

(b)

Fig.3. 4. Step Response (a) Open Loop Plant (b) Closed Loop Plant

The comparison between open loop and closed loop voltage stability:

The performance of the Non-Ideal Zeta converter under both open and closed-loop scenarios. Under constant load impedance of 6Ω, the converter displays a steady operational state. It is observed that the open-loop system's peak overshoot is 10.556%, the closed-loop application of the ZETA converter remarkably lowers the maximum peak overshoot to a mere 4.464%, signifying an enhanced system performance.

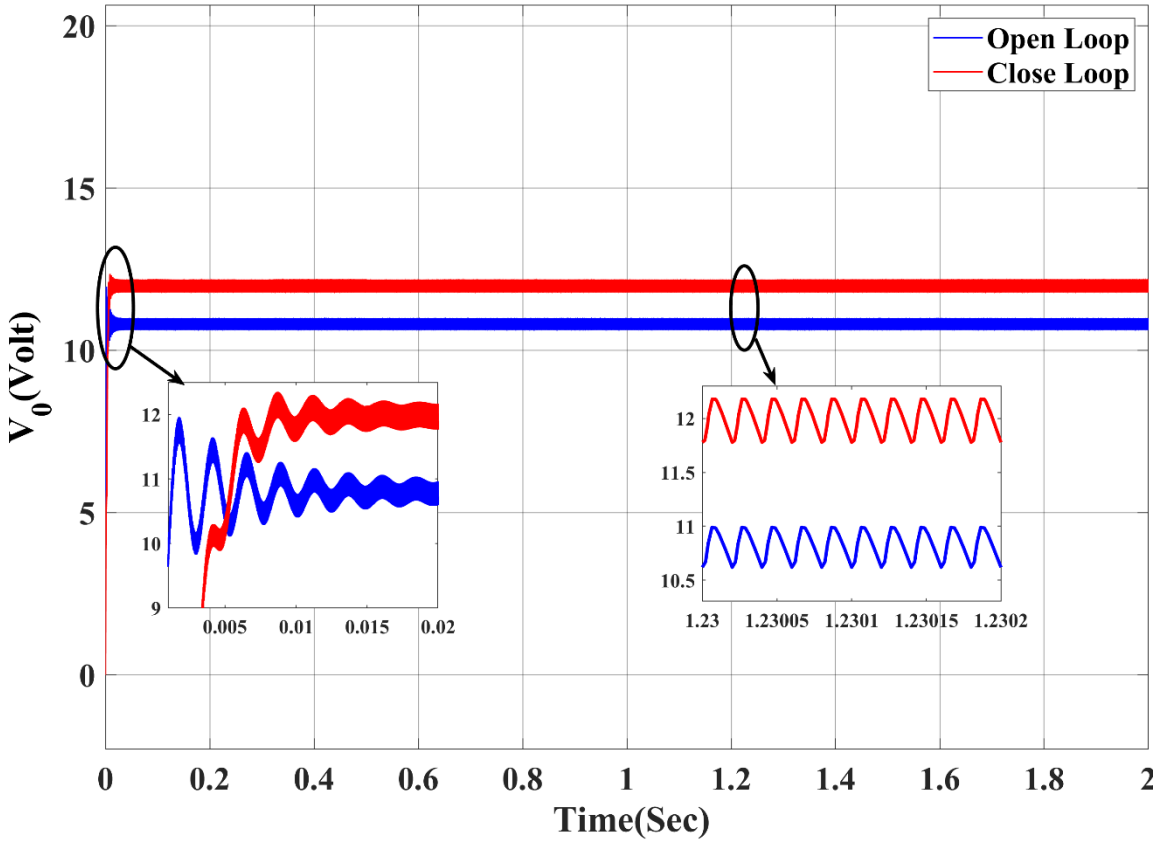

Fig.3. 5. Open loop vs closed loop Zeta converter output voltage

The regulation of output voltage under load variation

Investigated the control has been designed and developed to ensure a consistent output voltage within predetermined parameters, and it diligently monitors the load and adjusts the duty cycle as required. As depicted in Fig.3.6, modifying the load resistance from 6Ω to 14Ω results in fluctuations in both the output voltage and load current of the Zeta converter. The data presented in the study provides evidence supporting the converter's

capacity to maintain a consistent output voltage of 12V, even when subjected to varying load conditions in wide range.

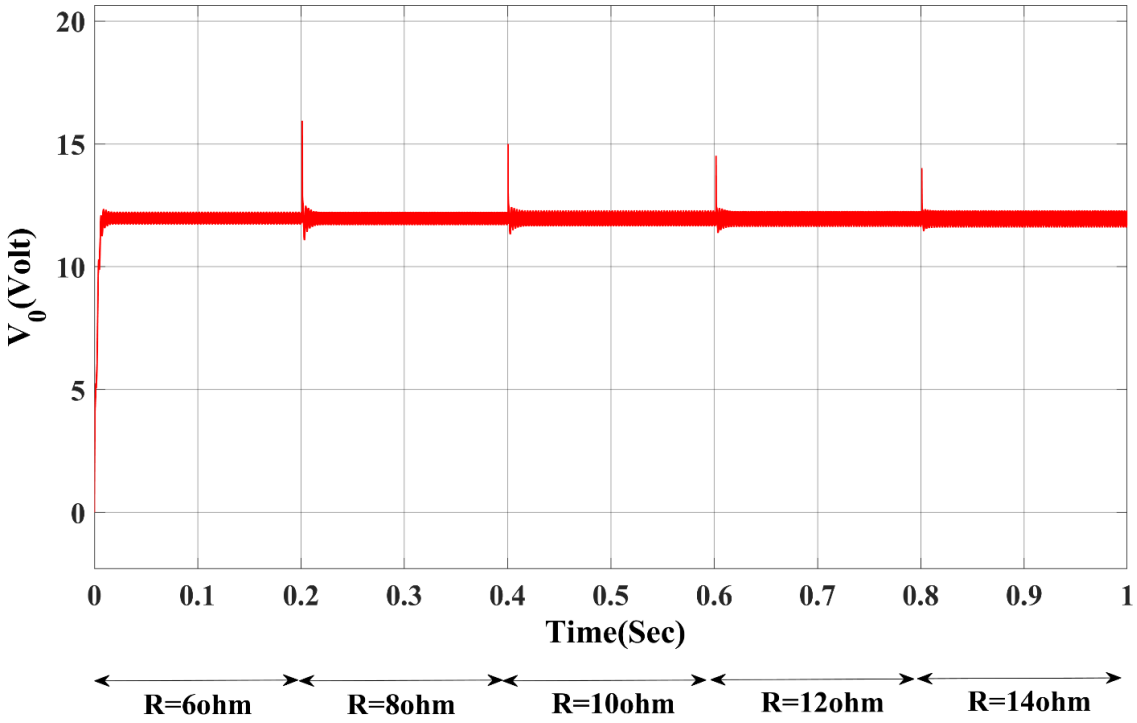

Fig.3. 6. Output Voltage and Current w. r. t. Load Variation

The regulation of load voltage with line variation

The efficiency of power converters can be affected by line variations, which are also known as fluctuations or disruptions in the input voltage. The closed-loop voltage mode control mitigates these effects by adaptively modifying the duty cycle of the converter. The converter commences its operation once the line voltage has achieved stability and has reached a state of equilibrium. In order to replicate power outages, the voltage of the power line is modified in distinct increments ranging from 24V to 48V. Fig.3.7 illustrates the ability of the control loop to maintain a consistent output voltage despite large fluctuations in the line voltage. This observation further confirms the effectiveness of well-designed control loop.

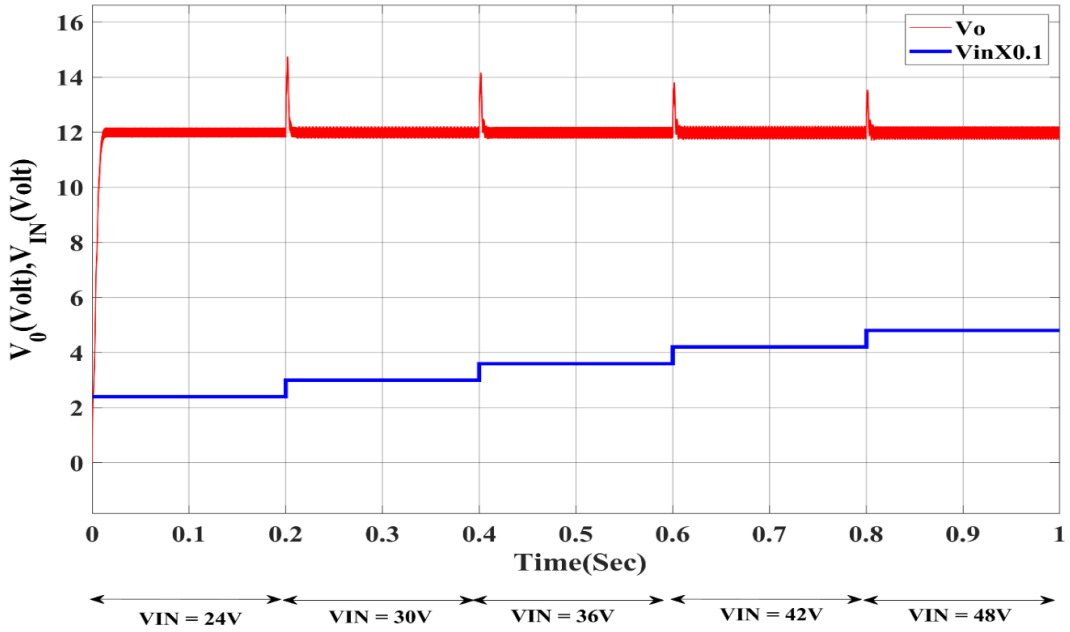

Fig.3. 7. Impact of Line variation on the Output Voltage

Comparison Between Ideal Zeta and Non-Ideal Zeta Converter

Output Voltage (Open Loop)

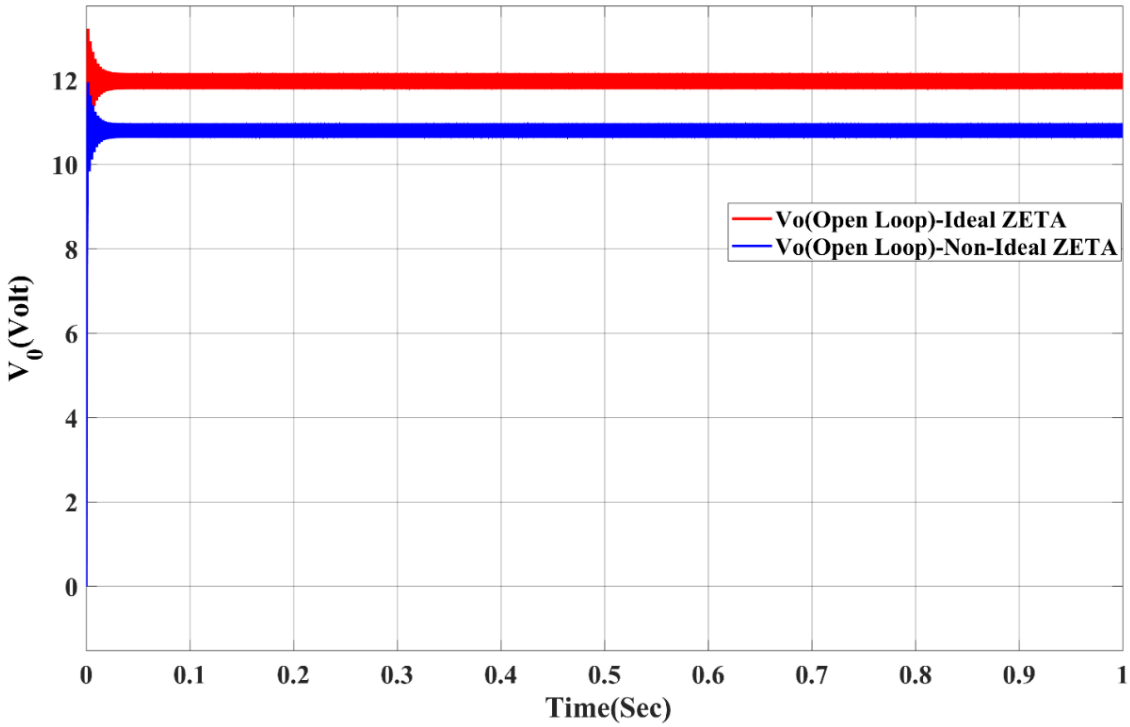

Fig.3. 8. Output Voltage of Ideal and Non-Ideal ZETA Converter (Open Loop)

Fig 3.8 illustrates the impact of parasitic components on the output voltage. The expected output voltage is 12V, but the actual output voltage is 10.82V, showing a significant drop. This reduction causes losses and can deteriorate the lifespan of the load. Addressing parasitic effects is crucial to maintain optimal performance and ensure the longevity of the system.

Output Voltage (Close Loop)

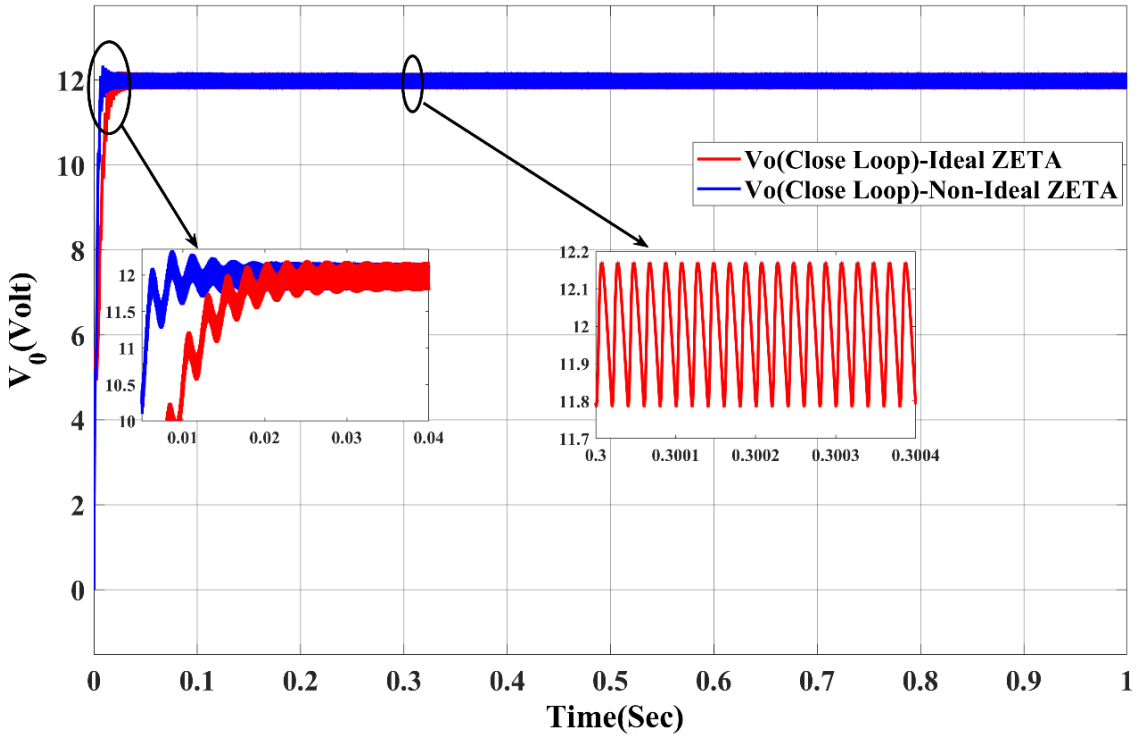

Fig.3. 9. Output Voltage of Ideal and Non-Ideal ZETA Converter (Close Loop)

Figure 3.9 indicates that the non-ideal Zeta converter, when operating in a closed-loop system, reaches its desired output faster (less rise time and settling time) compared to the ideal Zeta converter. However, this comes with a slight downside: it experiences a bit more overshoot, meaning it initially exceeds the desired output level before stabilizing.

3.5 Conclusions

This chapter focuses on modeling the non-ideal ZETA converter and designing a controller to maintain a constant output voltage despite changes in load and line conditions. It also compares the output voltage of the non-ideal and ideal ZETA converters in both open and closed-loop configurations.

We thoroughly examined the complexities of the non-ideal ZETA converter, emphasizing the importance of closed-loop voltage mode control for optimal performance. We started by exploring the parasitic components, such as resistances, inductances, and capacitances, which affect the converter. These parasitic elements cause additional losses and impact the converter's dynamic response.

After this detailed analysis of the non-ideal ZETA converter, we focused on designing an efficient closed-loop voltage mode control system. This control mechanism aims to precisely regulate the output voltage, reducing the negative effects of parasitic components. In conclusion, this chapter underscores the need for advanced control techniques to improve the performance and reliability of ZETA converters in real-world applications.

CHAPTER 4
MODELLING AND DESIGN OF BIDIRECTIONAL SEPIC/ZETA CONVERTER

4.1 Introduction

The importance of clean energy sources has surged due to the detrimental effects of fossil fuel usage on the environment. In recent times, there has been rapid development in PV system, fuel-cell, and wind-power generating systems. However, these systems often face challenges in providing stable power output. To address this issue, hybrid power systems combining renewable energy sources with batteries have emerged. In such systems, when renewable sources fail to meet the power demand, batteries step in to supply the shortfall. Additionally, these batteries can be used to store excess energy generated. Battery Energy Storage System (BEES) is generally performed as a storage system for energy. Bidirectional DC-DC converters play a crucial role in facilitating power transfer between different DC sources, making them essential components in renewable energy hybrid power systems, hybrid electric vehicles, and uninterruptible power supplies.

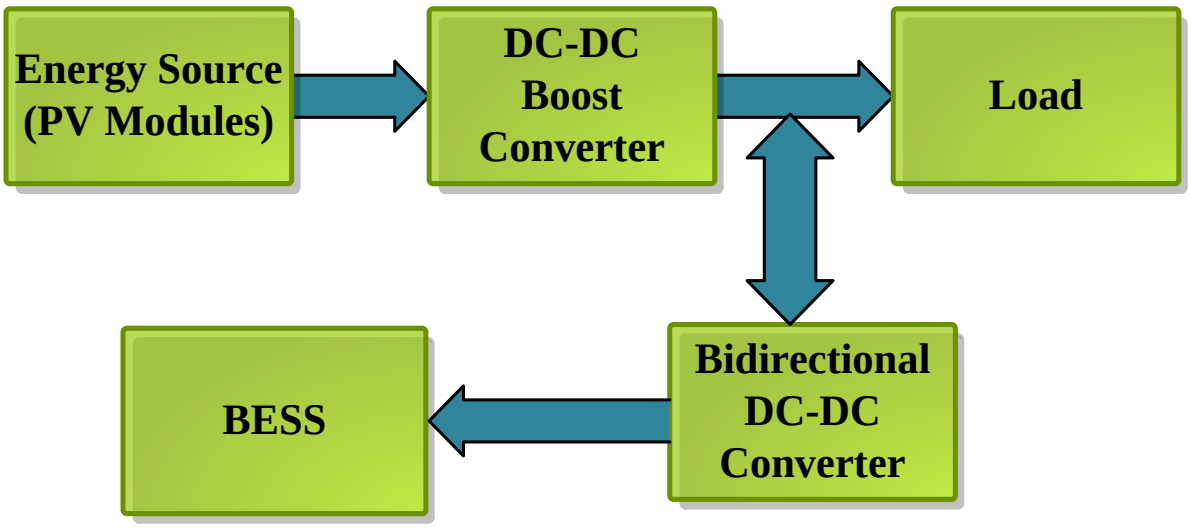

Fig.4. 1. System Block Diagram

Bidirectional DC-DC converters serve a dual purpose in battery charging and discharging systems. Fig. 4.2 shows the block diagram of the Bidirectional SEPIC/ZETA DC-DC Converter in which forward and reverse power flow condition have been shown.

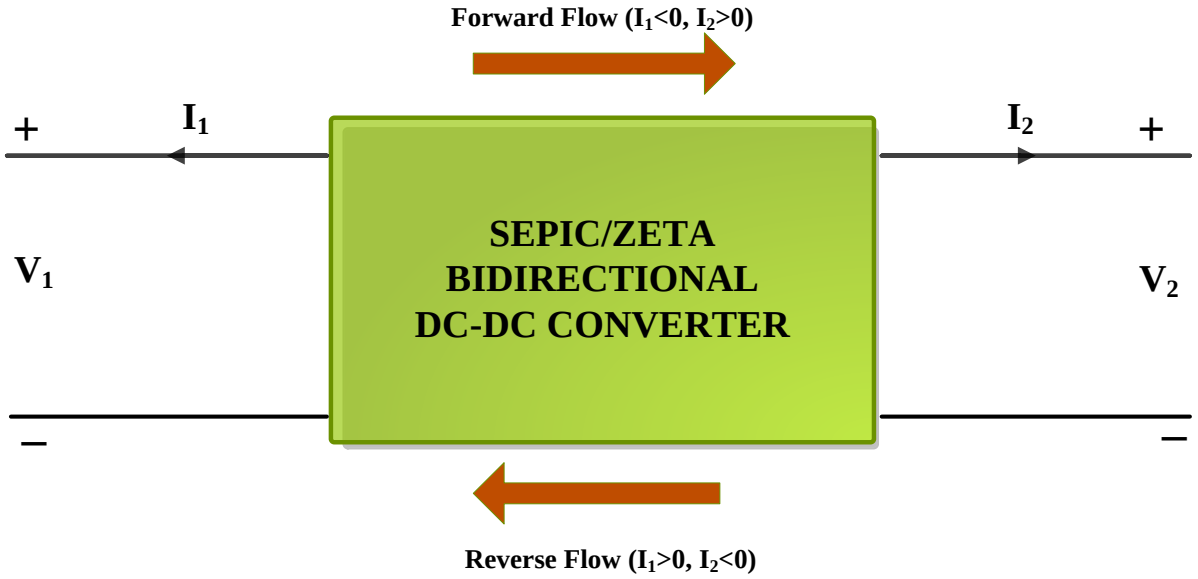

Fig.4. 2. Bidirectional SEPIC/ZETA DC-DC Converter

The proposal suggests utilizing a Bidirectional SEPIC/Zeta converter due to its advantageous feature of lower output voltage ripple when compared to other converters. This converter operates in two modes. In SEPIC mode, the battery acts as a source, supplying power to the DC grid with a voltage boost (Battery Discharging Mode). Conversely, Zeta mode allows the converter to draw power from the grid and charge the battery at a lower voltage (Battery Charging Mode). While an energy management system would typically handle mode selection, this chapter focuses on exploring SEPIC and ZETA modes independently.

The Bidirectional SEPIC/ZETA converter is used in various applications like EV battery management system, UPS, HVDC transmission, smart grid, etc [9]. This

paper explores the transfer function by performing converter's mathematical analysis relating the converter's output voltage to the duty cycle of its switches. The focus is on battery charging and discharging operations, with a deep dive into the different modes of the SEPIC/ZETA converter so that battery is charging and discharging with constant current. To optimize the performance of the PI controllers, the Ziegler-Nichols method is employed to determine the appropriate values for the proportional (Kp), integral (Ki), gains. The proportional component of controllers enhances transient response speed, while the integral component improves steady-state response and diminishes steady-state error.

4.2 System Under Consideration

Under this system there is an integration of Battery and Bidirectional DC-DC Converter. This integrated approach not only ensures seamless energy flow but also underscores the system's adaptability and efficiency in managing power resources. Battery and Bidirectional SEPIC/ZETA DC-DC Converter specification consideration have been discussed below:

Specifications of Battery*:*

Storage of the excess power is performed using a rechargeable battery for the DC bus and release it when needed, ensuring a stable voltage. It plays a crucial role in managing the charging and discharging processes to maintain optimal performance and prolong battery life. Monitoring the state of charge (SOC) helps determine when to charge or discharge the battery, contributing to its longevity. Table 4.1 outlines the battery specifications.

Table 4. 1 Specifications of Battery

Parameters	Values
Type	Lead Acid
Nominal voltage	48V
Rated capacity	25Ah
Internal resistance	0.0192Ω

Bidirectional SEPIC/ZETA DC-DC Converter:

This bidirectional converter, like regular SEPIC/ZETA converters, can both increase (boost) and decrease (buck) the voltage regardless of which direction power is flowing. The design uses two inductors (L_A and L_B), three capacitors (C_A, a coupling capacitor C_C, and C_B), and two switches (SW_A and SW_B) that can handle current in both directions, as illustrated in Fig.2. The system has a DC bus or Grid on one side and a battery on the other side. Table 4.2 summarizes how the converter operates under various conditions.

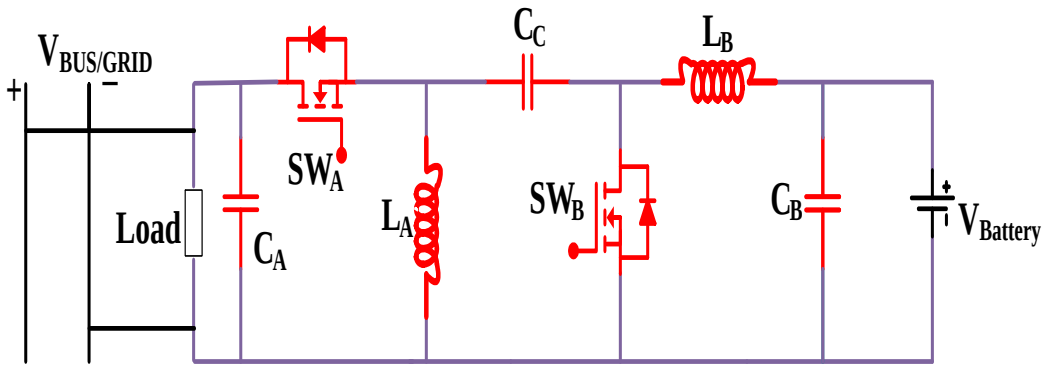

Fig.4. 3. Bidirectional SEPIC/ZETA DC-DC Converter Systematic Diagram

Table 4. 2 Operational Modes

Conditions	Operating Mode	Current Flow
Grid Voltage < load voltage	SEPIC	Battery to Grid
Grid Voltage > load voltage	ZETA	Grid to Battery
Grid voltage = load voltage	-	Battery in standby mode

4.3 Operational Modes

MODE 1: CHARGING (ZETA)

This mode charges the battery. Power flows from the DC bus (V_{BUS}), which is typically 80volts, to the 48volt battery through the Bidirectional Converter (BDC). In this scenario, the BDC acts like a Zeta converter, and switch (SW_A) turns on. To achieve the necessary voltage step-down for charging, the switch typically operates at a duty cycle below 50%.

MODE 2: DISCHARGING (SEPIC)

This mode handles battery discharge. Power flows from the battery ($V_{Battery}$), which is typically 48 volts, to the 80volt DC bus through the BDC. In this scenario, the BDC acts like a SEPIC converter, and switch (SW_B)takes over. To achieve the necessary voltage step-up for discharge, the switch generally operates at a duty cycle above 50%.

4.4 SEPIC Converter

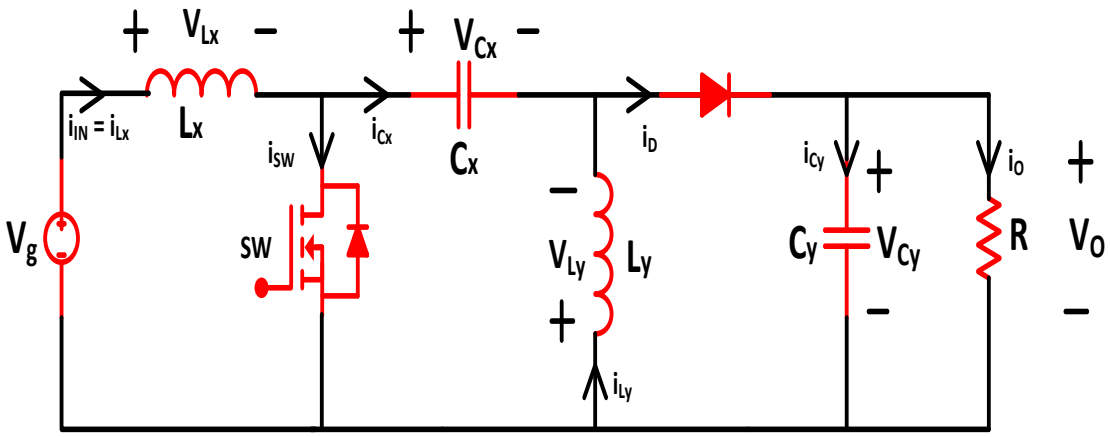

Fig.4. 4.SEPIC Converter Schematic Diagram

A SEPIC (Single-Ended Primary Inductor Converter) converter is a type of DC-DC converter that allows the output voltage to be higher than, lower than, or equal to the input voltage. This versatility makes SEPIC converters highly valuable in a variety of applications where the input voltage may vary above and below the desired output voltage.

The SEPIC converter, characterized by a non-linear fourth-order configuration because it has two capacitors and two inductors, belongs to the category of DC-DC converters designed to effectively modulate the output voltage in either an upward or downward direction. This converter is specifically categorized as a non-isolated type, signifying that there is a shared ground connection between the input and output voltages. Comprising two inductors ($\boldsymbol{L_x, L_y}$), two capacitors (C_x, C_y) and a switch (SW), the Zeta converter's configuration is illustrated in Fig.4.4.

4.4.1 Modes of Operation

MODE 1 (SW IS CLOSED)

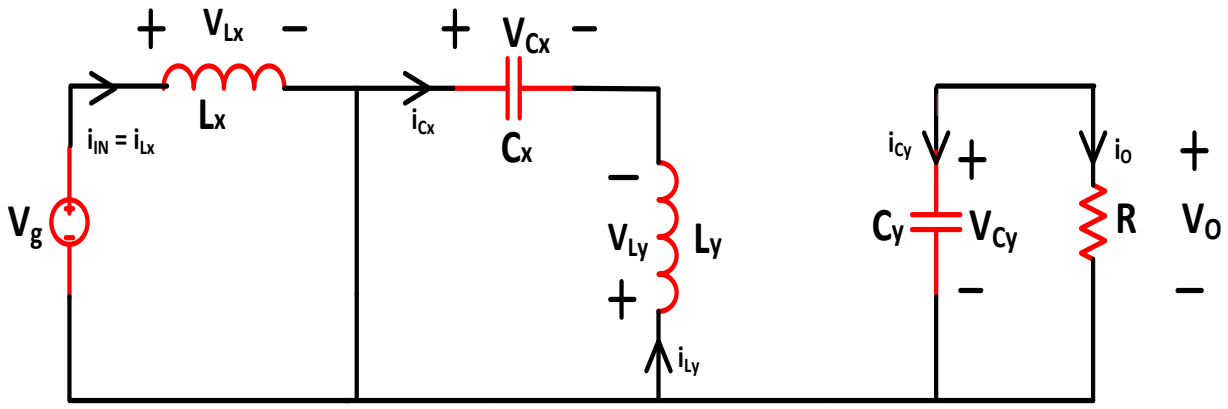

Fig.4. 5. Schematic diagram of SEPIC Converter in Mode 1 (SW is ON)

When SW is On, the diode will be in OFF state. The source voltage appears across the inductor $\boldsymbol{L_x}$ and causes its current ($\boldsymbol{i_{L_x}}$) to increase linearly, while the inductor $\boldsymbol{L_y}$ begins to store energy from the series capacitor via $\boldsymbol{C_x}$ which causes $\boldsymbol{i_{L_y}}$ to increase linearly and capacitor C_y discharges through the load.

$$V_{L_x} = V_g \tag{4.32}$$

$$V_{L_y} = V_{C_x} \tag{4.33}$$

$$i_{C_y} = -i_0 \tag{4.34}$$

$$i_{C_x} = -i_{L_y} \tag{4.35}$$

MODE 2 (SW IS OPEN)

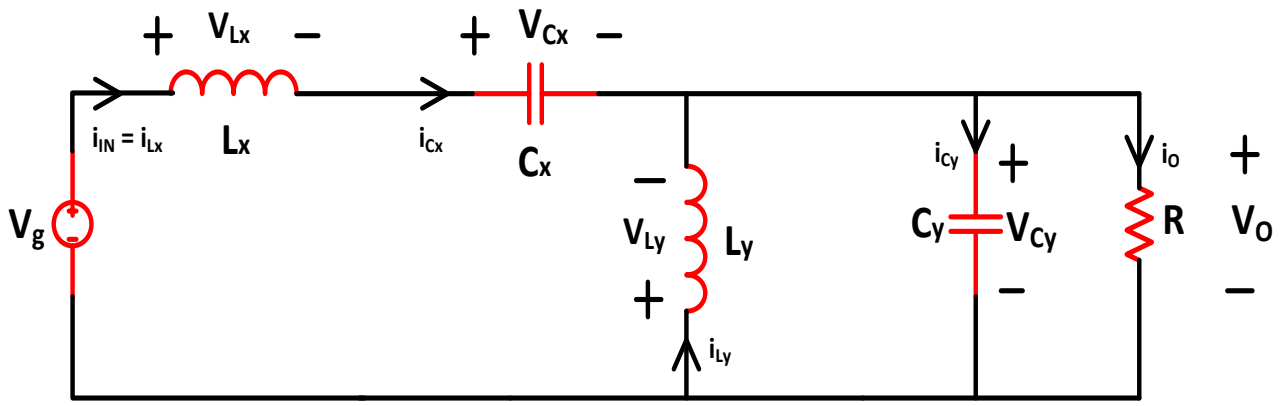

Fig.4. 6. Schematic diagram of SEPIC Converter in Mode 2 (SW is OFF)

In mode 2 Switch is open as shown in Fig.4.6. When SW is OFF, the diode will be in ON state. Inductor $L_x$charges the capacitor $C_x$in series, and Inductor L_y provides the output power, or discharges through the load which causes $i_{L_x}$and $i_{L_y}$to decrease linearly. This is how the Zeta converter operates and its output current is continuous.

$$V_{L_x} = V_g - V_0 - V_{C_x} \quad (4.36)$$

$$V_{L_y} = V_0 \quad (4.37)$$

$$i_{C_x} = i_{L_x} \quad (4.38)$$

$$i_{C_y} = i_{L_x} + i_{L_y} - i_0 \quad (4.39)$$

4.4.2 Circuit Expressions of SEPIC Converter

Output Voltage(V_0):

Applying Volt-Sec Balance:

$$V_g * D * T_s - V_0 * (1 - D) * T_s = 0 \quad (4.40)$$

$$V_0 = V_g * \frac{D}{1 - D} \quad (4.41)$$

Inductor Current$\left(I_{L_x} and\ I_{L_y}\right)$:

$$I_{L_x} = I_{IN} \tag{4.42}$$

$$I_{L_y} = I_0 \tag{4.43}$$

Inductor Values$\left(L_x and\ L_y\right)$:

$$L_x = V_g * \frac{D}{\Delta i_{L_x} * f_{SW}} \tag{4.44}$$

$$L_y = V_g * \frac{D}{\Delta i_{L_y} * f_{SW}} \tag{4.45}$$

Capacitor Values$\left(C_x and\ C_y\right)$:

$$C_x = \frac{D}{R * f_{SW} * \left(\frac{\Delta V_{C_x}}{V_0}\right)} \tag{4.46}$$

$$C_y = \frac{D}{R * f_{SW} * \left(\frac{\Delta V_{C_y}}{V_0}\right)} \tag{4.47}$$

4.5 Circuit Parameter Calculation of Bidirectional SEPIC/ZETA Converter

Considering the input voltage $V_{BUS} = 80V$, the output voltage $V_{Battery} = 48V$, the switching frequency $f_{SW} = 50KHz$, output power $P_0 = 240W$, the ripple current in inductors$(\Delta i_{L_1}, \Delta i_{L_2})$ and ripple in capacitor voltage $(\Delta V_{C_1}, \Delta V_{C_2})$ to be 3%.

Parameter Calculation for Charging Mode (Zeta Mode)

Duty Cycle(D):

By using eq. 2.14

$$V_{Battery} = D * \frac{V_{BUS}}{1 - D}$$

$$48 = D * \frac{80}{1 - D}$$

$$D = 0.375$$

Inductor Current(I_{L_A}):

By using eq. 2.26

$$I_{L_A} = I_{BUS}$$

By using eq. 2.19

$$I_{BUS} = D * \frac{I_{Battery}}{1 - D}$$

Put eq. 2.19 in eq. 2.26 then we get

$$I_{L_A} = D * \frac{I_{Battery}}{1 - D}$$

$$I_{L_A} = 0.375 * \frac{240/48}{1 - 0.375}$$

$$I_{L_A} = 3A$$

Inductor Current(I_{L_B}):

By using eq. 2.22

$$I_{L_B} = I_{Battery}$$

$$I_{L_2} = 5A$$

Inductor Value(L_A):

By using eq. 2.32

$$L_A = R * \frac{(1 - D)^2}{D * f_{SW} * \left(\frac{\Delta I_{L_A}}{I_{L_A}}\right)}$$

$$L_A = \frac{48}{5} * \frac{(1 - 0.375)^2}{0.375 * 50 * 10^3 * (0.03)}$$

$$L_A = 6.7mH$$

Inductor Value(L_B):

By using eq. 2.38

$$L_B = (1 - D) * \frac{R}{\left(\frac{\Delta I_{L_B}}{I_{L_B}}\right) * f_{SW}}$$

$$L_B = (1 - 0.375) * \frac{9.6}{(0.03) * 50 * 10^3}$$

$$L_B = 4mH$$

Capacitor Value(C_C):

By using eq. 2.44

$$C_C = \frac{D}{R * f_{SW} * \left(\frac{\Delta V_{C_C}}{V_{C_C}}\right)}$$

$$C_C = \frac{0.375}{9.6 * 50 * 10^3 * (0.03)}$$

$$C_C = 26.042uF$$

Capacitor Value(C_B):

By using eq. 2.51

$$C_B = \frac{(1 - D)}{8 * f_{SW}^2 * \left(\frac{\Delta V_{C_B}}{V_{C_B}}\right) * L_B}$$

$$C_B = \frac{(1 - 0.375)}{8 * (50 * 10^3)^2 * (0.03) * 4 * 10^{-3}}$$

$$C_B = 0.26uF$$

Parameter Calculation for Discharging Mode (SEPIC Mode)

Duty Cycle(D):

By using eq. 4.41

$$V_{BUS} = V_{Battery} * \frac{D}{1-D}$$

$$80 = 48 * \frac{D}{1-D}$$

$$D = 0.625$$

Inductor Current(I_{L_B}):

By using eq. 4.42

$$I_{L_B} = I_{Battery}$$

$$I_{L_B} = 5A$$

Inductor Current(I_{L_A}):

By using eq. 4.43

$$I_{L_A} = I_{BUS}$$

$$I_{L_A} = 3A$$

Inductor Value(L_B):

By using eq. 4.44

$$L_B = V_{Battery} * \frac{D}{\Delta i_{L_B} * f_{SW}}$$

$$L_B = 48 * \frac{0.625}{\frac{3*5}{100} * 50 * 10^3}$$

$$L_B = 4mH$$

Inductor Value(L_A):

By using eq. 4.45

$$L_A = V_{Battery} * \frac{D}{\Delta i_{L_A} * f_{SW}}$$

$$L_A = 48 * \frac{0.625}{\frac{3*3}{100} * 50 * 10^3}$$

$$L_A = 6.7mH$$

Capacitor Value(C_C):

By using eq. 4.46

$$C_c = \frac{D}{R * f_{SW} * \left(\frac{\Delta V_{C_c}}{V_c}\right)}$$

$$C_c = \frac{0.625}{\left(\frac{80}{3}\right) * 50 * 10^3 * (0.03)}$$

$$C_c = 15.624uF$$

Capacitor Value(C_A):

By using eq. 4.47

$$C_A = \frac{D}{R * f_{SW} * \left(\frac{\Delta V_{C_A}}{V_{C_A}}\right)}$$

$$C_A = \frac{0.625}{\left(\frac{80}{3}\right) * 50 * 10^3 * (0.03)}$$

$$C_A = 15.624uF$$

Parameters Of Bidirectional SEPIC/ZETA Converter

Table 4.3 shows detailed parameters related to SEPIC/ZETA Bidirectional (DC-DC) Converter.

Table 4. 3 Converter parameters.

PARAMETERS	RATINGS
V_{BUS}	80V
$V_{Battery}$	48V
$I_{Battery}$	5A
L_A	6.7mH
L_B	4mH
C_A	15.264µF
C_B	0.26µF
Load	26.667Ω
C_C **(Coupling capacitor)**	26.042µF
f_{SW} **(Switching frequency)**	50kHz

4.6 State Space Modelling of The Converter

In examining the state space modeling of ZETA and SEPIC converters, we delve into their dynamic behaviors and control mechanisms. By constructing state space equations, we uncover the intricate relationships among crucial parameters, offering insights into both transient and steady-state responses. This analytical approach not only allows for accurate system characterization but also facilitates the development of tailored control techniques, optimizing the performance and effectiveness of ZETA and SEPIC converters across various applications.

ZETA Mode (Charging)

Fig. 4.7 depicts the circuitry of the bidirectional converter configured in the ZETA arrangement during battery charging mode. The mathematical equations describing the ZETA circuit's behavior in both on and off modes, necessary for deriving the average state space model, are presented in equations (4.4) -(4.17).

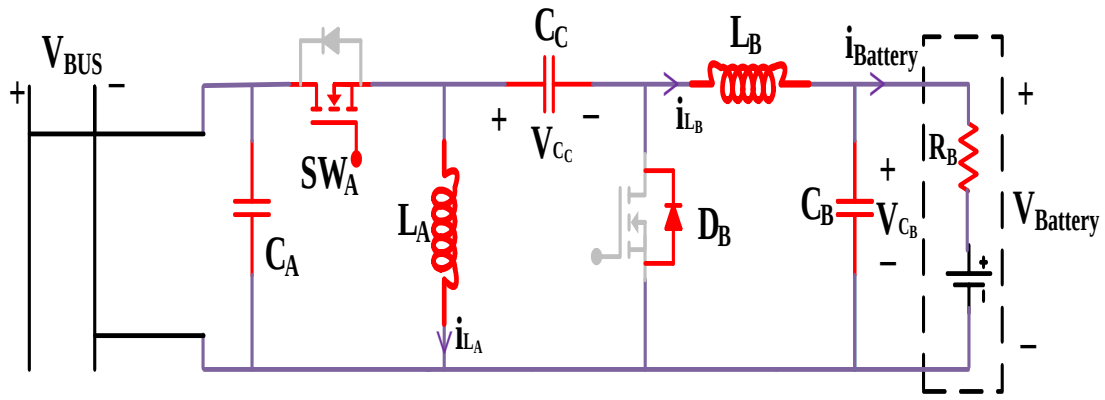

Fig.4. 7.ZETA mode configuration

Based on the state space representation obtained from the circuit equations, a small-signal model is built to examine the converter's small-signal behavior. The currents (i_{L_A} and i_{L_B}) passing through the inductors and the voltages (V_{C_C} and V_{C_B}) across the capacitors are identified in this research paper as the state variables of the Zeta converter. The output voltage functions as the output variable, and the input voltage is regulated as the controlled input variable. The equations listed below describe the Zeta converter.

$$x = \begin{bmatrix} i_{L_A} \\ i_{L_B} \\ V_{C_C} \\ V_{C_B} \end{bmatrix}, u = [V_{BUS}], y = \left[V_{Battery}\right] \tag{4.1}$$

This system is represented in state space model as:

$$\dot{x} = AX + BU \tag{4.2}$$

$$y = CX + EU \tag{4.3}$$

In mode I ZETA converter's state space equations are as follows:

$$\frac{di_{L_A}}{dt} = \frac{V_{BUS}}{L_A} \tag{4.4}$$

$$\frac{di_{L_B}}{dt} = \frac{V_{BUS} + V_{C_C} - V_{C_B}}{L_B} \tag{4.5}$$

$$\frac{dV_{C_C}}{dt} = -\frac{i_{L_B}}{C_C} \tag{4.6}$$

$$\frac{dV_{C_B}}{dt} = \frac{i_{L_B}}{C_B} - \frac{V_{C_B}}{R_B C_B} \tag{4.7}$$

$$V_{Battery} = V_{C_B} \tag{4.8}$$

$$\begin{bmatrix} \frac{di_{L_A}}{dt} \\ \frac{di_{L_B}}{dt} \\ \frac{dV_{C_C}}{dt} \\ \frac{dV_{C_B}}{dt} \end{bmatrix} = \begin{bmatrix} 0 & 0 & 0 & 0 \\ 0 & 0 & \frac{1}{L_B} & -\frac{1}{L_B} \\ 0 & -\frac{1}{C_C} & 0 & 0 \\ 0 & \frac{1}{C_B} & 0 & -\frac{1}{RC_B} \end{bmatrix} \begin{bmatrix} i_{L_A} \\ i_{L_B} \\ V_{C_C} \\ V_{C_B} \end{bmatrix} + \begin{bmatrix} \frac{1}{L_A} \\ \frac{1}{L_B} \\ 0 \\ 0 \end{bmatrix} [V_{BUS}] \tag{4.9}$$

$$\left[V_{Battery}\right] = [0 \quad 0 \quad 0 \quad 1]\begin{bmatrix} i_{L_A} \\ i_{L_B} \\ V_{C_C} \\ V_{C_B} \end{bmatrix} + [0][V_{BUS}] \tag{4.10}$$

In mode II ZETA converter's state space equations are as follows:

$$\frac{di_{L_A}}{dt} = -\frac{V_{C_C}}{L_A} \tag{4.11}$$

$$\frac{di_{L_B}}{dt} = -\frac{V_{C_B}}{L_B} \tag{4.12}$$

$$\frac{dV_{C_C}}{dt} = \frac{i_{L_A}}{C_C} \tag{4.13}$$

$$\frac{dV_{C_B}}{dt} = \frac{i_{L_B}}{C_B} - \frac{V_{C_B}}{R_B C_B} \tag{4.14}$$

$$V_{Battery} = V_{C_B} \tag{4.15}$$

$$\begin{bmatrix} \frac{di_{L_A}}{dt} \\ \frac{di_{L_B}}{dt} \\ \frac{dV_{C_C}}{dt} \\ \frac{dV_{C_B}}{dt} \end{bmatrix} = \begin{bmatrix} 0 & 0 & -\frac{1}{L_A} & 0 \\ 0 & 0 & 0 & -\frac{1}{L_B} \\ \frac{1}{C_C} & 0 & 0 & 0 \\ 0 & \frac{1}{C_B} & 0 & -\frac{1}{R_B C_B} \end{bmatrix} \begin{bmatrix} i_{L_A} \\ i_{L_B} \\ V_{C_C} \\ V_{C_B} \end{bmatrix} + \begin{bmatrix} 0 \\ 0 \\ 0 \\ 0 \end{bmatrix} [V_{BUS}] \tag{4.16}$$

$$\left[V_{Battery}\right] = [0 \quad 0 \quad 0 \quad 1]\begin{bmatrix} i_{L_A} \\ i_{L_B} \\ V_{C_C} \\ V_{C_B} \end{bmatrix} + [0][V_{BUS}] \tag{4.17}$$

SEPIC Mode (Discharging)

Fig.4.8 depicts the circuitry of the bidirectional converter configured in the SEPIC

arrangement during battery discharging mode. The mathematical equations describing the SEPIC circuit's behavior in both on and off modes, necessary for deriving the average state space model, are presented in equations (4.18) -(4.31).

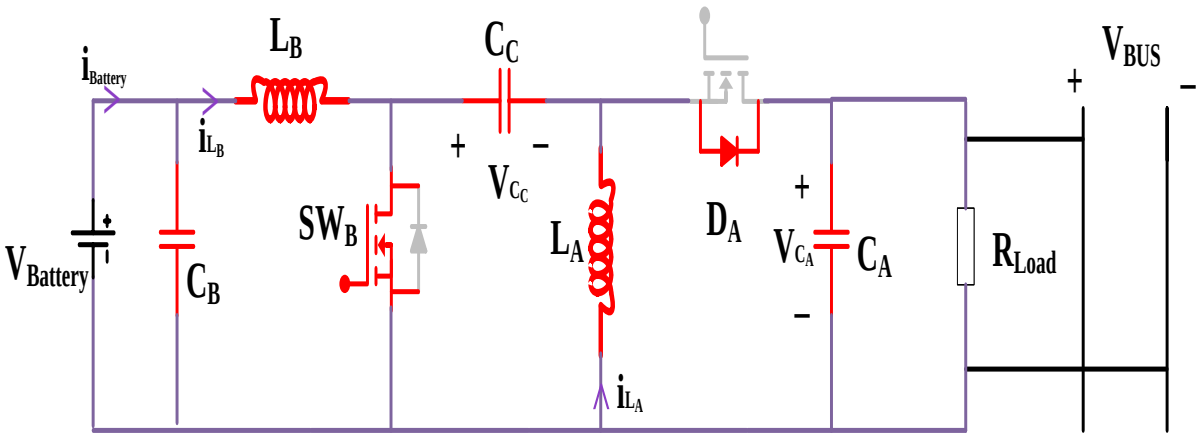

Fig.4. 8.SEPIC Mode configuration

In mode I SEPIC converter's state space equations are as follows:

$$\frac{di_{L_B}}{dt} = \frac{V_{Battery}}{L_B} \tag{4.18}$$

$$\frac{di_{L_A}}{dt} = \frac{V_{C_C}}{L_A} \tag{4.19}$$

$$\frac{dV_{C_C}}{dt} = -\frac{i_{L_A}}{C_C} \tag{4.20}$$

$$\frac{dV_{C_A}}{dt} = -\frac{V_{C_A}}{R_{Load}C_A} \tag{4.21}$$

$$V_0 = V_{C_A} \tag{4.22}$$

$$\begin{bmatrix} \frac{di_{L_B}}{dt} \\ \frac{di_{L_A}}{dt} \\ \frac{dV_{C_C}}{dt} \\ \frac{dV_{C_A}}{dt} \end{bmatrix} = \begin{bmatrix} 0 & 0 & 0 & 0 \\ 0 & 0 & \frac{1}{L_A} & 0 \\ 0 & -\frac{1}{C_C} & 0 & 0 \\ 0 & 0 & 0 & -\frac{1}{R_{Load}C_A} \end{bmatrix} \begin{bmatrix} i_{L_B} \\ i_{L_A} \\ V_{C_C} \\ V_{C_A} \end{bmatrix} + \begin{bmatrix} \frac{1}{L_B} \\ 0 \\ 0 \\ 0 \end{bmatrix} [V_{Battery}] \tag{4.23}$$

$$[V_{Bus}] = [0 \quad 0 \quad 0 \quad 1] \begin{bmatrix} i_{L_B} \\ i_{L_A} \\ V_{C_C} \\ V_{C_A} \end{bmatrix} + [0][V_{Battery}] \tag{4.24}$$

In mode II SEPIC converter's state space equations are as follows:

$$\frac{di_{L_B}}{dt} = \frac{V_{Battery} - V_{C_C} - V_{C_A}}{L_B} \tag{4.25}$$

$$\frac{di_{L_A}}{dt} = -\frac{V_{C_A}}{L_A} \tag{4.26}$$

$$\frac{dV_{C_C}}{dt} = \frac{i_{L_B}}{C_C} \tag{4.27}$$

$$\frac{dV_{C_A}}{dt} = \frac{i_{L_B}}{C_A} + \frac{i_{L_A}}{C_A} - \frac{V_{C_A}}{R_{Load}C_A} \tag{4.28}$$

$$V_{Bus} = V_{C_A} \tag{4.29}$$

$$\begin{bmatrix} \frac{di_{L_B}}{dt} \\ \frac{di_{L_A}}{dt} \\ \frac{dV_{C_C}}{dt} \\ \frac{dV_{C_A}}{dt} \end{bmatrix} = \begin{bmatrix} 0 & 0 & -\frac{1}{L_B} & -\frac{1}{L_B} \\ 0 & 0 & 0 & -\frac{1}{L_A} \\ \frac{1}{C_C} & 0 & 0 & 0 \\ \frac{1}{C_A} & \frac{1}{C_A} & 0 & -\frac{1}{R_{Load}C_A} \end{bmatrix} \begin{bmatrix} i_{L_B} \\ i_{L_A} \\ V_{C_C} \\ V_{C_A} \end{bmatrix} + \begin{bmatrix} \frac{1}{L_B} \\ 0 \\ 0 \\ 0 \end{bmatrix} [V_{Battery}] \tag{4.30}$$

$$[V_{Bus}] = [0 \quad 0 \quad 0 \quad 1]\begin{bmatrix} i_{L_B} \\ i_{L_A} \\ V_{C_C} \\ V_{C_A} \end{bmatrix} + [0][V_{Battery}] \tag{4.31}$$

The circuit calculations eliminate the switching ripple component by averaging across one switching period, resulting in the creation of the averaged switching model using eq. (2.68) -(2.71).

$$A = A_1 d + A_2(1-d)$$

$$B = B_1 d + B_2(1-d)$$

$$C = C_1 d + C_2(1-d)$$

$$E = E_1 d + E_2(1-d)$$

Before obtaining the small-signal model of the converter, it's necessary to linearize the nonlinear averaged state-space model around a specific operating point. This involves introducing small disturbances, termed perturbations, to the state variables of the system and its parameter, also to its input variables as well using eq. (2.72) -(2.75).

$$d = D + \hat{d},\ x = X + \hat{x},\ u = U + \hat{u},\ y = Y + \hat{y}$$

By replacing the averaged state space model (eq. 32-35) from the perturbed variables and neglecting steady-state terms and higher-order influences, the linearized small-signal model is obtained in the following manner using eq. (2.76) -(2.78).

$$s\hat{x}(s) = A\hat{x}(s) + B\hat{u}(s) + \big((A_1 - A_2)X(s) + (B_1 - B_2)U(s)\big)\hat{d}(s)$$

$$\hat{y}(s) = C\hat{x}(s) + E\hat{u}(s) + ((A_1 - A_2)X(s) + (E_1 - E_2)U(s))\hat{d}(s)$$

$$\frac{\hat{x}(s)}{\hat{d}(s)} = (sI - A)^{-1}\big((A_1 - A_2)X(s) + (B_1 - B_2)U(s)\big)$$

The transfer function for the ZETA mode, determined through small signal analysis and averaging while incorporating circuit parameters in terms of duty cycle, can be represented as:

$$\frac{\widehat{v_0}(s)}{\hat{d}(s)} = \frac{1.069e08\, s^3 + 2.086e11\, s^2 + 1.288e13\, s + 1.178e18}{s^5 + 4e05\, s^4 + 1.07e09\, s^3 + 1.644e12\, s^2 + 2.162e15\, s + 1.178e18} \quad (4.32)$$

Likewise, for the SEPIC mode, the transfer function can be formulated as follows:

$$\frac{\widehat{v_0}(s)}{\hat{d}(s)} = \frac{-5.12e05\, s\text{^}3 + 1.229e09\, s\text{^}2 - 1.842e12\, s + 4.422e15}{s\text{^}4 + 2400\, s\text{^}3 + 7.198e06\, s\text{^}2 + 8.637e09\, s + 1.295e13} \quad (4.33)$$

4.7 Control Strategy For ZETA/SEPIC Bidirectional Converter

Fig.4.9 shows the basic idea of the control strategy (PI) which is proposed for the system. Using the ZETA mode for charging and the SEPIC mode for discharging, a PI controller is used in this configuration to control both charging and discharging operations. The reference values (V_{Ref_L}, V_{Ref_B}), feedback, and control output of the PI system are modified in accordance with whether the system is in ZETA or SEPIC mode.

The tuning of the PI controller for the system is carried out using the classical Ziegler-Nichols (ZN) method. This involves determining the parameters by performing the averaging of the state space model for the transfer function. As a result, the PI gains obtained are presented in Table 4.4.

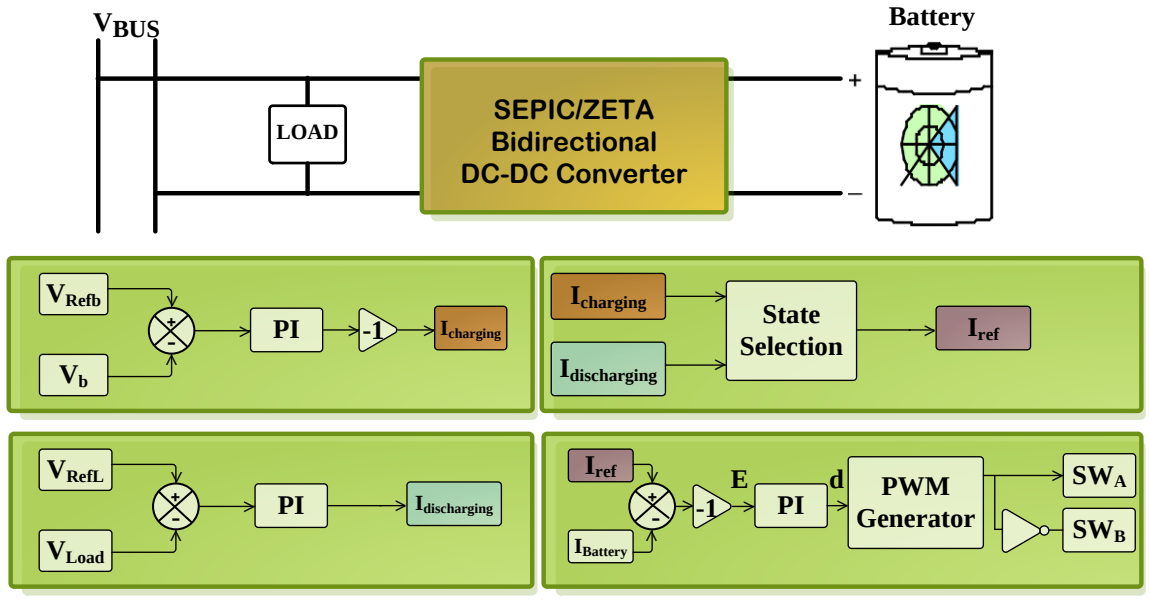

Fig.4. 9. Proposed Control Strategy

Table 4. 4 Parameters of Controller

Loop	Mode	K_p	K_i
Voltage Loop	Charging	50	10e3
	Discharging	0.5	50
Current Loop	Charging/ Discharging	0.05	10

4.8 Results and Analysis

The output results for the converter are evaluated in MATLAB/SIMULINK for scenarios involving both charging and discharging of the battery.

4.8.1 Charging Mode (Zeta Converter):

During the charging phase, the state of charge (SOC%) of the battery gradually increases, accompanied by a rise in battery voltage. The corresponding waveforms

depicting the battery current are illustrated in Fig.4.10.

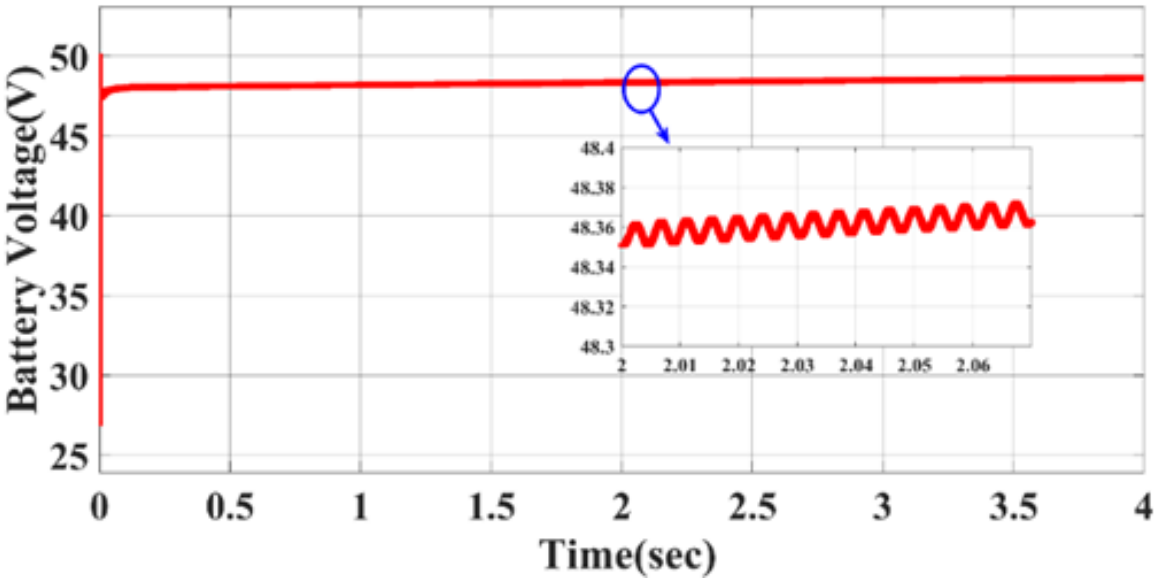

(a)

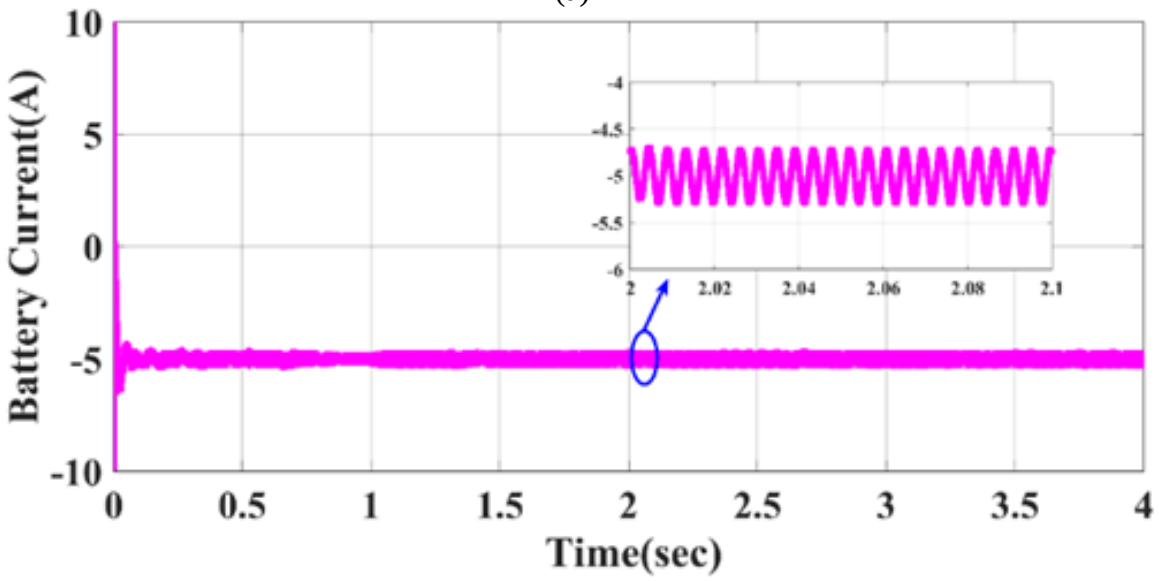

(b)

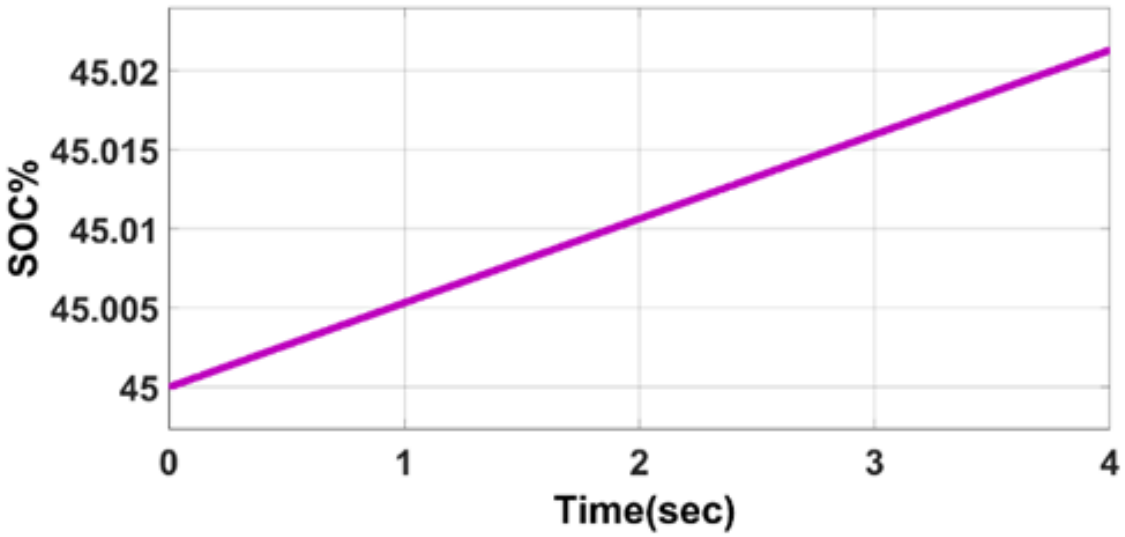

(c)

Fig.4. 10. Charging mode (a) Battery Voltage (b) Battery Current (c) %SOC

4.8.2 Discharging Mode (SEPIC Converter)

During the charging phase, the state of charge (SOC%) of the battery gradually decreases, accompanied by a fall in battery voltage. The corresponding waveforms depicting the battery current are illustrated in Fig.4.11.

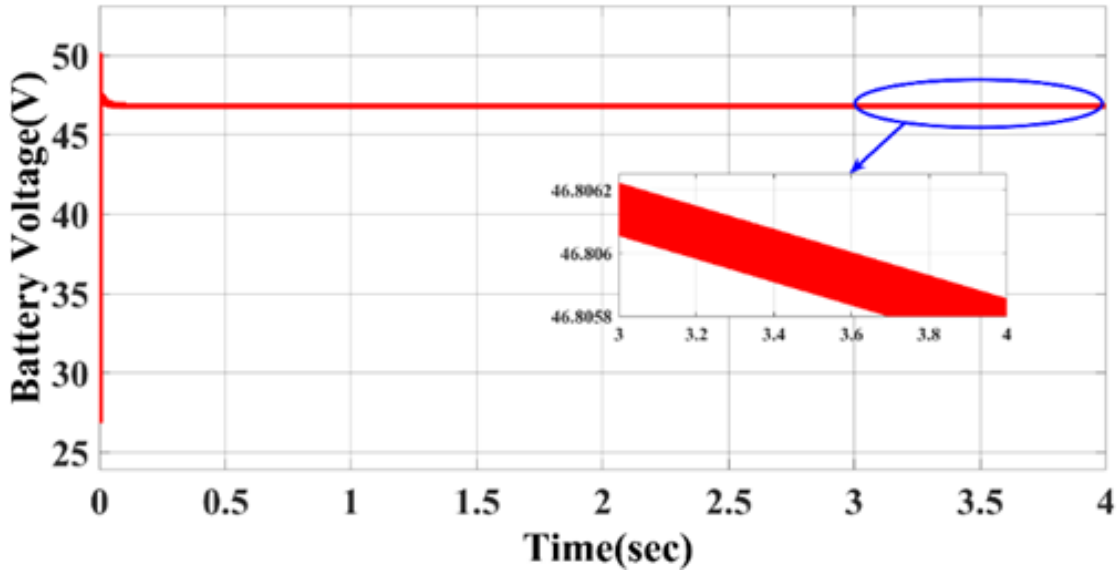

(a)

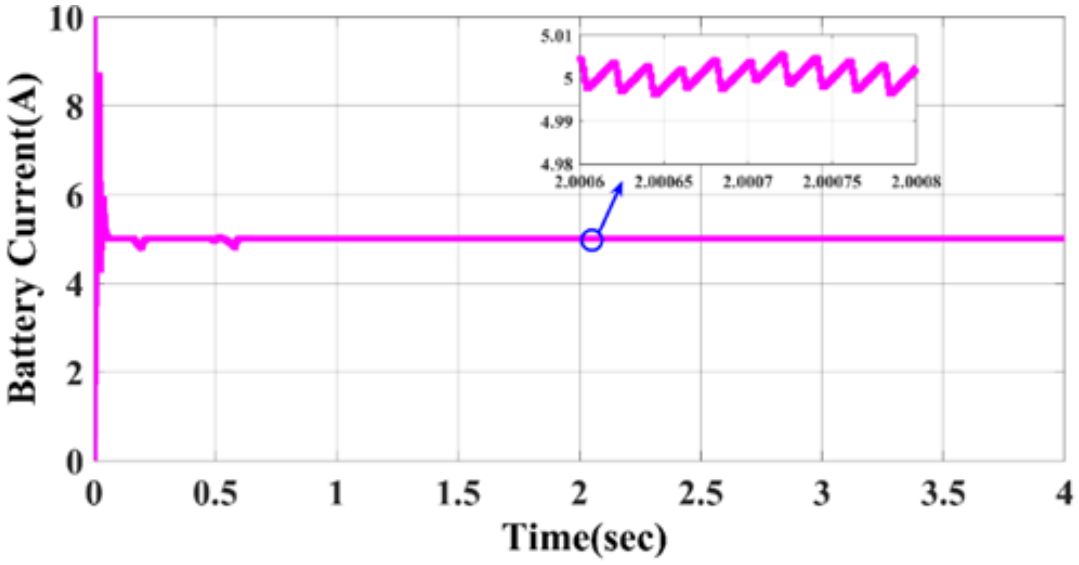

(b)

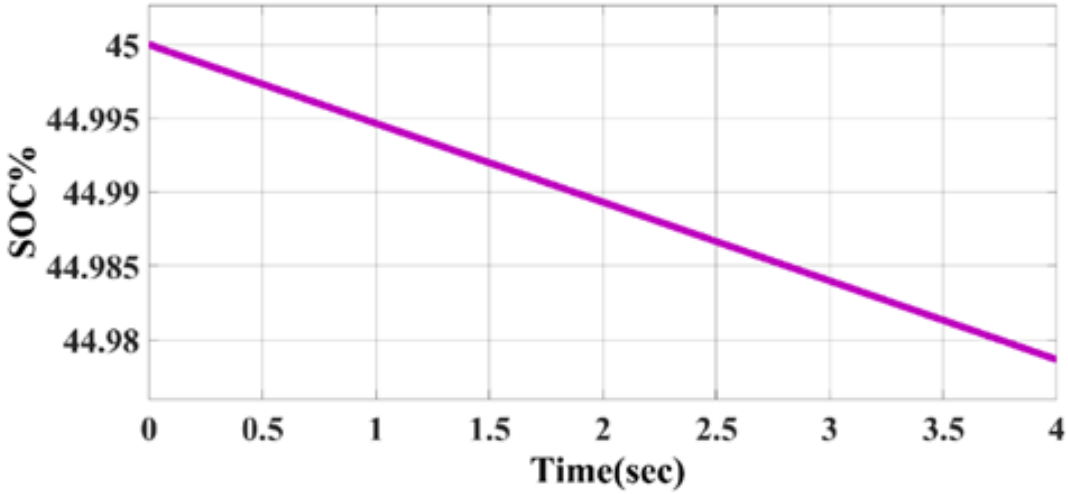

(c)

Fig.4. 11. Discharging mode (a) Battery Voltage (b) Battery Current (c) %SOC

4.8.3 Charging and Discharging Mode

The bidirectional converter showcases its effectiveness in both charging and discharging modes, as evidenced by the comprehensive depiction in Fig.4.12. These figures vividly illustrate the converter's adeptness in seamlessly handling operations in both modes, underscoring its efficiency and versatility.

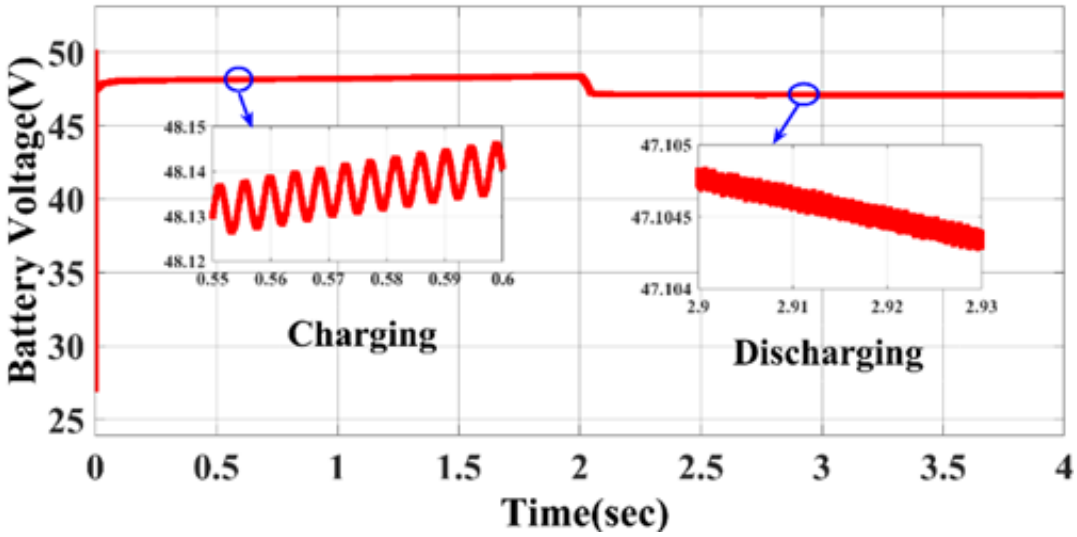

(a)

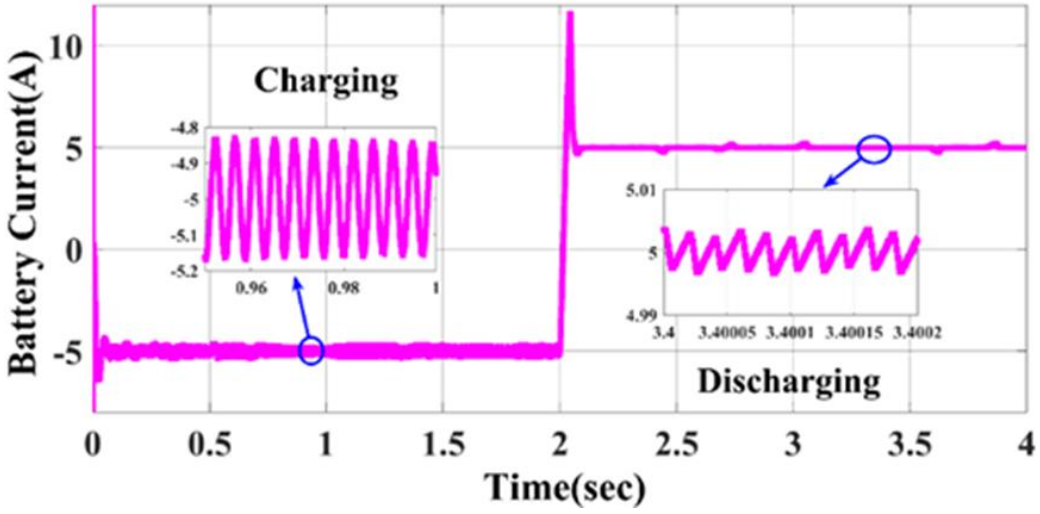

(b)

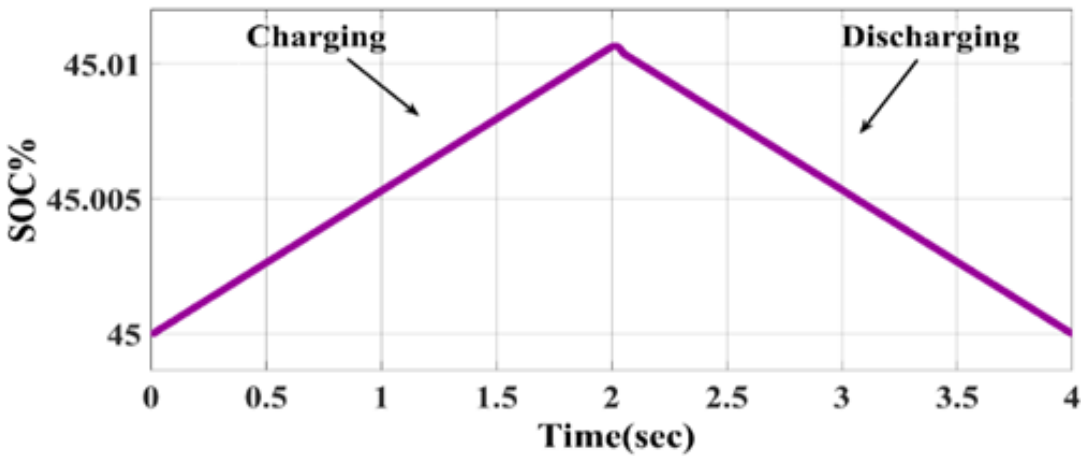

(c)

Fig.4. 12. Charging and Discharging mode (a) Battery Voltage (b) Battery Current (c) %SOC

4.9 Conclusion

This chapter focuses on modeling the Bidirectional SEPIC/ZETA converter and designing a control system to ensure the battery charges and discharges with a constant current. The Bidirectional SEPIC/ZETA converter is chosen because it has low output voltage ripple, making it ideal for applications like EV battery management, UPS, HVDC transmission, and smart grids.

The chapter examines the SEPIC and Zeta modes separately, with an emphasis on maintaining a constant current during battery charging and discharging. The Ziegler-Nichols method is used to optimize the PI controllers, which improves transient response and reduces steady-state error. This allows for successful control of battery charging and discharging with a constant current of 5A. The robust control system ensures efficient and stable battery management.

CHAPTER 5
CONCLUSION AND FUTURE SCOPE

5.1 Conclusion

In this work, the comprehensive study on Zeta converters delves into their operating modes, design aspects, and the development of small signal models, offering valuable insights into their functionality and control mechanisms. Closed-loop voltage mode control, known for its simplicity and ease of implementation, has been thoroughly analysed. By employing a Proportional-Integral-Derivative (PID) controller, this control method demonstrates significant effectiveness in maintaining a stable and accurate output voltage. The PID controller's ability to mitigate the effects of non-idealities such as component tolerances and parameter variations is particularly noteworthy. Experimental results reveal that the closed-loop voltage mode control effectively reduces output voltage deviations during load variations from 5W to 20W and maintains a stable output voltage of 12V despite input voltage fluctuations ranging from 24V to 48V. This robust performance in line regulation showcases the potential of the closed-loop voltage mode control for applications that prioritize precise voltage regulation.

Moreover, the implementation of the PID controller within this control scheme leads to a notable improvement in system efficiency. The reduction in peak overshoot by 28% and the swift response of the PID controller contribute to enhanced overall performance. These findings validate the significant benefits of using a PID controller within closed-loop voltage mode control for non-ideal Zeta converters. However, it is essential to recognize that while this method excels in precise voltage regulation, its ability to handle dynamic load conditions and input voltage fluctuations may be limited compared to alternative control approaches.

Furthermore, the study extends its analysis to the modelling of a bidirectional DC-DC converter using SEPIC/Zeta circuitry, specifically designed for battery-

related applications. The implementation of a PID control system effectively manages the battery charging and discharging processes, resulting in satisfactory state of charge (SOC) levels as validated by MATLAB/SIMULINK simulations. The Ziegler-Nichols method employed to ascertain the PID parameters (Kp, Ki, and Kd) enhances the converter's control performance, ensuring a constant current during both charging and discharging modes.

In summary, the research demonstrates the effectiveness of PID control in both closed-loop voltage mode and bidirectional converter applications. The closed-loop voltage mode control, with its simplicity and efficiency in voltage regulation, proves suitable for applications requiring stable output voltage. Conversely, the closed-loop current mode control offers robust performance in handling dynamic load conditions and input voltage fluctuations, making it ideal for diverse applications. The comprehensive modelling and validation of the bidirectional converter further emphasize the practicality and efficiency of PID control in battery management systems.

5.2 Future Scope

1. Optimization of PID Parameters:

Future research should focus on optimizing PID parameters for diverse operating conditions to enhance Zeta converter performance. Advanced optimization techniques such as Particle Swarm Optimization (PSO), Genetic Algorithms (GA), and Fuzzy Logic should be explored to achieve better tuning precision and control performance, particularly in dynamic scenarios where the Ziegler-Nichols method shows limitations.

2. Hardware Implementation Validation:

Validating the proposed system through hardware implementation is essential. Real-world hardware testing will provide practical insights and highlight challenges not apparent in MATLAB/SIMULINK simulations. Comparing hardware results with simulation data will help identify discrepancies and areas for improvement, ensuring system robustness and reliability in actual applications.

3. Exploration of Adaptive Control Strategies:

Research should explore adaptive control strategies that dynamically adjust PID parameters in real-time based on operating conditions. This approach can enhance the system's ability to manage varying load conditions and input voltage fluctuations more effectively. Integrating machine learning algorithms for predictive control and optimization can further advance the field, enabling the converter to anticipate and adapt to changes proactively.

REFERENCES

[1]. Singh, Prashant, Alka Singh, and Ankita Arora. "A Comprehensive Study on the Closed Loop Performance of a Zeta Converter." *2023 11th National Power Electronics Conference (NPEC)*. IEEE, 2023.

[2]. P. R. Babu, S. R. Prasath and R. Kiruthika, "Simulation and performance analysis of CCM Zeta converter with PID controller," 2015 International Conference on Circuits, Power and Computing Technologies [ICCPCT-2015], Nagercoil, India, 2015.

[3]. Niculescu, E., Mioara-Purcaru, D., Niculescu, M. C., Purcaru, I., & Maria, M. (2009, July). A simplified steady-state analysis of the PWM Zeta converter. In *WSEAS International Conference. Proceedings. Mathematics and Computers in Science and Engineering*.

[4]. C. Sudhakarababu and M. Veerachary, Zeta Converter for Power Factor Correction and Voltage Regulation, 2004 TENCON Proc., vol. 4, 2004

[5]. J.-L., Lin, S.-P., Yang, and P.-W. Lin, Small Signal Analysis and Controller Design for an Isolated Zeta Converter with High Power Factor Correction, Electric Power Systems Research 76, © 2005 Elsevier B.V., 2005, pp. 67–76.

[6]. Mittal, S., Singh, A., & Chittora, P. (2022, October). EV Control in G2V and V2G modes using SOGI Controller. In *2022 IEEE 3rd Global Conference for Advancement in Technology (GCAT)*.

[7]. Vuthchhay,Eng and Chanin Bunlaksananusorn, “Dynamic modelling of a Zeta converter with State-Space averaging technique”, In Electrical Engineering/Electronics, Computer, Telecommunications and Information Technology 2008,ECTI-CON 2008,5th International Conference on, vol. 2,IEEE 2008.

[8]. Kochcha, Pijit and Sarawut Sujitjorn, “Isolated zeta converter: principle of operation and design in continuous conduction mode”, WSEAS Transactions on Circuits and Systems 9, no. 7 (2010).

[9]. Rashid, Muhammad Harunur. Power electronics: circuits, devices, and Applications. Vol. 2. NJ: Prentice Hall, 1988.

[10]. Preeja, J. P. and S. V. Kayalvizhi, “Transient Response Improvement of Cuk Converter using SMC & FLC”.

[11]. Shi-Peng Huang, Hua-Qing Xu and Yan-Fei Liu, "Sliding-mode controlled Cuk switching regulator with fast response and first-order dynamic characteristic," 20th Annual IEEE Power Electronics Specialists Conference, Milwaukee, WI, USA, 1989 vol.1, doi: 10.1109/PESC.1989.48481.

[12]. P. K. Singh, Y. V. Hote and M. M. Garg, "Comments on "PI and sliding mode control of a cuk converter"," in IEEE Transactions on Power Electronics, vol. 29, no. 3, pp. 1551-1552, March 2014, doi: 10.1109/TPEL.2013.2278856.

[13]. Z. Chen, "PI and Sliding Mode Control of a Cuk Converter," in IEEE Transactions on Power Electronics, vol. 27, no. 8, pp. 3695-3703, Aug. 2012, doi: 10.1109/TPEL.2012.2183891.

[14]. A. Safari and S. Mekhilef, "Simulation and Hardware Implementation of Incremental Conductance MPPT With Direct Control Method Using Cuk Converter," in IEEE Transactions on Industrial Electronics, vol. 58, no. 4, pp. 1154-1161, April 2011, doi: 10.1109/TIE.2010.2048834.

[15]. M. S. Bashir, S. Jamil, Z. Yamin and H. Ullah, "Small Signal Modelling and Observer based Stability Analysis of Cuk Converter via Lyapunov's Direct Method," 2021 International Conference on Emerging Power Technologies (ICEPT), Topi, Pakistan, 2021, pp. 1-6, doi: 10.1109/ICEPT51706.2021.9435568.

[16]. R. Katoch and D. Joshi, "Comparitive Analysis of Positive Output Elementary Superlift Luo Converter using PI and Fuzzy Controller," 2022 IEEE 10th Power India International Conference (PIICON), New Delhi, India, 2022, pp. 1-6, doi: 10.1109/PIICON56320.2022.10045271.

[17]. S. Upadhyaya, K. Rana, M. Taneja and D. Joshi, "Modelling and Control of Non-Isolated Multiport DC/DC Converter," 2020 First IEEE International Conference

on Measurement, Instrumentation, Control and Automation (ICMICA), Kurukshetra, India, 2020, pp. 1-5, doi: 10.1109/ICMICA48462.2020.9242764

[18]. Lin, C-C., L-S. Yang, and G. W. Wu. "Study of a non-isolated bidirectional DC–DC converter." *IET Power Electronics* (2013)

[19]. Sebaje, Alex Sander, Mário Lúcio da Silva Martins, and Carlos. "A hybrid bidirectional DC-DC converter based on a SEPIC/Zeta converter with a modified switched capacitor cell." *2021 Brazilian* IEEE, 2021.

[20]. Sunarno, Epyk, et al. "Design and implementation bidirectional SEPIC/ZETA converter using Fuzzy Logic Controller in DC microgrid application." *Journal of Physics: Conference Series* 2019.

[21]. Ravi, Deepak, et al. "Bidirectional DC to DC converters: an overview of various topologies, switching schemes and control techniques." *International Journal of Engineering & Technology* 7.4.5 (2018).

[22]. Lithesh, Gottapu, Bekkam Krishna "Review and comparative study of bi-directional DC-DC converters." *2021 IEEE International Power and Renewable Energy Conference (IPRECON)*.

[23]. Sharma, Vasudha, Narendra Kumar, and Ram Bhagat. "Tuning of PID Controller in Magnetic Levitation System Applying Honey Badger Algorithm." IEEE 2023.

[24]. Verma, Sujata, S. K. Singh, and A. G. Rao, “Overview of control Techniques for DC-DC converters”, Research Journal of Engineering Sciences ISSN 2278 (2013): 9472.

[25]. Slobodan Cuk, R.D. Middlebrook, "DC-DC Switching Converter," U.S.Patent applied for,California Institute of Technology, Sept.26,1977.

[26]. Middlebrook, Richard D., and Slobodan Cuk. "A general unified approach to modelling switching-converter power stages." In 1976 IEEE Power Electronics Specialists Conference, pp. 18-34. IEEE, 1976.

[27]. Cuk, Slobodan, and R. D. Middlebrook. "A new optimum topology switching dc-to-dc converter." (1977): 160-179

[28]. Niculescu, Elena, Dorina Mioara-Purcaru, Marius-Cristian Niculescu, Ion Purcaru and Marian Maria, “A simplified steady-state analysis of the PWM Zeta converter”, In WSEAS International Conference. Proceedings. Mathematics and Computers in Science and Engineering, edited by N. E. Mastorakis, V. Mladenov, Z. Bojkovic, S. Kartalopoulos, A. Varonides, and M. Jha, no. 13., World Scientific and Engineering Academy and Society, 2009.

[29]. Niculescu, Elena, Dorina-Mioara Purcaru, and M. C. Niculescu, “A steady-state analysis of PWM SEPIC converter”, In Proceedings of the 10th WSEAS international conference on Circuits, pp. 217-222. World Scientific and Engineering Academy and Society (WSEAS), 2006.

[30]. Ioinovici, Adrian. Fundamentals and hard-switching converters. John Wiley & Sons, 2013.

[31]. Wu, Tasi-Fu, and Yu-Kai Chen, “Modelling PWM DC/DC converters out of basic converter units”, Power Electronics, IEEE Transactions on 13, no. 5 (1998): 870-881. X

[32]. Vuthchhay,Eng and Chanin Bunlaksananusorn, “Dynamic modelling of a Zeta converter with State-Space averaging technique”, In Electrical Engineering/Electronics, Computer, Telecommunications and Information Technology 2008,ECTI-CON 2008,5th International Conference on, vol. 2, pp. 969-972,IEEE 2008.

[33]. Kochcha, Pijit and Sarawut Sujitjorn, “Isolated zeta converter: principle of operation and design in continuous conduction mode”, WSEAS Transactions on Circuits and Systems 9, no. 7 (2010): 483-492.

[34]. Preeja, J. P. and S. V. Kayalvizhi, “Transient Response Improvement of Cuk Converter using SMC & FLC”.

[35]. Banaei, Mohamad Reza, and Hossein Ajdar Faeghi Bonab. "A high efficiency nonisolated buck–boost converter based on ZETA converter." IEEE Transactions on Industrial Electronics 67.3 (2019): 1991-1998.

[36]. Kim, In-Dong. "Design of bidirectional PWM Sepic/Zeta DC-DC converter." *2007 7th* IEEE.

[37]. Gorji, Saman A., et al. "Topologies and control schemes of bidirectional DC–DC power converters: An overview." IEEE (2019).

[38]. M. Jain, M. Daniele, and P. K. Jain, "A Bidirectional DC-DC Converter Topology for Low Power Application", IEEE Trans. Power Electronics, vol. 15, no. 4, pp. 595-606, July 2000.

[39]. F. Caricchi, F. Crescimbini, and A. Di Napoli, "20kW Water-Cooled Prototype of a Buck-Boost Bidirectional DC-DC Converter Topology for Electrical Vehicle Motor Drives", IEEE APEC Rec., 1995, pp. 887-892

[40]. F. Z. Peng, H. Li, GJ. Su, and lS. Lawler, "A New ZVS Bidirectional DC-DC Converter for Fuel Cell and Battery Application", IEEE Trans. Power Electronics, vol. 19, no. 1, pp. 54-65, Jan 2004.

[41]. K.-W. Ma, and Y. S. Lee, "A Novel Uninterruptible dc-dc Converter for UPS Applications", IEEE Trans. Industry Applications vol. IA-28, no. 4, pp. 808-815, July/Aug. 1992.

[42]. Mittal, Sudhanshu, Alka Singh, and Prakash Chittora. "Solar PV Array based Grid-Connected Bi-Directional EV Charger Controlled using NARLMMN Algorithm." 2023 9th IEEE India International Conference on Power Electronics (IICPE). IEEE, 2023.

[43]. Mittal, Sudhanshu, Alka Singh, and Prakash Chittora. "EV Control in G2V and V2G modes using SOGI Controller." 2022 IEEE 3rd Global Conference for Advancement in Technology (GCAT). IEEE, 2022.

[44]. D. M. Sable, F. C. Lee, and B. H. Cho, "A Zero-Voltage-Switching Bidirectional Battery Charger / Discharger for the NASA EOS Satellite", IEEE APEC Rec., 1992.

LIST OF PUBLICATIONS

- Singh, Prashant, Alka Singh, and Ankita Arora. "**A Comprehensive Study on the Closed Loop Performance of a Zeta Converter**." *2023 11th National Power Electronics Conference (NPEC)*. IEEE, 2023. (**Published**)
- Singh, Prashant, Alka Singh, and Ankita Arora. "**Dynamic Modelling and PID Control Design for Bidirectional SEPIC/ZETA DC-DC Converter in Battery Applications**" in 2024 IEEE *4th Series of CONIT (The International Conference for Intelligent Technologies)* (**Accepted**)